CR-61646

TR-DA1568
21 October 1967

SUMMARY REPORT:
VENUS SWINGBY TRAJECTORIES; ESTIMATION OF INERTIAL PLATFORM ERRORS; INTERPLANETARY NAVIGATION AND GUIDANCE ANALYSIS

GPO PRICE $ _____

CFSTI PRICE(S) $ _____

Contract No. NAS8-20358

Hard copy (HC) 3.00

Microfiche (MF) .65

ff 653 July 65

Prepared for
NATIONAL AERONAUTICS AND SPACE ADMINISTRATION
MARSHALL SPACE FLIGHT CENTER
Huntsville, Alabama

PHILCO Ford

PHILCO-FORD CORPORATION
Space & Re-entry Systems Division
Palo Alto, California

TR-DA1568
21 October 1967

SUMMARY REPORT:
VENUS SWINGBY TRAJECTORIES;
ESTIMATION OF INERTIAL PLATFORM ERRORS;
INTERPLANETARY NAVIGATION AND GUIDANCE ANALYSIS

Contract No. NAS8-20358

21 October 1967

Prepared by
PHILCO-FORD CORPORATION
Space & Re-Entry Systems Division
Palo Alto, California

for
National Aeronautics and Space Administration
Marshall Space Flight Center
Huntsville, Alabama

SUMMARY REPORT

TASK 1

HANDBOOK

MARS-VENUS-EARTH SWINGBY TRAJECTORIES

1971-1999

TASK 2

ESTIMATION OF INERTIAL

PLATFORM ERRORS

TASK 3

EFFECT OF BIAS ERRORS ON

INTERPLANETARY NAVIGATION AND

GUIDANCE SYSTEM PERFORMANCE

FOREWORD

The research presented in this report was performed for the Astrionics Laboratory of the George C. Marshall Flight Center, Huntsville, Alabama. The report is a summary of the final reports prepared under NASA Contract NAS8-20358 for three tasks. The three tasks are: (1) Preparation of a Mars-Venus-Earth swingby trajectory handbook, (2) Analysis of the feasibility of estimating inertial platform sensor errors from tracking data, and (3) Analysis of the effects of bias errors on interplanetary navigation and guidance system requirements. The task final reports that are summarized are the following:

1. Handbook Mars-Venus-Earth Swingby Trajectories 1971-1999, Philco-Ford SRS-TR 147, Palo Alto, California, 15 April 1967.

2. Estimation of Inertial Platform Errors, Philco-Ford SRS TR-DA1569, Palo Alto, California, 21 October 1967.

3. Effect of Bias Errors on Interplanetary Navigation and Guidance System Performance, Philco-Ford SRS-TR 148, Palo Alto, California, 11 August 1967.

TASK 1
HANDBOOK
MARS-VENUS-EARTH SWINGBY TRAJECTORIES
1971-1999
(SUMMARY)

Contract No. NAS8-20358

21 October 1967

Prepared by

Paul J. Rohde

PHILCO-FORD CORPORATION

Space & Re-Entry Systems Division

Palo Alto, California

for

National Aeronautics and Space Administration

Marshall Space Flight Center

Huntsville, Alabama

SECTION 1
INTRODUCTION

The increasing interest in the manned exploration of the planet Mars places a direct emphasis on the analysis of the round trip trajectories from Earth to Mars. A number of good trajectory handbooks[1,2]* are available showing direct trajectories to and from Mars. The purpose of this handbook is to present Mars return trajectories that utilize Venus as an intermediate body. The use of a Venus swingby trajectory was first reported by Hollister[3] and Sohn[4]. The mission advantages gained by using them as part of a round trip trajectory are shown in studies by Deerwester[5] and Sohn[6,7].

The swingby return trajectory analysis is restricted to specific times of interest. Low energy direct outbound trajectories to Mars exist for each Earth-Mars opposition. The analysis reported here investigates the availability of swingby return trajectories to meet these outbound trajectories with short stay times at Mars. Figure 1 shows a pictorial sketch of a hyperbolic excess speed contour plot from Reference 1. The cross hatched section in the figure shows the extent of the time region that is analyzed. The date at Mars is varied $\pm$ 50 days from the arrival date of the minimum energy outbound. The return flight time is varied from 200 days to 400 days. The analysis of this type of time region is done with a 10 day by 10 day grid for each opposition from 1971 to 1999 inclusive.

The three body program and planetary ephemeris used in the computation of the trajectory data are described in Section 2. Section 3 contains an example of the type of trajectory data generated for each opposition from 1971 to 1999. The data presented are for the 1971 opposition.

---

* Superscripts refer to the references presented in Section 4.

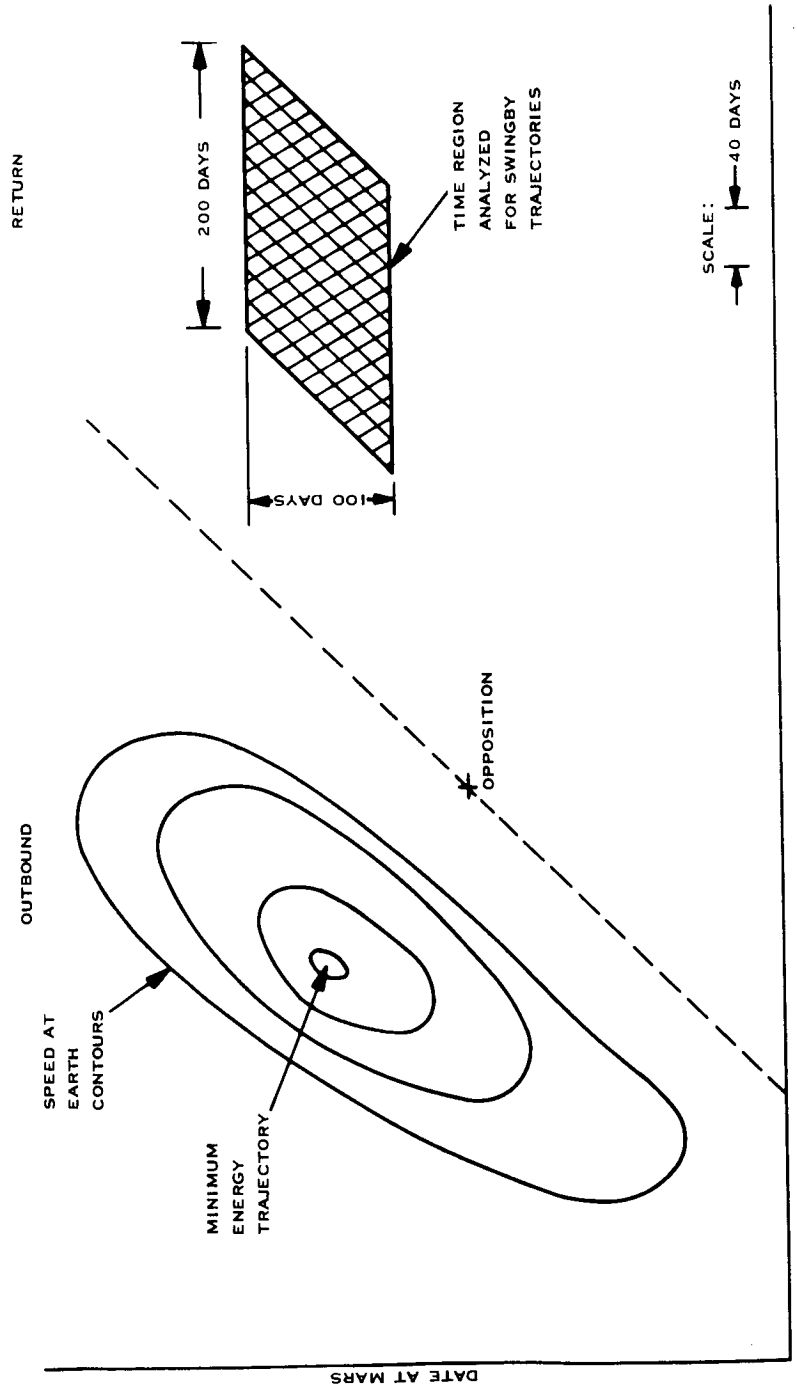

Figure 1 Time Region Analyzed

SECTION 2
TRAJECTORY COMPUTATIONS

The Philco Quick Look Three Body Program was used to generate the swingby trajectory data in Section 3. This program is the outgrowth of two earlier versions of powered assist swingby programs. The program accepts as inputs a launch date and flight time. It then automatically searches the swingby ΔV curve as a function of first leg flight time (Figure 2). and iterates to locate the zero points. These are the unpowered or free swingby trajectories.

2.1 TECHNIQUES

The following is a general description of the computation methods employed in the Quick Look Three Body Program. Each choice of a launch date, L, and time of flight, T, determines the heliocentric geometry of the "launch" body and "target" body. The division of the time of flight into first and second leg flight times, T_1 and $T_2 = T - T_1$, determines the position of the intermediate body. The launch date, L, and time of flight, T_1, determines the conic trajectory between the first and second bodies ("first leg") and yields the hyperbolic approach asymptote $\vec{S}_1$ relative to the second body. The arrival date, $(L + T_1)$, at the second body becomes the departure date for the conic trajectory to the third or target body ("second leg"). The time of flight, T_2, for the second leg determines the hyperbolic departure asymptote, $\vec{S}_2$.

The transition from the hyperbolic path (relative to the intermediate body) having asymptotes $\vec{S}_1$ and $\vec{S}_1'$, to the path with asymptote $\vec{S}_2$, will in general require a corrective change ΔV. The computer program searches for the value of flight time, T_1, that makes the magnitude of ΔV zero.

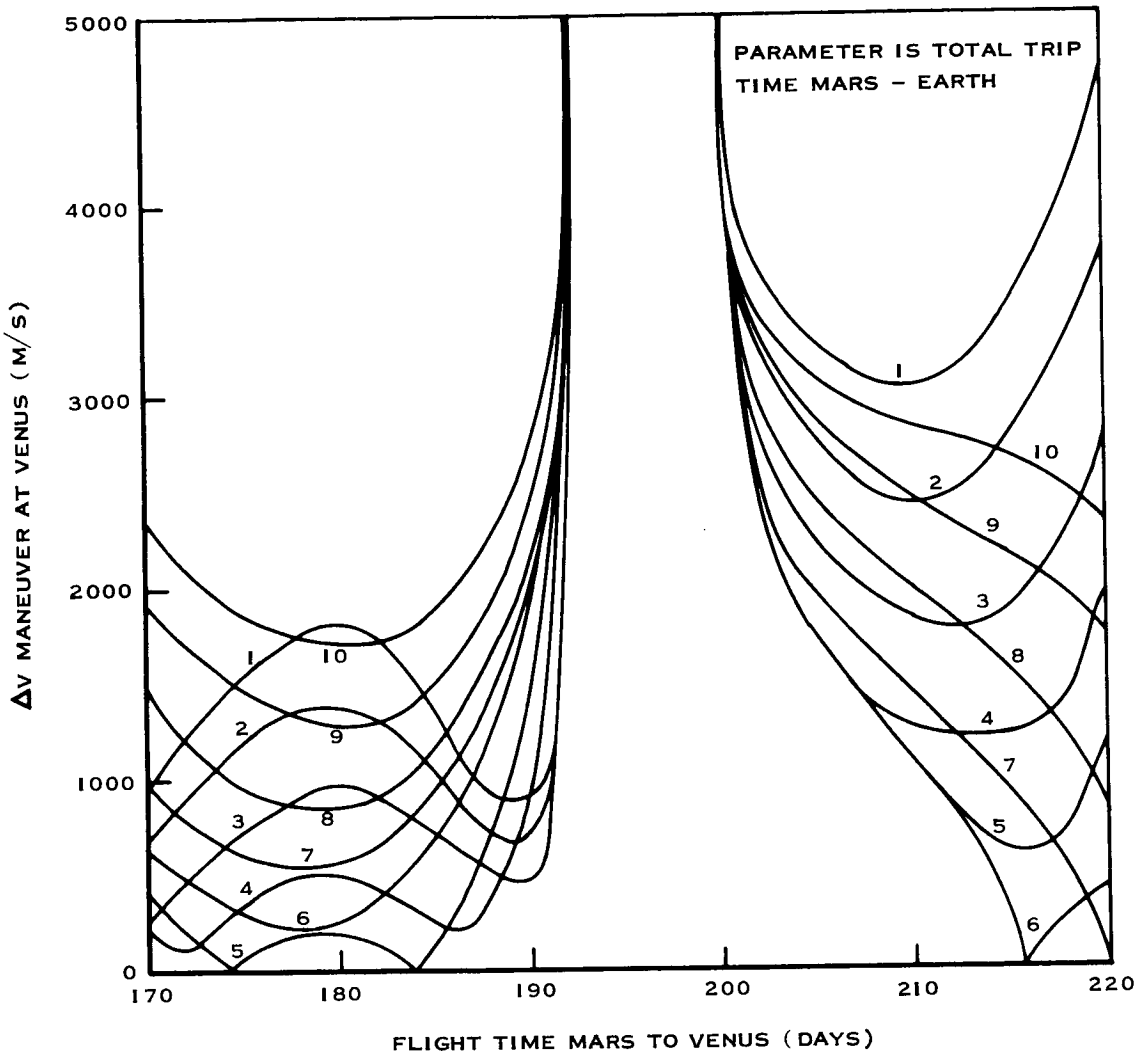

Figure 2 Venus Swingby ΔV Curves

A detailed description of the theory and operation of subroutine CONBR is presented in Reference 8. The purpose of this subroutine is to determine the particular heliocentric conic section connecting either the launch and intermediate bodies or the intermediate and target bodies for a specified transfer angle and time of flight. The subroutine solves the problem by means of an iteration process on the flight path angle at the first body.

PANTRY is the planetary ephemeris subroutine that rapidly provides planetary positions and velocities. The ephemeris calculated by this package is approximate, being derived from mean orbital elements of the various planets, but is in all cases, in error by less than one milliradian in angular position and usually much less. Figure 3 shows the position deviation of Venus obtained when comparing the data from the mean element computations in PANTRY with the JPL ephemeris tape[9]. The Three Body Program is capable of using the JPL ephemeris by direct substitution of subroutines. The major disadvantage of using the JPL ephemeris tape is the fact that it is significantly slower and reduces the speed of the program by a factor of five to seven times when the program is used to scan launch and arrival dates. The theoretical aspects of the mean element computations are described in Reference 10.

The program logic is set up so the program operates in the following manner. For a specified launch date, L, starting first leg flight time, T_1, and total flight time, T, the program goes through the following search and iteration procedure to obtain the free swingby trajectories.

1. PANTRY computes the heliocentric positions and velocities of the launch, intermediate and target bodies for the times L, L + T_1, and L + T respectively.

2. CONBR with the flight times for the two legs, T_1 and $T_2 = T - T_1$, and the computed transfer angles ψ_1 and ψ_2 computes the two heliocentric conic trajectories.

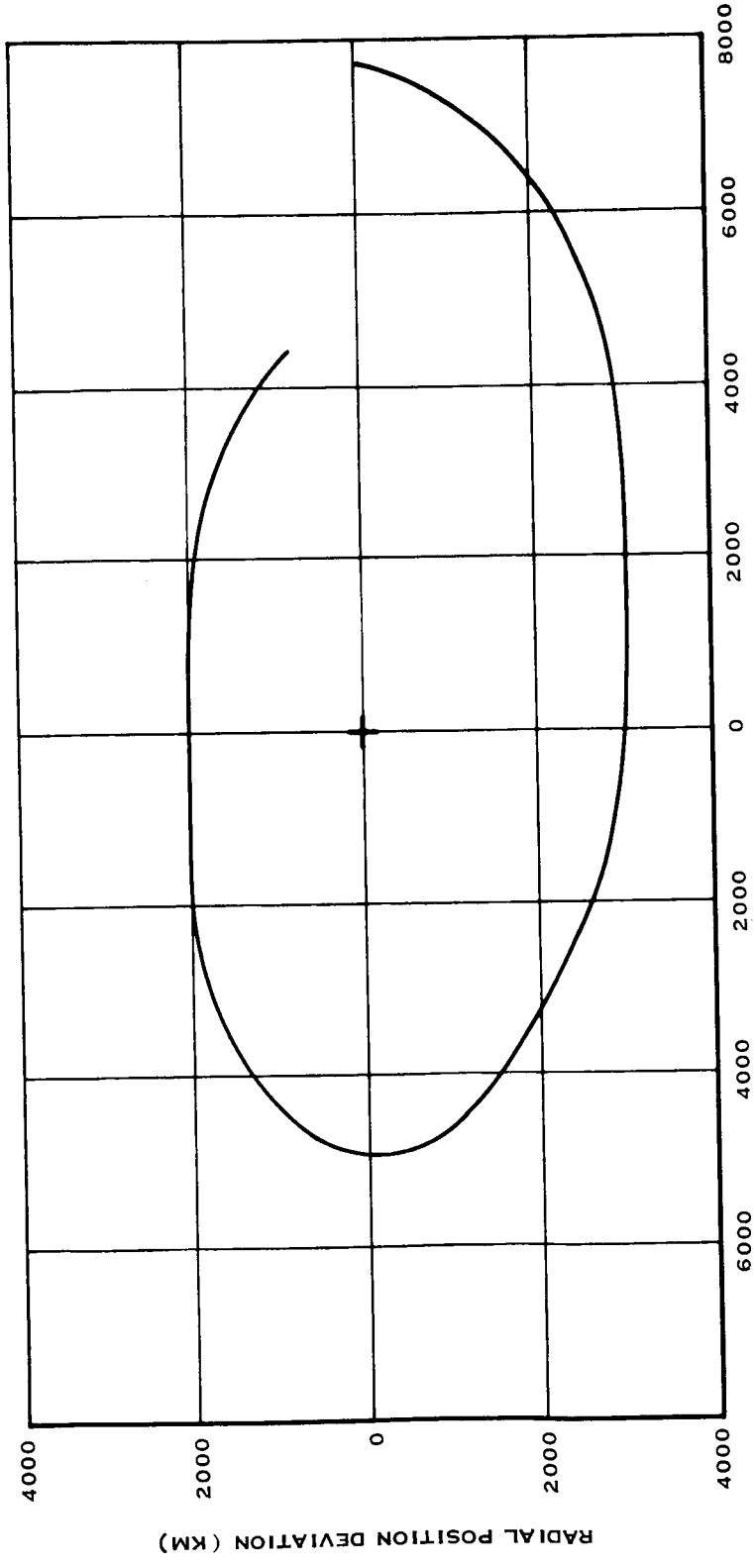

Figure 3 Deviation of Mean Element Ephemeris

3. The magnitude of the first leg approach velocity relative to the intermediate body is compared with the departure velocity relative to the body required for the second leg.

   If the difference between the magnitudes is less than a prescribed value, the periapsis radius is computed that will furnish the required rotation of the approach asymptote (Equation 3). If the radius is equal to or greater than some R_{MIN} then a free swingby has been obtained.

4. If either the magnitude or periapsis radius test fails in step 3, the first leg flight time, T_1, is incremented, ΔT_1, and the steps are repeated.

The iteration process is controlled such that when the computed difference in the approach and departure velocity magnitude is below a selected level the incremental step ΔT_1 is reduced to produce a fine search for a zero. Each time the sign of the velocity difference, $\Delta V = |\vec{S}_1| - |\vec{S}_2|$, near a zero changes sign indicating a zero was crossed, the ΔT_1 step size is halved and its sign changed to force the process to seek a zero. Following location of a zero, the program continues to increment T_1 and locate additional zeros until an upper limit on T_1 is reached. As shown in Figure 2 and the data in Section 3, a given launch date and flight time may have multiple free swingby trajectories. The zero search process described here for a given launch date and flight time requires approximately 20 seconds with the search and iteration levels set so about 150 trajectory pairs are examined.

For each launch date, L_o, the program will automatically step through a specified number of total flight times T. Finally, in an "outer loop" the launch date is incremented through a specified range. This permits the study of a selected grid of launch dates and arrival dates.

For present purposes, there are no constraints to satisfy as to the manner in which the probe passes the intermediate body, except for the radius of closest approach, R_p. Hence, the vectors $\vec{S}_1$ and $\vec{S}_2$ may be assumed to define the plane of the orbit relative to the intermediate body.

For any hyperbolic trajectory, the radius of closest approach, R_p, is related to the half angle, β, between the two asymptotes by

$$R_p = \frac{\mu}{C_3}\left(\frac{1}{\cos \beta} - 1\right) \tag{1}$$

where

$$C_3 = v^2 - \frac{2\mu}{r} \text{ (twice) energy} \tag{2}$$

μ = central body gravitational constant

Let β_o be the half-angle between $-\vec{S}_1$ and $\vec{S}_2$. The corresponding R_p is then

$$R_o = R_p(\beta_o) = \frac{\mu}{\vec{S}_1 \cdot \vec{S}_1}\left(\frac{1}{\cos \beta_o} - 1\right) \tag{3}$$

Suppose R_{MIN} is a pre-assigned minimum approach radius for the intermediate body. If $R_o \geq R_{MIN}$, the direction of $\vec{S}_1$ can be altered during encounter to match the direction of $\vec{S}_2$. Trajectory pairs relative to the intermediate body with characteristics such that $|\vec{S}_1| - |\vec{S}_2| \leq \epsilon$ and $R_o \geq R_{MIN}$ represent free swingby trajectories. In the analysis, ϵ was selected to be 10 meters/sec and R_{MIN} was 6050 kilometers (Venus radius).

2.2 QUICK LOOK THREE BODY PROGRAM

The Quick Look Three Body Program has two basic subroutines and a main driver which contains the logic for automatically scanning a parametric range of launch and arrival dates. The two basic subroutines are CONBR and PANTRY.

SECTION 3

SWINGBY TRAJECTORY DATA

This section is an example of the detailed Mars-Venus-Earth free swingby trajectory data. The mathematical analyses used for the calculations and the planetary ephemeris used are described in the previous section. For the 1971 Earth-Mars opposition, four types of data are presented. The data in Section 3.1 are a bar graph presentation of the energies required for direct outbound and swingby return trajectories. The last three types of data are presented in Section 3.2. The data on the first page for the opposition is a three year ephemeris on Earth, Venus, and Mars in ecliptic of 1950 coordinates. This data allows the user to look at the geometrical relationships between the three planets for specific dates of interest. The second page for the opposition contains a conversion of Julian Dates to Calendar Dates for the span of dates used in the analysis. The remaining pages for the opposition contain the tabulated trajectory data. The data for each trajectory is presented on one line that spans across facing pages.

3.1 GRAPHICAL DATA

The bar graphs in Figure 4 show the launch and arrival hyperbolic excess speeds for outbound and return trajectories. The abscissa on each graph is the date at Mars. This permits the analyst to combine a direct outbound and a swingby return using the Mars stay time as a parameter. The speed data for the outbound direct trajectories are taken from Reference 1. For each date at Mars, the trajectory with the minimum departure speed at Earth was selected. The return swingby trajectory data are taken from Section 3.2. For each date at Mars, the trajectory with the minimum arrival speed at Earth was selected.

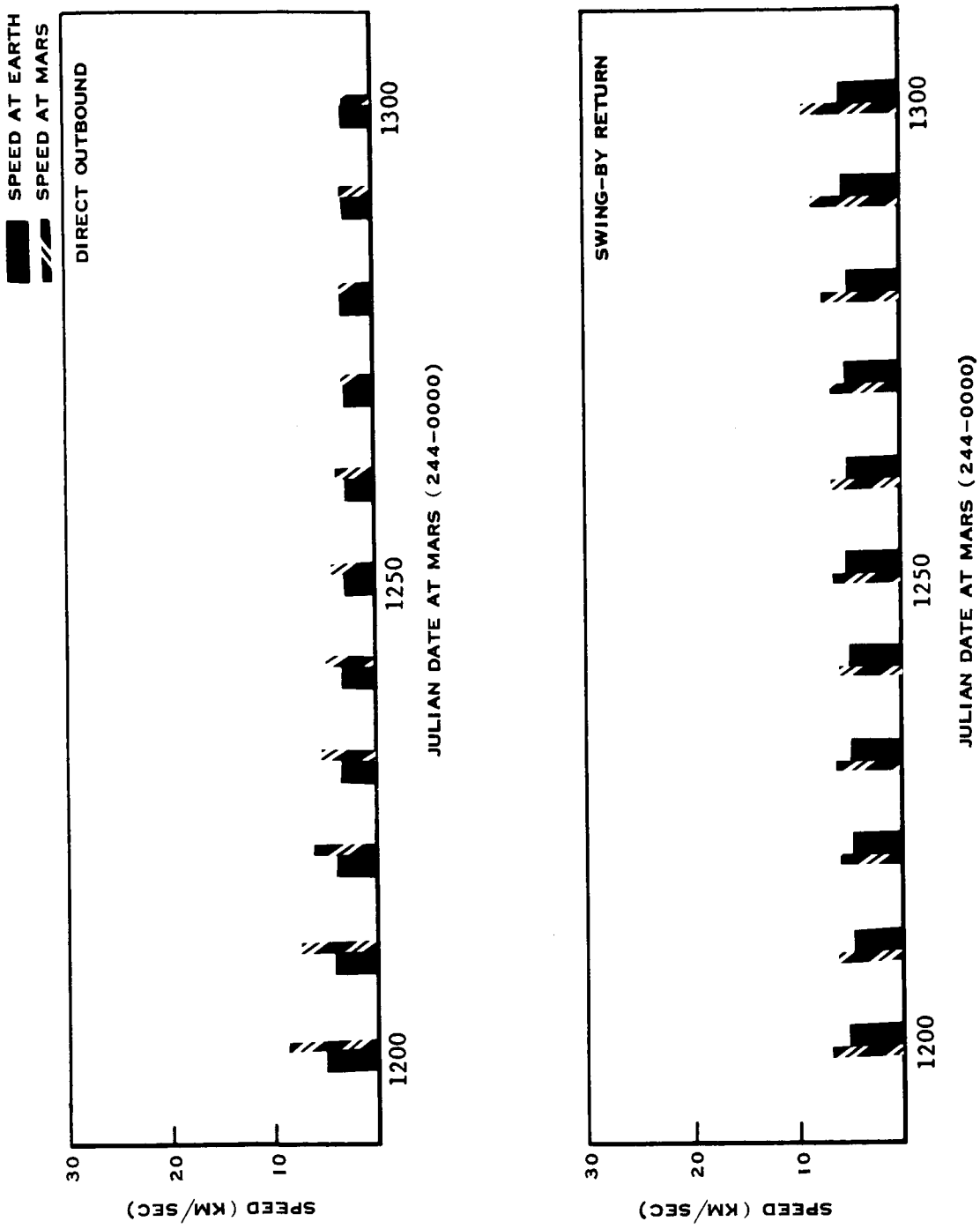

Figure 4 1971 Opposition

3.2 TABULAR DATA

The tabulated trajectory data are presented in a format similar to that used in Reference 1. To aid in the construction of round trip trajectories with Venus swingby return trajectories, the date at Mars is held constant while the trip time to Earth is varied from 200 days to 400 days in 10-day increments. In some instances there are multiple free swingby trajectories for a given Mars departure date and flight time and in other cases there are no trajectories. This accounts for the absence of some departure dates and flight times and the multiple occurrence of others. The Mars departure date is presented at the extreme left-hand side of the page. In the Space Flight Handbook, Volume 3, Part 2 that contains tabulated direct Earth-Mars trajectories, the Mars arrival date is presented in the extreme right-hand column of each page. Therefore, by placing this manual to the right of the Handbook, the analyst may make up round trip Earth-Mars-Earth trajectories with various stopover times at Mars.

Three cartesian coordinate frames of reference are used in the presentation of the trajectory data. They are the following: (1) Target coordinates for data relative to Mars and Venus, (2) Ecliptic coordinates for data relative to the Sun, and (3) Earth Equator coordinates for data relative to the Earth. These coordinate frames are oriented as follows:

Target Coordinates : x axis from the planet toward the Sun
z axis normal to planet orbit plane
y axis forms right handed system

Ecliptic Coordinates : x axis in ecliptic plane directed toward vernal equinox
y axis normal to x in ecliptic plane
z axis normal to ecliptic plane

Earth Equator Coordinates : x axis in earth equatorial plane directed toward vernal equinox
y axis in earth equatorial plane and normal to x
z axis normal to the earth equatorial plane

The time epochs associated with the coordinate frames are the following. The Mars departure and Venus arrival dates are used to fix the Target coordinates for the Mars and Venus data respectively. The Ecliptic coordinates are fixed at the Mars departure date. The Earth Equator coordinates are for the Earth arrival date.

The following is a list of the symbols used in Section 3.2 to present the trajectory data and their definitions.

SYMBOLS AND DEFINITIONS FOR TRAJECTORY DATA

COLUMN	SYMBOL	DEFINITION
1		Julian date of Mars departure (244 - 3120 last five numbers)
2		Julian date of Venus passage
3		Julian date of Earth Arrival
4		Total trip duration in days
		MARS ASYMPTOTE*
5	SPEED	Magnitude of hyperbolic excess Mars departure velocity (km/sec).
6	DECL	Declination of the hyperbolic excess velocity, measured in degrees positive above and negative below Mars' orbit plane.
7	RA	Right ascension of the hyperbolic excess velocity, measured in degrees in Mars' orbit plane from the Mars-Sun line.
		MARS-VENUS HELIOCENTRIC TRANSFER**
8	VELM	Heliocentric velocity at Mars departure (km/sec).
9	PTHM	Path angle of heliocentric velocity at Mars departure (deg).
10	INCL	Inclination of heliocentric trajectory to the ecliptic plane (deg).
11	ECC	Eccentricity of heliocentric conic.
12	SMA	Semimajor axis of heliocentric conic (Astronomical Units).
13	PERIH	Perihelion of heliocentric conic (Astronomical Units).
14	LAN	Longitude of the ascending node (deg).
15	APF	Argument of perifocus (deg).
16	THETM	True anomaly of Mars at departure measured in the transfer orbit (deg).
17	THETV	True anomaly of Venus at passage measured in the transfer orbit (deg). THETV-THETM equals the heliocentric transfer angle.
		VENUS ASYMPTOTE*
18	SPEED	Magnitude of hyperbolic excess Venus arrival velocity (km/sec).
19	DECL	Analogous to the Mars departure velocity case; however, this is the declination of the position at which the arrival velocity vector would emerge from Venus' celestial sphere (deg).
20	RA	Right ascension of the position at which the arrival velocity vector would emerge from Venus' celestial sphere (deg).

VENUS PASSAGE*

21	INCL	Inclination of the Venus centered swingby trajectory to the orbit plane (deg).
22	RCA	Distance of closest approach to Venus required to satisfy the asymptote turn angle to meet the outgoing asymptote to Earth (deg).
23	DECL	Declination of the position at which a vector directed from Venus through the point of closest approach would emerge from Venus' celestial sphere (deg).
24	RA	Right ascension of the position at which vector from Venus through the point of closest approach would emerge from Venus' celestial sphere (deg).

VENUS-EARTH HELIOCENTRIC TRANSFER**

25	VELE	Heliocentric velocity at Earth arrival (km/sec).
26	PTHE	Path angle of heliocentric velocity at Earth arrival (deg).
27	INCL	Inclination of heliocentric trajectory to the ecliptic plane (deg).
28	ECC	Eccentricity of heliocentric conic.
29	SMA	Semimajor axis of heliocentric conic (Astronomical Units).
30	PERIN	Perihelion of heliocentric conic (Astronomical Units).
31	LAN	Longitude of the ascending node (deg).
32	APF	Argument of perifocus (deg).
33	THETV	True anomaly of Venus at passage measured in the transfer orbit (deg).
34	THETE	True anomaly of Earth at arrival measured in the transfer orbit (deg).

EARTH ASYMPTOTE***

35	SPEED	Magnitude of hyperbolic excess Earth arrival velocity (km/sec).
36	DECL	Declination of the position at which the arrival velocity vector would emerge from Earth's celestial sphere (deg).
37	RA	Right ascension of the position at which time arrival velocity vector would emerge from Earth's celestial sphere (deg).

Coordinate Frames Used :

*Target Coordinate

** Ecliptic Coordinates of Mars Departure Date

*** Earth Equator Coordinates of Earth Arrival Date

PLANETARY EPHEMERIS - ECLIPTIC OF 1950

DATE	EARTH			VENUS			MARS		
	R	DE	RA	R	DE	RA	R	DE	RA
7101.01	0.98	-0.00	99.6	0.72	2.76	130.7	1.62	1.00	-163.5
7102.01	0.99	-0.00	131.2	0.72	3.28	-179.0	1.59	0.58	-149.0
7103.01	0.99	-0.00	159.5	0.72	1.70	-133.9	1.56	0.15	-135.4
7104.01	1.00	0.00	-169.7	0.73	-1.11	-84.7	1.52	-0.36	-119.6
7105.01	1.01	0.00	-140.3	0.73	-3.12	-37.2	1.48	-0.85	-103.5
7106.01	1.01	0.00	-110.4	0.73	-3.06	12.0	1.45	-1.30	-86.0
7107.01	1.02	0.00	-81.8	0.72	-0.95	60.0	1.41	-1.64	-68.2
7108.01	1.02	0.00	-52.2	0.72	1.89	110.0	1.39	-1.83	-49.1
7109.01	1.01	0.00	-22.4	0.72	3.38	160.4	1.38	-1.81	-29.6
7110.01	1.00	-0.00	6.9	0.72	2.49	-151.1	1.39	-1.59	-10.5
7111.01	0.99	-0.00	37.6	0.73	-0.13	-101.6	1.40	-1.19	8.8
7112.01	0.99	-0.00	67.8	0.73	-2.59	-54.2	1.43	-0.70	27.0
7201.01	0.98	-0.00	99.4	0.73	-3.35	-5.0	1.46	-0.13	45.0
7202.01	0.99	-0.00	130.9	0.72	-1.79	44.4	1.50	0.41	62.1
7203.01	0.99	-0.00	160.2	0.72	0.88	91.1	1.54	0.87	77.2
7204.01	1.00	0.00	-168.9	0.72	3.08	141.4	1.58	1.27	92.7
7205.01	1.01	0.00	-139.6	0.72	3.10	-169.9	1.61	1.57	107.0
7206.01	1.01	0.00	-109.7	0.72	0.96	-120.2	1.64	1.76	121.2
7207.01	1.02	0.00	-81.1	0.73	-1.76	-72.7	1.66	1.84	134.6
7208.01	1.01	0.00	-51.5	0.73	-3.34	-23.6	1.66	1.82	148.2
7209.01	1.01	0.00	-21.7	0.72	-2.62	25.7	1.66	1.71	161.8
7210.01	1.00	-0.00	7.6	0.72	-0.14	73.8	1.66	1.50	174.9
7211.01	0.99	-0.00	38.4	0.72	2.52	124.3	1.64	1.20	-171.2
7212.01	0.99	-0.00	68.6	0.72	3.37	172.7	1.61	0.83	-157.5
7301.01	0.98	-0.00	100.1	0.72	1.87	-137.3	1.58	0.38	-142.8
7302.01	0.99	-0.00	131.7	0.73	-0.93	-88.0	1.54	-0.11	-127.3
7303.01	0.99	-0.00	159.9	0.73	-2.94	-43.7	1.51	-0.58	-112.7
7304.01	1.00	0.00	-169.2	0.73	-3.20	5.5	1.47	-1.06	-95.7
7305.01	1.01	0.00	-139.8	0.72	-1.31	53.4	1.43	-1.47	-78.4
7306.01	1.01	0.00	-110.0	0.72	1.55	103.4	1.40	-1.75	-59.7
7307.01	1.02	0.00	-81.3	0.72	3.29	152.1	1.39	-1.85	-40.9
7308.01	1.01	0.00	-51.7	0.72	2.74	-157.7	1.38	-1.74	-21.3
7309.01	1.01	0.00	-21.9	0.73	0.25	-108.1	1.39	-1.43	-1.7
7310.01	1.00	-0.00	7.3	0.73	-2.32	-60.6	1.41	-0.99	16.8
7311.01	0.99	-0.00	38.1	0.73	-3.39	-11.6	1.44	-0.44	35.3
7312.01	0.99	-0.00	68.3	0.72	-2.18	36.3	1.48	0.10	52.3

JULIAN-CALENDAR DATE CONVERSIONS, 1971 OPPOSITION

JULIAN DATE	CALENDAR DATE	JULIAN DATE	CALENDAR DATE
244-1200.5	7109.06	244-1550.5	7208.21
244-1210.5	7109.16	244-1560.5	7208.31
244-1220.5	7109.26	244-1570.5	7209.10
244-1230.5	7110.06	244-1580.5	7209.20
244-1240.5	7110.16	244-1590.5	7209.30
244-1250.5	7110.26	244-1600.5	7210.10
244-1260.5	7111.05	244-1610.5	7210.20
244-1270.5	7111.15	244-1620.5	7210.30
244-1280.5	7111.25	244-1630.5	7211.09
244-1290.5	7112.05	244-1640.5	7211.19
244-1300.5	7112.15	244-1650.5	7211.29
244-1310.5	7112.25	244-1660.5	7212.09
244-1320.5	7201.04	244-1670.5	7212.19
244-1330.5	7201.14	244-1680.5	7212.29
244-1340.5	7201.24	244-1690.5	7301.08
244-1350.5	7202.03	244-1700.5	7301.18
244-1360.5	7202.13	244-1710.5	7301.28
244-1370.5	7202.23	244-1720.5	7302.07
244-1380.5	7203.04	244-1730.5	7302.17
244-1390.5	7203.14	244-1740.5	7302.27
244-1400.5	7203.24	244-1750.5	7303.09
244-1410.5	7204.03	244-1760.5	7303.19
244-1420.5	7204.13	244-1770.5	7303.29
244-1430.5	7204.23	244-1780.5	7304.08
244-1440.5	7205.03	244-1790.5	7304.18
244-1450.5	7205.13	244-1800.5	7304.28
244-1460.5	7205.23	244-1810.5	7305.08
244-1470.5	7206.02	244-1820.5	7305.18
244-1480.5	7206.12	244-1830.5	7305.28
244-1490.5	7206.22	244-1840.5	7306.07
244-1500.5	7207.02	244-1850.5	7306.17
244-1510.5	7207.12	244-1860.5	7306.27
244-1520.5	7207.22	244-1870.5	7307.07
244-1530.5	7208.01	244-1880.5	7307.17
244-1540.5	7208.11	244-1890.5	7307.27

MARS DEPART	VENUS PASS	EARTH ARRIVE	TRIP TIME	MARS ASYMPTOTE SPEED	DECL	R A	VELM	PTHM	MARS-VENUS HELIOCENTRIC TRANSFER INCL	ECC	SMA	PERIH	LAN	APF	THETM	THETV	VENUS SPEED
4-1200	4-1374	4-1450	250.	8.39	-1.2	116.6	19.4	11.0	1.79	0.451	0.976	0.535	65.7	102.2	166.0	280.0	14.96
4-1200	4-1381	4-1460	260.	7.66	-0.4	115.6	19.9	9.4	1.82	0.415	0.997	0.584	53.8	113.9	166.2	290.8	12.86
4-1200	4-1388	4-1470	270.	7.07	1.0	114.3	20.3	8.1	1.97	0.384	1.016	0.626	39.5	127.8	166.6	302.0	10.94
4-1200	4-1395	4-1480	280.	6.60	3.6	113.0	20.6	7.0	2.41	0.359	1.032	0.662	21.8	145.0	167.2	314.2	9.17
4-1200	4-1421	4-1490	290.	7.04	-29.3	109.8	21.1	5.5	9.16	0.320	1.058	0.720	142.7	23.2	168.1	358.6	7.54
4-1200	4-1469	4-1510	310.	8.32	-3.1	127.5	20.5	14.1	1.97	0.413	1.029	0.604	88.6	87.4	157.9	424.6	12.21
4-1200	4-1478	4-1520	320.	9.61	-1.8	131.7	20.3	18.1	1.84	0.459	1.020	0.551	77.7	100.7	155.5	436.5	14.80
4-1200	4-1401	4-1550	350.	6.35	8.0	111.8	20.8	6.3	3.41	0.342	1.042	0.686	5.5	160.7	167.6	324.9	8.01
4-1200	4-1420	4-1550	350.	7.81	-35.7	109.0	21.1	5.5	12.20	0.320	1.058	0.719	145.6	20.3	168.2	355.9	9.13
4-1200	4-1424	4-1550	350.	6.56	-23.1	110.4	21.1	5.6	6.81	0.320	1.058	0.720	138.7	27.3	167.9	362.6	6.49
4-1200	4-1406	4-1560	360.	6.41	16.2	110.9	20.9	5.9	5.69	0.332	1.049	0.701	352.2	173.7	168.0	334.0	7.78
4-1200	4-1413	4-1560	360.	10.53	46.1	106.9	21.0	5.6	21.78	0.324	1.055	0.712	338.4	187.1	168.1	344.1	15.77
4-1200	4-1432	4-1560	360.	6.22	-13.8	112.5	21.1	6.1	4.03	0.324	1.057	0.715	127.6	39.5	166.9	374.9	5.96
4-1200	4-1438	4-1570	370.	6.27	-10.9	114.0	21.0	6.7	3.32	0.329	1.055	0.708	121.3	46.6	166.1	382.5	6.36
4-1200	4-1442	4-1580	380.	6.39	-9.1	115.5	21.0	7.3	2.93	0.336	1.052	0.699	116.3	52.5	165.1	389.0	6.92
4-1200	4-1446	4-1590	390.	6.56	-7.7	117.2	20.9	8.0	2.67	0.343	1.049	0.689	111.7	58.1	164.1	395.0	7.56
4-1210	4-1376	4-1450	240.	8.11	-1.0	110.5	19.1	9.1	1.74	0.453	0.967	0.529	62.6	109.0	168.7	278.6	15.13
4-1210	4-1382	4-1460	250.	7.38	-0.1	109.1	19.7	7.6	1.83	0.414	0.990	0.580	50.7	120.6	169.0	289.7	12.97
4-1210	4-1389	4-1470	260.	6.80	1.3	107.4	20.1	6.3	2.05	0.383	1.010	0.623	37.9	132.8	169.6	301.1	11.02
4-1210	4-1396	4-1480	270.	6.35	3.8	105.5	20.5	5.3	2.52	0.357	1.027	0.660	23.5	146.3	170.4	313.5	9.21
4-1210	4-1406	4-1490	280.	6.06	11.2	103.4	20.8	4.3	4.29	0.333	1.043	0.695	4.0	164.9	171.3	330.3	7.56
4-1210	4-1410	4-1490	280.	6.16	17.1	102.8	20.9	4.1	5.90	0.328	1.047	0.704	357.3	171.4	171.5	336.2	7.54
4-1210	4-1426	4-1490	280.	6.85	-30.2	102.2	21.0	3.9	8.95	0.318	1.055	0.720	149.2	19.7	171.5	362.6	7.60
4-1210	4-1451	4-1500	290.	6.33	-7.7	111.2	20.8	6.8	2.42	0.344	1.043	0.684	114.8	58.8	166.8	397.8	7.85
4-1210	4-1473	4-1520	310.	8.07	-2.7	123.8	20.3	13.3	1.78	0.415	1.020	0.597	84.7	95.9	159.7	426.9	12.53
4-1210	4-1481	4-1530	320.	9.13	-1.6	128.1	20.2	16.8	1.73	0.454	1.012	0.552	73.4	109.5	157.3	436.6	14.66
4-1210	4-1401	4-1550	340.	6.13	6.7	104.3	20.7	4.7	3.17	0.343	1.036	0.681	13.3	156.1	170.9	322.3	8.18
4-1210	4-1406	4-1560	350.	6.06	11.2	103.4	20.8	4.3	4.29	0.333	1.043	0.695	4.0	164.9	171.3	330.3	7.56
4-1210	4-1432	4-1560	350.	6.12	-19.0	103.6	21.0	4.2	5.09	0.320	1.054	0.717	140.5	29.0	170.9	371.3	6.17
4-1210	4-1438	4-1570	360.	6.02	-13.3	105.7	21.0	4.9	3.59	0.325	1.052	0.710	131.5	39.0	169.8	380.4	6.28
4-1210	4-1443	4-1580	370.	6.08	-10.7	107.6	20.9	5.5	2.99	0.331	1.049	0.702	124.9	46.6	168.7	387.2	6.75
4-1210	4-1447	4-1590	380.	6.20	-8.9	109.5	20.9	6.1	2.63	0.338	1.046	0.693	119.2	53.4	167.7	393.2	7.33
4-1210	4-1451	4-1600	390.	6.36	-7.5	111.5	20.8	6.9	2.38	0.346	1.042	0.682	113.8	59.9	166.5	398.7	7.97
4-1210	4-1349	4-1610	400.	12.84	-2.0	111.7	15.4	18.7	2.03	0.678	0.848	0.273	102.1	67.7	170.5	237.2	25.92
4-1220	4-1377	4-1450	230.	7.90	-0.8	103.6	18.9	6.9	1.72	0.455	0.960	0.524	59.5	115.6	171.5	277.4	15.31
4-1220	4-1384	4-1460	240.	7.17	0.1	101.5	19.5	5.5	1.87	0.415	0.985	0.576	48.4	126.0	172.2	288.7	13.11
4-1220	4-1390	4-1470	250.	6.60	1.5	99.1	20.0	4.2	2.13	0.382	1.006	0.621	37.2	136.3	173.1	300.5	11.07
4-1220	4-1398	4-1480	260.	6.18	3.9	96.8	20.4	3.3	2.61	0.356	1.024	0.659	25.7	146.9	174.0	313.0	9.24
4-1220	4-1407	4-1490	270.	5.89	9.4	94.4	20.7	2.4	3.88	0.334	1.040	0.693	11.6	159.8	175.1	328.6	7.55
4-1220	4-1414	4-1490	270.	6.15	21.2	93.1	20.9	2.0	7.16	0.323	1.048	0.710	359.8	171.0	175.7	341.5	7.52
4-1220	4-1430	4-1490	270.	6.75	-30.6	93.7	21.0	2.2	8.76	0.317	1.053	0.719	155.9	15.6	175.2	366.8	7.74
4-1220	4-1444	4-1500	280.	5.90	-12.2	98.7	20.8	3.6	3.07	0.328	1.047	0.703	134.2	39.8	172.6	386.6	6.74
4-1220	4-1462	4-1510	290.	6.52	-5.4	109.3	20.5	7.2	1.86	0.364	1.030	0.654	104.4	75.1	167.0	410.4	9.53
4-1220	4-1470	4-1520	300.	7.05	-3.7	114.3	20.3	9.4	1.71	0.387	1.021	0.626	92.1	90.1	164.4	419.4	11.01
4-1220	4-1476	4-1530	310.	7.64	-2.6	118.6	20.2	11.7	1.65	0.411	1.014	0.597	81.7	102.8	162.1	427.0	12.44
4-1220	4-1483	4-1540	320.	8.54	-1.5	123.4	20.0	14.9	1.66	0.445	1.006	0.558	69.7	117.2	159.7	435.8	14.32
4-1220	4-1406	4-1560	340.	5.90	9.1	94.5	20.7	2.5	3.79	0.335	1.039	0.691	12.3	159.2	175.1	327.9	7.60
4-1220	4-1411	4-1570	350.	5.94	15.5	93.5	20.8	2.1	5.47	0.326	1.046	0.705	4.0	166.9	175.5	337.0	7.22
4-1220	4-1438	4-1570	350.	5.94	-17.1	95.9	20.9	2.8	4.28	0.321	1.050	0.713	144.1	28.5	174.1	377.9	6.37
4-1220	4-1443	4-1580	360.	5.89	-12.7	98.1	20.8	3.4	3.18	0.327	1.047	0.705	135.5	38.2	172.9	385.5	6.67
4-1220	4-1448	4-1590	370.	5.95	-10.3	100.5	20.8	4.1	2.65	0.333	1.044	0.696	128.3	46.6	171.7	391.5	7.17
4-1220	4-1452	4-1600	380.	6.06	-8.5	102.8	20.7	4.9	2.32	0.341	1.040	0.686	121.6	54.6	170.4	397.1	7.75
4-1220	4-1348	4-1610	390.	13.41	-1.9	106.2	14.2	17.0	1.96	0.717	0.822	0.232	109.6	64.1	172.9	231.3	27.70
4-1220	4-1456	4-1610	390.	6.21	-7.1	105.3	20.6	5.7	2.09	0.349	1.036	0.675	114.8	62.7	169.1	402.4	8.41
4-1220	4-1357	4-1620	400.	11.19	-1.9	106.7	16.2	13.1	1.72	0.620	0.869	0.331	93.6	81.4	171.7	245.4	23.25
4-1230	4-1385	4-1460	230.	7.06	0.3	92.8	19.4	3.0	1.91	0.416	0.982	0.573	46.6	130.6	175.7	288.0	13.21
4-1230	4-1392	4-1470	240.	6.52	1.7	89.9	19.9	1.9	2.21	0.383	1.004	0.620	37.1	138.8	176.9	300.1	11.13
4-1230	4-1399	4-1480	250.	6.13	3.9	86.9	20.3	1.0	2.68	0.357	1.023	0.658	28.1	146.6	178.2	312.8	9.26
4-1230	4-1407	4-1490	260.	5.88	8.2	84.1	20.6	0.2	3.68	0.335	1.039	0.691	17.7	155.6	179.6	327.8	7.55
4-1230	4-1418	4-1490	260.	6.26	23.5	82.7	20.9	-0.1	8.05	0.320	1.051	0.715	3.9	168.6	180.3	346.6	7.51
4-1230	4-1445	4-1500	270.	5.87	-14.2	88.4	20.8	1.4	3.34	0.327	1.047	0.704	145.4	30.5	177.1	385.8	6.81
4-1230	4-1460	4-1510	280.	6.11	-6.7	98.2	20.5	4.3	1.82	0.353	1.031	0.668	115.1	65.9	172.0	405.6	8.81
4-1230	4-1467	4-1520	290.	6.42	-4.8	103.4	20.3	6.1	1.62	0.370	1.023	0.645	100.6	83.0	169.4	413.9	10.03
4-1230	4-1472	4-1530	300.	6.75	-3.6	107.4	20.2	7.7	1.55	0.386	1.017	0.624	89.8	95.7	167.4	420.1	11.06
4-1230	4-1478	4-1540	310.	7.21	-2.5	112.0	20.0	9.7	1.55	0.406	1.010	0.600	78.9	108.9	165.1	426.6	12.26
4-1230	4-1485	4-1550	320.	7.99	-1.3	117.6	19.8	12.8	1.61	0.437	1.001	0.563	66.1	124.5	162.4	435.0	14.00
4-1230	4-1406	4-1560	330.	5.89	7.6	84.3	20.6	0.3	3.54	0.337	1.038	0.688	18.7	154.7	179.5	326.3	7.69
4-1230	4-1411	4-1570	340.	5.86	11.5	83.4	20.7	0.0	4.51	0.328	1.045	0.702	12.9	160.1	179.9	334.5	7.07
4-1230	4-1419	4-1580	350.	6.32	24.4	82.7	20.9	-0.1	8.36	0.320	1.051	0.715	3.5	169.0	180.3	347.1	7.63
4-1230	4-1422	4-1580	350.	7.92	39.1	83.3	20.9	-0.1	14.93	0.318	1.053	0.718	358.7	173.8	180.3	353.0	10.90
4-1230	4-1443	4-1580	350.	5.90	-15.6	87.6	20.8	1.2	3.70	0.325	1.048	0.707	148.3	27.1	177.5	383.5	6.72
4-1230	4-1448	4-1590	360.	5.86	-12.0	90.0	20.7	1.9	2.81	0.331	1.044	0.698	139.6	37.1	176.2	390.1	7.10
4-1230	4-1452	4-1600	370.	5.90	-9.7	92.5	20.6	2.6	2.32	0.337	1.040	0.689	131.3	46.7	174.9	395.7	7.62
4-1230	4-1346	4-1610	380.	14.15	-1.9	100.1	12.9	14.2	1.92	0.759	0.797	0.192	119.7	57.9	175.4	225.4	29.63
4-1230	4-1456	4-1610	380.	5.99	-8.0	95.5	20.5	3.5	2.01	0.345	1.036	0.678	123.0	56.6	173.4	400.9	8.21
4-1230	4-1356	4-1620	390.	11.72	-1.9	100.5	15.1	10.7	1.61	0.657	0.845	0.290	99.8	78.9	174.3	239.4	24.96
4-1230	4-1366	4-1630	400.	9.58	-1.6	99.3	17.1	7.5	1.55	0.554	0.899	0.401	78.4	100.6	173.9	255.8	20.28
4-1240	4-1386	4-1460	220.	7.10	0.5	83.1	19.3	0.2	1.96	0.418	0.982	0.571	45.5	134.0	179.8	287.6	13.32
4-1240	4-1393	4-1470	230.	6.61	1.8	79.6	19.8	-0.8	2.28	0.384	1.006	0.619	37.6	140.2	181.3	300.1	11.18
4-1240	4-1400	4-1480	240.	6.27	3.7	76.3	20.2	-1.6	2.74	0.358	1.026	0.659	30.4	145.8	182.9	313.0	9.28

ASYMPTOTE		VENUS PASSAGE						VENUS-EARTH HELIOCENTRIC TRANSFER								EARTH ASYMPTOTE		
DECL	R A	INCL	R C A	DECL	R A	VELE	PTHE	INCL	ECC	SMA	PERIH	LAN	APF	THETV	THETE	SPEED	DECL	R A
-4.1	355.2	170.50	7741.9	7.8	75.5	34.1	31.1	1.16	0.588	1.501	0.619	52.3	87.3	308.3	452.7	17.27	-20.0	228.4
-5.4	349.3	173.81	13530.6	-3.6	72.3	32.9	28.4	2.15	0.517	1.321	0.637	62.0	85.0	311.7	455.0	15.35	-24.1	236.9
-7.7	342.4	150.64	22700.8	-28.9	69.5	31.8	25.6	3.01	0.454	1.201	0.655	71.5	82.3	315.6	457.7	13.58	-28.0	245.5
-12.1	333.6	113.61	25157.9	-65.8	71.7	30.9	22.9	3.71	0.399	1.119	0.673	81.1	79.3	320.7	460.7	12.04	-31.5	254.3
51.3	274.5	70.14	7561.8	54.1	151.3	32.2	23.3	3.53	0.430	1.248	0.711	90.7	90.0	343.7	450.0	12.76	-31.6	271.8
4.7	194.2	139.18	55766.1	-40.2	277.6	28.9	23.0	1.22	0.393	0.974	0.591	109.7	61.0	69.8	119.0	11.69	-26.1	276.9
3.9	187.3	162.44	11797.4	-16.6	269.6	25.6	20.0	0.13	0.415	0.813	0.476	119.4	35.4	100.1	144.5	10.33	-23.7	268.6
-20.0	324.2	88.56	8175.8	47.5	322.1	26.9	2.6	9.50	0.181	0.861	0.705	328.0	191.7	331.2	528.3	5.55	29.7	267.3
61.2	280.8	87.54	22231.3	-20.0	275.4	27.1	3.8	14.26	0.175	0.871	0.719	148.0	18.5	355.3	521.5	7.71	-83.2	278.4
40.8	266.5	87.52	24284.2	-35.1	262.6	27.1	4.0	9.62	0.175	0.872	0.720	148.0	19.6	1.2	160.4	5.75	-74.8	287.9
-34.5	314.9	87.37	13346.3	38.7	311.0	27.0	1.0	9.92	0.174	0.861	0.711	337.7	184.9	337.2	535.1	5.58	33.0	266.2
-77.5	325.4	83.65	12787.8	5.5	294.6	27.0	1.6	23.68	0.172	0.864	0.715	337.7	187.6	344.3	532.4	11.90	42.4	265.0
22.5	244.6	90.89	16632.1	-46.9	245.9	27.1	2.1	7.94	0.171	0.865	0.717	157.7	10.2	14.3	169.8	4.82	-74.0	280.3
16.3	233.0	92.60	12252.7	-50.3	236.9	27.0	0.2	7.88	0.171	0.860	0.713	167.4	0.9	22.4	179.1	4.69	-75.7	265.7
12.8	224.6	93.07	9307.8	-52.2	229.3	27.1	-1.6	8.15	0.173	0.858	0.709	177.1	352.6	28.3	187.4	4.80	-76.0	250.5
10.4	217.9	92.99	7196.4	-53.4	222.5	27.1	-3.2	8.61	0.178	0.857	0.705	186.9	345.1	33.0	194.9	5.12	-74.7	241.5
-4.2	356.0	172.21	6874.2	5.7	75.6	34.5	31.5	1.32	0.603	1.566	0.621	52.3	88.5	309.3	451.5	17.64	-20.4	229.0
-5.5	350.0	173.25	11768.5	-4.6	72.1	33.2	28.7	2.24	0.530	1.360	0.640	62.0	86.3	312.8	453.7	15.66	-24.4	237.6
-7.7	343.1	153.41	19691.2	-26.1	69.0	32.0	26.0	3.04	0.464	1.227	0.657	71.5	83.6	316.7	456.4	13.85	-28.1	246.3
-11.8	334.2	119.75	24246.7	-59.7	69.0	31.1	23.3	3.69	0.407	1.136	0.674	81.1	80.6	321.8	459.4	12.26	-31.4	255.1
-25.0	318.7	91.03	15624.6	-80.4	132.2	30.5	21.0	4.02	0.363	1.088	0.693	90.7	78.7	330.0	461.3	11.03	-33.8	265.2
-35.2	312.2	86.94	10688.3	-74.9	145.7	30.9	21.5	3.89	0.376	1.119	0.697	90.7	81.4	332.9	458.6	11.41	-33.2	266.8
52.2	266.4	69.94	7135.3	53.5	144.2	32.7	23.9	3.43	0.453	1.308	0.715	90.7	92.8	347.9	447.2	13.27	-31.1	273.4
10.7	215.1	13.05	26791.4	9.0	133.0	32.0	23.3	2.58	0.426	1.231	0.707	100.2	88.7	22.3	91.3	12.68	-29.0	282.1
5.0	192.9	163.10	17189.5	-15.5	275.0	26.4	17.9	0.67	0.363	0.845	0.538	119.3	39.9	88.3	140.1	9.27	-25.2	272.5
4.2	187.3	166.06	8641.2	-12.5	267.5	24.0	13.7	0.24	0.409	0.756	0.447	308.8	201.6	109.1	158.4	8.44	-22.6	262.3
-16.9	326.7	89.86	6894.9	48.6	326.5	26.9	2.6	9.82	0.181	0.861	0.706	328.0	191.9	331.5	528.1	5.68	30.4	267.3
-25.0	318.7	89.58	10365.1	44.2	318.1	26.9	1.0	9.48	0.175	0.860	0.710	337.7	184.7	336.7	535.3	5.39	32.1	266.0
32.5	250.5	93.45	21138.7	-40.8	255.7	27.1	2.1	8.38	0.171	0.866	0.718	157.7	10.1	13.1	169.9	5.00	-75.3	280.3
21.1	236.1	95.21	15095.8	-48.0	243.9	27.0	0.2	7.70	0.171	0.860	0.713	167.4	0.9	22.9	179.1	4.62	-75.1	265.8
15.8	226.8	95.31	11350.8	-51.0	234.9	27.0	-1.6	7.74	0.174	0.857	0.708	177.1	352.5	29.3	187.5	4.63	-74.7	251.1
12.6	219.8	94.78	8737.5	-52.9	227.2	27.1	-3.2	8.06	0.178	0.857	0.704	186.9	345.1	34.0	194.9	4.90	-73.0	242.5
10.4	214.1	93.79	6741.9	-53.9	220.0	27.2	-4.6	8.63	0.183	0.857	0.700	196.8	338.7	37.2	201.3	5.33	-72.1	243.2
-1.9	16.1	87.06	8561.4	84.3	345.0	27.0	-41.2	4.78	0.672	0.844	0.277	206.7	322.8	237.6	577.2	19.87	-24.0	232.2
-4.3	356.6	173.33	6163.8	4.2	75.7	34.8	31.8	1.45	0.619	1.637	0.623	52.3	89.8	310.3	450.2	18.01	-20.7	229.6
-5.6	350.6	173.01	10455.0	-5.0	72.1	33.4	29.0	2.32	0.542	1.401	0.641	62.0	87.5	313.7	452.5	15.96	-24.6	238.2
-7.7	343.5	155.56	17645.7	-23.9	68.7	32.3	26.2	3.07	0.474	1.252	0.659	71.5	84.8	317.7	455.2	14.09	-28.1	246.9
-11.4	334.6	125.01	23425.8	-54.5	66.9	31.3	23.5	3.67	0.414	1.153	0.676	81.1	81.7	322.8	458.3	12.45	-31.3	255.7
-21.1	320.5	95.69	18591.1	-80.4	102.3	30.5	21.0	4.00	0.365	1.092	0.694	90.7	79.1	330.4	460.9	11.09	-33.7	265.5
-41.8	305.1	85.74	8622.7	-71.2	141.6	31.4	22.2	3.74	0.396	1.164	0.703	90.7	84.9	337.0	455.1	11.93	-32.6	268.9
52.7	258.1	69.57	6712.8	53.1	137.1	33.2	24.5	3.33	0.478	1.376	0.718	90.7	95.2	352.1	444.8	13.81	-30.7	274.8
18.9	227.6	28.71	26917.0	24.6	142.8	31.7	22.1	2.86	0.402	1.199	0.718	100.2	88.4	12.0	91.6	11.99	-30.0	282.0
8.0	204.1	157.95	186069.2	-20.0	288.4	29.3	20.6	1.75	0.353	1.003	0.649	109.7	67.2	53.0	112.8	10.61	-27.6	280.8
6.3	197.6	164.98	22930.6	-12.8	280.0	26.9	16.7	1.02	0.332	0.867	0.579	119.3	43.5	78.9	136.5	8.68	-26.4	275.6
5.3	192.8	166.17	12195.1	-11.8	273.1	25.0	12.3	0.35	0.351	0.789	0.512	128.8	24.9	97.7	155.1	7.40	-24.6	266.7
4.5	187.7	167.26	7928.3	-10.9	267.0	23.3	7.8	0.45	0.401	0.734	0.440	318.4	192.0	112.3	168.0	7.22	-21.4	256.1
-20.5	321.2	90.86	8667.8	46.3	322.4	26.9	1.0	9.58	0.175	0.861	0.710	337.7	184.7	336.8	535.3	5.43	32.3	266.1
-32.1	310.9	90.27	13865.7	39.7	311.3	27.0	-0.4	9.66	0.170	0.861	0.714	347.4	177.9	342.6	542.1	5.41	33.7	264.9
26.4	239.7	97.61	18523.3	-43.2	251.0	27.0	0.2	7.88	0.171	0.860	0.713	167.4	0.9	22.4	179.1	4.69	-75.7	265.7
19.8	228.9	97.53	13578.9	-48.9	240.4	27.0	-1.6	7.54	0.174	0.857	0.708	177.1	352.5	29.8	187.5	4.56	-74.0	251.4
15.3	221.6	96.49	10349.2	-51.8	231.7	27.1	-3.1	7.71	0.179	0.856	0.703	186.9	345.3	34.5	194.7	4.76	-72.0	244.0
12.4	215.7	95.26	8001.0	-53.5	224.0	27.2	-4.6	8.13	0.184	0.857	0.699	196.8	338.7	38.0	201.3	5.14	-70.6	243.8
-1.9	19.1	96.77	7612.9	81.6	73.0	27.0	-44.2	5.62	0.709	0.844	0.246	206.7	324.7	233.7	575.3	21.29	-24.4	233.2
10.3	210.7	93.86	6190.1	-54.3	216.8	27.4	-5.9	8.76	0.189	0.859	0.696	206.7	333.1	40.3	206.9	5.62	-70.2	247.9
-2.4	12.2	79.12	14033.9	78.2	304.9	27.3	-36.9	2.35	0.616	0.851	0.327	216.7	319.5	244.2	580.5	17.95	-23.7	241.3
-5.6	351.0	172.88	9500.5	-5.2	72.1	33.7	29.3	2.39	0.555	1.444	0.643	62.0	88.6	314.6	451.4	16.25	-24.8	238.8
-7.6	343.8	157.36	16140.6	-22.1	68.2	32.5	26.5	3.09	0.482	1.277	0.661	71.5	85.9	318.7	454.1	14.31	-28.2	247.5
-10.9	334.8	129.19	22857.7	-50.4	65.3	31.4	23.7	3.65	0.420	1.168	0.678	81.1	82.7	323.7	457.3	12.62	-31.2	256.3
-18.7	321.2	99.45	20843.4	-78.5	83.3	30.6	21.2	3.98	0.367	1.098	0.695	90.7	79.6	330.9	460.4	11.16	-33.6	265.8
-46.1	297.3	84.13	7511.4	-68.5	138.6	31.8	22.8	3.62	0.415	1.210	0.708	90.7	87.9	340.8	452.1	12.40	-32.0	270.6
22.9	228.5	39.85	26560.9	35.3	137.0	31.7	22.2	2.83	0.404	1.203	0.717	100.2	88.5	12.9	91.5	12.06	-29.9	282.0
10.1	207.9	151.40	237671.8	26.8	300.7	29.5	20.1	1.90	0.344	1.012	0.663	109.7	69.0	47.7	111.0	10.39	-28.1	281.9
7.8	201.5	167.81	27889.9	-8.4	284.4	27.2	16.1	1.25	0.314	0.882	0.605	119.3	46.0	72.1	134.0	8.35	-27.2	277.7
6.6	197.2	166.97	15467.3	-10.0	277.2	25.6	11.6	0.71	0.318	0.811	0.553	128.8	27.6	89.2	152.4	6.87	-26.0	270.1
5.7	193.1	167.04	10829.6	-10.5	272.3	24.3	7.2	0.13	0.345	0.766	0.502	138.5	14.1	101.8	165.9	6.24	-23.7	260.1
4.8	188.2	167.78	7913.3	-10.2	267.1	23.1	2.9	0.60	0.393	0.728	0.442	328.0	184.5	113.0	175.5	6.53	-20.0	250.4
-17.6	322.8	91.59	7550.4	47.5	325.1	27.0	1.0	9.76	0.174	0.861	0.710	337.7	184.8	337.0	535.2	5.51	32.7	266.1
-24.9	313.7	91.57	11400.8	43.8	315.9	27.0	-0.5	9.38	0.171	0.861	0.714	347.4	177.7	342.2	542.3	5.29	33.1	264.7
-47.6	296.6	90.02	19622.3	-29.6	296.6	27.2	-1.7	11.22	0.167	0.863	0.718	357.1	171.6	350.8	548.4	6.09	36.9	264.6
-68.5	289.4	89.03	18233.4	14.1	286.7	27.2	-1.5	16.90	0.166	0.863	0.719	357.1	172.5	355.8	547.5	8.71	41.7	266.4
25.6	231.4	99.68	16141.2	-45.1	246.0	27.0	-1.6	7.65	0.174	0.857	0.708	177.1	352.5	29.5	187.5	4.60	-74.4	251.3
18.7	223.3	98.28	12022.0	-49.9	236.1	27.1	-3.2	7.56	0.179	0.856	0.703	186.9	345.2	34.8	194.8	4.71	-71.5	244.2
14.7	217.1	96.68	9227.0	-52.5	227.6	27.2	-4.6	7.83	0.184	0.857	0.699	196.8	338.7	38.5	201.3	5.03	-69.5	244.1
-1.9	22.0	105.65	6590.2	73.6	94.3	27.0	-47.5	6.64	0.747	0.844	0.213	206.7	326.9	229.5	573.1	22.83	-24.9	234.3
12.0	212.1	94.98	7156.8	-53.9	220.0	27.4	-5.9	8.33	0.190	0.859	0.696	206.7	333.1	40.8	206.9	5.46	-68.8	248.2
-2.3	15.2	91.47	12560.6	85.4	33.9	27.3	-39.8	2.94	0.653	0.851	0.295	216.7	321.2	240.2	578.8	19.31	-24.2	242.1
-3.0	7.3	53.88	26611.6	53.6	283.5	27.5	-32.2	0.21	0.549	0.858	0.387	226.7	316.1	252.1	583.9	15.80	-22.6	250.7
-5.6	351.2	172.91	8792.8	-5.3	71.8	34.0	29.6	2.44	0.566	1.484	0.645	62.0	89.6	315.5	450.4	16.51	-24.9	239.3
-7.4	343.8	158.78	15138.4	-20.7	67.5	32.7	26.7	3.11	0.490	1.300	0.663	71.5	86.8	319.6	453.2	14.50	-28.2	248.0
-10.5	334.7	132.30	22584.8	-47.3	64.2	31.6	23.9	3.63	0.426	1.182	0.679	81.1	83.6	324.6	456.4	12.77	-31.2	256.8

MARS DEPART	VENUS PASS	EARTH ARRIVE	TRIP TIME	MARS ASYMPTOTE SPEED	DECL	R A	VELM	PTHM	MARS-VENUS HELIOCENTRIC TRANSFER INCL	ECC	SMA	PERIH	LAN	APF	THETM	THETV	VENUS SPEED
4-1240	4-1408	4-1490	250.	6.05	7.2	73.3	20.6	-2.3	3.58	0.337	1.043	0.691	22.5	152.2	184.5	327.8	7.54
4-1240	4-1422	4-1490	250.	6.53	24.6	72.0	20.9	-2.5	8.78	0.320	1.057	0.718	8.4	165.2	185.4	351.9	7.54
4-1240	4-1446	4-1500	260.	6.02	-15.3	78.3	20.7	-0.7	3.53	0.329	1.048	0.703	155.5	22.2	181.5	386.9	7.08
4-1240	4-1459	4-1510	270.	5.99	-7.8	86.3	20.4	1.5	1.80	0.347	1.034	0.675	127.3	54.7	177.2	402.7	8.46
4-1240	4-1465	4-1520	280.	6.13	-5.8	91.4	20.2	3.0	1.53	0.360	1.026	0.656	110.7	73.8	174.7	409.9	9.42
4-1240	4-1470	4-1530	290.	6.30	-4.5	95.5	20.1	4.3	1.44	0.372	1.020	0.641	98.2	88.4	172.7	415.4	10.24
4-1240	4-1474	4-1540	300.	6.53	-3.4	99.6	20.0	5.7	1.42	0.385	1.014	0.623	86.8	101.7	170.7	420.6	11.09
4-1240	4-1480	4-1550	310.	6.90	-2.3	104.5	19.8	7.7	1.47	0.403	1.006	0.600	74.9	115.9	168.4	426.7	12.21
4-1240	4-1487	4-1560	320.	6.08	6.4	73.8	20.5	-2.2	3.39	0.340	1.040	0.686	23.9	151.0	184.2	325.1	7.81
4-1240	4-1487	4-1560	320.	7.60	-1.1	111.5	19.6	10.9	1.61	0.434	0.996	0.564	61.3	132.7	165.1	435.1	13.93
4-1240	4-1411	4-1570	330.	6.02	9.1	72.6	20.7	-2.4	4.07	0.332	1.047	0.700	19.6	154.7	184.9	333.2	7.08
4-1240	4-1417	4-1580	340.	6.07	14.0	71.7	20.8	-2.6	5.44	0.325	1.053	0.711	14.3	159.4	185.4	342.6	6.67
4-1240	4-1441	4-1580	340.	6.30	-21.8	76.1	20.8	-1.4	5.48	0.324	1.052	0.711	164.2	12.1	182.9	380.3	7.21
4-1240	4-1448	4-1590	350.	5.99	-14.2	79.0	20.7	-0.6	3.24	0.330	1.047	0.701	153.2	24.9	181.2	388.5	7.15
4-1240	4-1452	4-1600	360.	5.94	-11.0	81.7	20.6	0.2	2.43	0.336	1.042	0.691	143.5	36.1	179.7	394.4	7.57
4-1240	4-1456	4-1610	370.	5.96	-8.9	84.5	20.5	1.0	1.98	0.343	1.037	0.681	133.5	47.5	178.2	399.7	8.11
4-1240	4-1365	4-1630	390.	10.10	-1.6	92.2	16.3	4.6	1.43	0.588	0.879	0.362	82.2	100.2	176.8	249.8	21.85
4-1240	4-1377	4-1640	400.	8.11	-0.8	87.8	18.2	1.9	1.65	0.481	0.941	0.489	58.7	122.6	178.0	270.6	16.72
4-1250	4-1387	4-1460	210.	7.34	0.6	72.7	19.2	-3.1	2.02	0.421	0.986	0.571	44.9	136.2	184.3	287.6	13.41
4-1250	4-1394	4-1470	220.	6.91	1.8	68.9	19.8	-4.0	2.34	0.388	1.011	0.619	38.6	140.5	186.3	300.2	11.25
4-1250	4-1401	4-1480	230.	6.62	3.5	65.4	20.3	-4.6	2.78	0.362	1.033	0.660	32.9	144.3	188.2	313.5	9.29
4-1250	4-1409	4-1490	240.	6.45	6.1	62.5	20.6	-5.1	3.48	0.342	1.050	0.691	27.0	148.4	190.0	327.8	7.58
4-1250	4-1426	4-1490	240.	6.98	24.4	61.6	20.9	-5.2	9.37	0.324	1.065	0.720	13.2	161.1	191.0	357.7	7.60
4-1250	4-1449	4-1500	250.	6.34	-15.7	68.5	20.6	-3.1	3.68	0.334	1.051	0.700	165.1	14.2	186.2	389.1	7.48
4-1250	4-1459	4-1510	260.	6.14	-8.8	74.8	20.4	-1.3	1.83	0.347	1.038	0.678	140.9	42.1	182.4	401.1	8.36
4-1250	4-1464	4-1520	270.	6.16	-6.5	79.5	20.2	0.0	1.43	0.357	1.030	0.662	121.6	63.9	180.0	407.9	9.19
4-1250	4-1469	4-1530	280.	6.22	-5.2	83.1	20.1	1.1	1.31	0.366	1.024	0.649	107.0	80.4	178.1	412.7	9.86
4-1250	4-1472	4-1540	290.	6.30	-4.2	86.8	19.9	2.2	1.28	0.375	1.018	0.636	94.8	94.4	176.3	416.7	10.47
4-1250	4-1477	4-1550	300.	6.46	-3.1	91.4	19.8	3.7	1.32	0.387	1.011	0.620	81.7	109.6	174.1	421.7	11.28
4-1250	4-1407	4-1560	310.	6.48	5.4	63.1	20.5	-5.0	3.29	0.346	1.047	0.685	28.3	147.4	189.6	324.6	7.92
4-1250	4-1482	4-1560	310.	6.76	-2.0	97.3	19.6	5.8	1.44	0.406	1.002	0.596	68.6	125.4	171.4	428.0	12.41
4-1250	4-1411	4-1570	320.	6.42	7.3	61.8	20.7	-5.2	3.82	0.337	1.054	0.699	25.0	149.9	190.4	332.7	7.12
4-1250	4-1490	4-1570	320.	7.40	-0.7	105.7	19.3	9.3	1.67	0.437	0.990	0.557	55.5	142.3	167.6	436.7	14.19
4-1250	4-1416	4-1580	330.	6.41	10.3	61.0	20.8	-5.3	4.68	0.330	1.060	0.710	21.3	153.1	191.0	341.4	6.55
4-1250	4-1424	4-1590	340.	6.65	18.8	61.1	20.9	-5.3	7.36	0.325	1.065	0.719	15.4	158.8	191.2	353.7	6.80
4-1250	4-1433	4-1590	340.	15.09	51.1	72.5	20.9	-4.7	35.73	0.324	1.064	0.720	7.2	167.8	190.0	366.6	23.05
4-1250	4-1447	4-1590	340.	6.46	-18.2	67.5	20.7	-3.4	4.48	0.332	1.053	0.703	168.8	9.8	186.9	386.5	7.50
4-1250	4-1452	4-1600	350.	6.23	-12.7	70.4	20.5	-2.5	2.80	0.338	1.047	0.693	158.2	22.3	185.0	393.2	7.66
4-1250	4-1456	4-1610	360.	6.15	-9.8	73.3	20.4	-1.7	2.07	0.344	1.041	0.683	147.0	35.1	183.3	398.6	8.10
4-1250	4-1461	4-1620	370.	6.14	-7.8	76.5	20.3	-0.8	1.64	0.351	1.035	0.672	134.1	49.8	181.5	403.7	8.65
4-1250	4-1375	4-1640	390.	8.71	-0.9	79.8	17.6	-1.4	1.55	0.510	0.926	0.453	61.2	123.0	181.3	264.5	18.20
4-1250	4-1393	4-1650	400.	6.95	1.7	69.2	19.8	-3.9	2.31	0.390	1.009	0.615	39.1	140.2	186.1	299.1	11.43
4-1260	4-1388	4-1460	200.	7.84	0.7	62.1	19.3	-7.0	2.07	0.426	0.996	0.571	44.7	137.3	189.6	288.2	13.51
4-1260	4-1395	4-1470	210.	7.48	1.7	58.1	19.9	-7.6	2.40	0.393	1.023	0.621	39.7	139.9	192.0	301.1	11.30
4-1260	4-1402	4-1480	220.	7.24	3.1	54.8	20.4	-8.0	2.82	0.368	1.046	0.661	35.3	142.0	194.3	314.6	9.31
4-1260	4-1409	4-1490	230.	7.10	5.2	52.1	20.7	-8.4	3.45	0.349	1.064	0.693	30.8	144.6	196.3	329.3	7.54
4-1260	4-1451	4-1500	240.	6.84	-15.7	59.3	20.6	-5.7	3.88	0.342	1.057	0.695	174.7	5.9	191.1	391.7	7.98
4-1260	4-1459	4-1510	250.	6.53	-9.2	64.3	20.3	-4.1	1.86	0.352	1.045	0.677	154.2	29.8	187.7	401.2	8.54
4-1260	4-1464	4-1520	260.	6.44	-6.9	68.3	20.2	-2.9	1.34	0.360	1.036	0.664	134.2	52.1	185.3	407.1	9.20
4-1260	4-1468	4-1530	270.	6.42	-5.6	71.5	20.0	-2.0	1.18	0.366	1.030	0.653	117.1	71.0	183.4	411.2	9.73
4-1260	4-1472	4-1540	280.	6.42	-4.6	74.7	19.9	-1.0	1.13	0.373	1.024	0.642	101.8	88.0	181.7	415.0	10.26
4-1260	4-1476	4-1550	290.	6.46	-3.5	78.7	19.8	0.2	1.17	0.382	1.017	0.628	86.5	105.5	179.7	419.3	10.93
4-1260	4-1480	4-1560	300.	6.55	-2.5	83.8	19.6	1.8	1.29	0.395	1.009	0.611	72.8	121.6	177.2	424.2	11.74
4-1260	4-1411	4-1570	310.	7.08	5.9	51.6	20.8	-8.4	3.66	0.345	1.068	0.699	29.6	145.3	196.6	333.0	7.18
4-1260	4-1486	4-1570	310.	6.79	-1.3	90.9	19.3	4.3	1.50	0.414	0.998	0.585	60.4	137.3	173.9	430.7	12.93
4-1260	4-1416	4-1580	320.	7.05	7.9	50.9	20.9	-8.4	4.29	0.339	1.074	0.710	26.9	147.5	197.2	341.5	6.53
4-1260	4-1495	4-1580	320.	7.44	0.0	101.4	19.0	8.5	1.86	0.450	0.983	0.541	49.2	153.1	169.4	440.2	14.91
4-1260	4-1422	4-1590	330.	7.08	11.8	50.8	21.0	-8.4	5.57	0.334	1.078	0.718	23.3	150.8	197.5	351.6	6.26
4-1260	4-1451	4-1600	340.	6.83	-15.5	59.4	20.6	-5.6	3.81	0.342	1.057	0.695	174.3	6.3	191.0	391.9	7.98
4-1260	4-1456	4-1610	350.	6.61	-11.0	62.2	20.4	-4.7	2.38	0.348	1.050	0.685	163.2	19.4	189.0	397.8	8.24
4-1260	4-1461	4-1620	360.	6.50	-8.5	65.3	20.3	-3.8	1.68	0.354	1.042	0.674	149.4	35.2	187.0	402.8	8.71
4-1260	4-1373	4-1640	380.	9.54	-1.0	71.4	17.1	-5.7	1.44	0.543	0.915	0.418	63.5	123.3	184.9	258.9	19.73
4-1260	4-1389	4-1650	390.	7.77	0.8	61.4	19.4	-7.1	2.13	0.420	1.001	0.580	43.8	137.8	190.0	290.3	13.12
4-1260	4-1418	4-1660	400.	7.05	8.9	50.8	20.9	-8.4	4.62	0.337	1.075	0.713	25.8	148.4	197.4	344.8	6.37
4-1270	4-1395	4-1470	200.	8.35	1.6	47.9	20.1	-11.7	2.45	0.402	1.044	0.625	41.0	138.1	198.6	302.8	11.35
4-1270	4-1402	4-1480	210.	8.15	2.7	44.9	20.6	-11.9	2.85	0.377	1.068	0.665	37.6	138.9	201.2	316.6	9.31
4-1270	4-1410	4-1490	220.	8.02	4.3	42.7	21.0	-12.0	3.41	0.360	1.087	0.696	34.2	140.2	203.3	331.3	7.53
4-1270	4-1454	4-1500	230.	7.53	-15.1	51.0	20.6	-8.5	4.07	0.354	1.067	0.689	183.9	357.6	196.2	394.9	8.61
4-1270	4-1460	4-1510	240.	7.13	-9.2	55.0	20.3	-7.1	1.94	0.360	1.054	0.674	167.6	17.1	193.0	402.3	8.91
4-1270	4-1465	4-1520	250.	6.96	-6.9	58.4	20.2	-6.0	1.26	0.366	1.045	0.662	147.5	39.6	190.6	407.5	9.44
4-1270	4-1469	4-1530	260.	6.87	-5.6	61.2	20.0	-5.1	1.03	0.372	1.038	0.652	127.3	61.7	188.7	411.2	9.89
4-1270	4-1472	4-1540	270.	6.81	-4.6	64.0	19.9	-4.2	0.97	0.377	1.031	0.642	108.0	82.7	187.0	414.6	10.34
4-1270	4-1475	4-1550	280.	6.76	-3.7	67.4	19.7	-3.1	1.02	0.384	1.024	0.631	89.4	103.2	185.0	418.3	10.88
4-1270	4-1480	4-1560	290.	6.74	-2.7	71.9	19.5	-1.7	1.17	0.394	1.015	0.615	73.7	121.4	182.6	422.7	11.58
4-1270	4-1412	4-1570	300.	8.00	4.7	42.4	21.0	-12.0	3.55	0.358	1.090	0.700	33.6	140.5	203.6	334.1	7.26
4-1270	4-1485	4-1570	300.	6.77	-1.7	77.8	19.3	0.3	1.39	0.407	1.005	0.596	62.0	136.1	179.6	428.0	12.46
4-1270	4-1416	4-1580	310.	7.96	6.1	41.8	21.1	-12.0	4.05	0.351	1.096	0.711	31.5	142.0	204.2	342.6	6.58
4-1270	4-1492	4-1580	310.	6.98	-0.5	86.4	19.0	3.3	1.71	0.429	0.991	0.566	52.4	149.7	175.6	435.1	13.81
4-1270	4-1422	4-1590	320.	7.93	8.5	41.7	21.2	-11.8	4.92	0.347	1.099	0.718	29.1	144.2	204.4	352.1	6.19
4-1270	4-1502	4-1590	320.	7.67	0.9	99.1	18.5	8.5	2.16	0.471	0.973	0.514	44.4	163.1	170.3	445.2	16.07

ASYMPTOTE		VENUS PASSAGE						VENUS-EARTH HELIOCENTRIC TRANSFER								EARTH ASYMPTOTE	
DECL	R A	INCL	R C A	DECL	R A	VELE	PTHE	INCL	ECC	SMA	PERIH	LAN	APF	THETV	THETE	SPEED	DECL	R A
-16.9	321.2	102.21	22711.9	-76.5	73.5	30.7	21.3	3.94	0.371	1.105	0.696	90.7	80.3	331.6	459.7	11.25	-33.5	266.2
-49.2	287.9	81.82	6716.9	-66.1	136.4	32.3	23.4	3.51	0.435	1.261	0.712	90.7	90.6	344.6	449.4	12.87	-31.5	272.2
25.6	226.9	49.10	24743.5	44.1	128.4	31.8	22.5	2.76	0.411	1.214	0.715	100.2	88.8	15.6	91.2	12.25	-29.6	282.2
12.4	210.4	124.86	142187.5	53.1	313.4	29.5	19.9	1.97	0.340	1.015	0.670	109.7	69.8	45.1	110.2	10.26	-28.3	282.3
9.5	204.4	169.82	31263.7	-2.5	287.6	27.4	15.7	1.40	0.303	0.891	0.621	119.3	47.7	67.6	132.3	8.16	-27.7	279.0
8.0	200.4	168.25	17736.0	-7.3	280.8	25.9	11.3	0.92	0.301	0.824	0.576	128.8	29.4	83.7	150.6	6.61	-27.0	272.4
6.9	196.9	167.49	13033.7	-9.1	276.0	24.9	7.0	0.46	0.315	0.784	0.537	138.4	15.7	94.9	164.2	5.77	-25.3	263.1
6.0	193.0	167.37	10323.5	-9.9	271.6	24.1	2.9	0.07	0.343	0.756	0.497	328.0	185.7	103.9	174.4	5.63	-22.2	253.2
-15.4	323.9	91.99	6701.1	48.2	326.7	27.0	1.0	9.99	0.174	0.861	0.711	337.7	184.9	337.3	535.1	5.60	33.1	266.2
5.0	188.1	168.21	7990.2	-9.6	267.1	23.1	-1.1	0.81	0.391	0.726	0.442	337.7	178.2	113.3	181.8	6.38	-18.6	245.8
-20.8	315.1	92.20	9882.4	45.8	318.2	27.0	-0.5	9.38	0.171	0.861	0.714	347.4	177.7	342.2	542.3	5.29	33.1	264.7
-30.9	302.6	91.50	15629.0	40.5	304.7	27.2	-1.8	9.40	0.168	0.862	0.717	357.1	171.0	348.0	549.0	5.30	33.6	263.4
37.8	235.4	100.65	19202.4	-36.4	251.7	27.1	-1.5	8.77	0.173	0.858	0.710	177.1	352.6	27.0	187.4	5.05	-77.6	249.4
23.6	225.0	99.83	13760.2	-46.8	239.9	27.1	-3.1	7.69	0.179	0.856	0.703	186.9	345.3	34.5	194.7	4.76	-72.0	244.0
17.6	218.4	98.08	10432.1	-50.9	231.0	27.2	-4.6	7.71	0.185	0.857	0.698	196.8	338.7	38.7	201.3	4.99	-69.1	244.3
14.0	213.2	96.00	7997.0	-53.1	222.7	27.3	-5.9	8.12	0.190	0.858	0.695	206.7	333.1	41.1	206.9	5.39	-68.1	248.3
-2.8	10.1	70.59	26379.4	70.0	293.3	27.5	-34.8	0.57	0.585	0.858	0.356	226.7	317.4	248.2	582.6	17.03	-23.1	251.3
-4.0	0.1	4.11	32071.5	0.9	271.9	27.7	-26.7	1.57	0.468	0.866	0.461	56.8	132.5	262.6	587.5	13.27	-20.2	260.0
-5.5	351.2	172.97	8314.6	-5.3	71.5	34.2	29.8	2.49	0.576	1.525	0.646	62.0	90.5	316.2	449.5	16.75	-25.1	239.8
-7.2	343.7	159.87	14540.8	-19.6	67.1	32.8	26.9	3.12	0.498	1.322	0.664	71.5	87.6	320.2	452.4	14.69	-28.3	248.5
-10.0	334.2	134.22	22789.1	-45.4	63.0	31.7	24.1	3.62	0.430	1.195	0.680	81.1	84.4	325.3	455.6	12.90	-31.1	257.3
-15.3	321.0	103.86	24576.1	-75.3	66.6	30.8	21.4	3.93	0.373	1.111	0.696	90.7	80.7	332.0	459.2	11.33	-33.4	266.4
-50.9	276.6	78.66	6133.9	-63.8	134.9	32.7	24.0	3.41	0.457	1.318	0.716	90.7	93.1	348.5	446.9	13.35	-31.1	273.6
27.3	224.0	57.03	22508.0	51.4	117.8	31.9	22.9	2.66	0.419	1.223	0.711	100.2	88.8	19.4	91.2	12.47	-29.3	282.1
14.6	211.8	117.89	87834.7	59.4	320.5	29.5	19.8	1.99	0.339	1.016	0.672	109.7	70.0	44.4	110.0	10.23	-28.4	282.5
11.1	206.0	168.68	31311.6	3.6	290.4	27.4	15.6	1.45	0.300	0.894	0.626	119.3	48.2	65.9	131.7	8.10	-27.9	279.5
9.3	202.3	169.21	18724.6	-4.0	283.0	26.0	11.2	1.03	0.293	0.830	0.587	128.8	30.3	81.0	149.7	6.50	-27.4	273.4
8.1	199.4	168.27	14317.8	-6.9	278.5	25.2	6.9	0.65	0.300	0.794	0.556	138.4	16.7	90.8	163.3	5.54	-26.3	264.7
7.0	196.1	167.68	11826.3	-8.7	274.7	24.5	3.0	0.21	0.319	0.770	0.525	148.0	6.4	98.6	173.5	5.22	-23.7	255.1
-13.8	324.3	92.06	6078.7	48.8	327.2	27.0	1.1	10.20	0.174	0.861	0.711	337.7	185.0	337.5	535.0	5.70	33.5	266.3
6.0	192.2	167.73	9914.2	-9.4	270.9	23.9	-0.7	0.34	0.348	0.749	0.488	337.7	178.6	105.8	181.4	5.57	-20.3	247.1
-18.0	315.6	92.38	8797.8	47.0	318.9	27.0	-0.5	9.49	0.170	0.861	0.714	347.4	177.8	342.3	542.2	5.33	33.3	264.8
5.0	187.3	168.82	7935.6	-9.0	266.5	23.2	-4.6	1.10	0.398	0.724	0.436	347.4	173.0	114.1	187.0	6.67	-17.4	244.0
-24.8	304.0	91.95	13330.0	43.9	306.8	27.2	-1.8	9.16	0.168	0.862	0.717	357.1	171.0	347.6	549.0	5.19	33.1	263.2
-41.7	284.0	90.18	20948.3	33.8	284.3	27.3	-3.0	10.41	0.167	0.864	0.720	6.9	165.0	355.9	555.0	5.81	34.8	263.2
-84.5	115.8	93.63	9420.8	-7.9	261.9	27.3	-2.6	37.61	0.167	0.864	0.720	6.9	166.7	8.0	193.3	18.54	40.3	270.9
32.1	226.9	100.89	15635.3	-40.7	243.3	27.1	-3.2	8.46	0.178	0.857	0.705	186.9	345.1	33.3	194.9	5.06	-74.2	241.8
21.6	219.5	99.08	11445.5	-48.2	233.4	27.2	-4.6	7.91	0.184	0.857	0.699	196.8	338.7	38.3	201.3	5.06	-69.8	244.1
16.5	214.1	96.89	8686.3	-51.7	225.0	27.3	-5.9	8.12	0.190	0.858	0.695	206.7	333.1	41.1	206.9	5.39	-68.1	248.3
13.1	209.5	94.88	6708.2	-53.4	217.3	27.5	-7.0	8.61	0.196	0.861	0.693	216.7	328.3	42.7	211.7	5.86	-67.3	256.0
-3.7	3.1	7.01	36111.2	5.9	274.9	27.7	-29.1	1.36	0.502	0.865	0.431	56.8	133.5	258.4	586.5	14.40	-20.9	260.3
-7.0	344.4	26.22	23700.4	-25.8	257.3	28.0	-18.8	2.90	0.344	0.875	0.574	66.9	129.3	282.3	590.7	9.61	-15.4	269.8
-5.4	350.9	173.04	8048.5	-5.2	70.9	34.4	30.0	2.53	0.586	1.564	0.648	62.0	91.3	316.9	448.7	16.96	-25.2	240.2
-7.0	343.1	160.44	14439.4	-19.1	66.3	33.0	27.1	3.13	0.505	1.342	0.665	71.5	88.4	320.8	451.6	14.85	-28.3	248.9
-9.6	333.3	134.82	23581.8	-44.9	61.5	31.8	24.2	3.61	0.434	1.205	0.681	81.1	85.0	325.9	455.0	13.00	-31.1	257.6
-14.2	319.3	102.58	26705.7	-76.7	65.8	30.8	21.5	3.90	0.376	1.117	0.697	90.7	81.3	332.8	458.7	11.40	-33.3	266.8
28.6	220.7	63.37	19637.3	56.9	106.8	32.0	23.4	2.55	0.428	1.234	0.705	100.2	88.7	23.3	91.3	12.75	-28.9	282.0
16.4	211.6	117.79	60094.4	58.7	322.7	29.5	19.9	1.95	0.341	1.014	0.668	109.7	69.6	45.9	110.4	10.30	-28.3	282.2
12.4	206.6	165.17	29277.3	9.3	291.9	27.4	15.6	1.45	0.300	0.894	0.626	119.3	48.2	65.9	131.7	8.10	-27.9	279.5
10.5	203.4	169.30	18600.2	-0.5	284.2	26.1	11.1	1.06	0.290	0.832	0.591	128.8	30.6	80.0	149.4	6.46	-27.6	273.8
9.1	200.7	168.94	14559.7	-4.5	279.7	25.3	6.9	0.71	0.295	0.798	0.562	138.4	17.1	89.4	162.9	5.47	-26.6	265.4
7.9	197.7	168.30	12348.8	-7.0	276.2	24.7	3.0	0.32	0.309	0.775	0.536	148.0	6.8	96.4	173.2	5.07	-24.4	256.0
6.8	194.6	167.95	10850.1	-8.5	273.0	24.3	-0.5	0.13	0.330	0.760	0.509	337.7	178.9	102.0	181.1	5.24	-21.3	248.0
-15.9	315.1	92.11	7998.4	47.9	318.0	27.0	-0.4	9.61	0.170	0.861	0.714	347.4	177.8	342.5	542.2	5.39	33.6	264.9
5.7	190.6	168.34	9384.4	-9.0	269.6	23.8	-4.0	0.72	0.362	0.743	0.474	347.4	172.9	108.2	187.1	5.97	-18.4	244.3
-21.0	303.7	91.69	11758.8	45.9	306.1	27.2	-1.8	9.16	0.168	0.862	0.717	357.1	171.0	347.6	549.0	5.19	33.1	263.2
4.7	185.4	169.94	7523.4	-8.0	265.2	23.0	-7.9	1.54	0.419	0.718	0.417	357.1	168.8	116.5	191.2	7.37	-16.6	244.8
-30.2	287.4	90.04	17504.3	41.1	287.4	27.3	-3.0	9.37	0.168	0.864	0.719	6.9	164.7	354.0	555.3	5.36	32.7	262.3
28.2	220.5	99.50	12270.0	-43.5	234.8	27.2	-4.6	8.63	0.183	0.857	0.700	196.8	338.7	37.2	201.3	5.33	-72.1	243.2
19.7	214.8	97.45	9111.5	-49.4	226.2	27.4	-5.9	8.41	0.190	0.859	0.696	206.7	333.1	40.7	206.9	5.49	-69.1	248.1
15.1	210.2	95.43	6980.7	-52.2	218.7	27.5	-7.0	8.75	0.195	0.861	0.693	216.7	328.3	42.6	211.7	5.91	-67.8	256.0
-3.4	5.8	12.47	39401.0	11.9	277.1	27.7	-31.6	1.12	0.538	0.865	0.400	56.8	134.7	254.2	585.3	15.60	-21.5	260.8
-5.7	349.7	23.86	22886.4	-23.5	262.1	28.0	-21.4	2.79	0.384	0.874	0.539	66.9	129.6	275.5	590.4	10.84	-16.7	269.6
-23.5	298.8	36.31	14007.4	-33.5	219.5	28.3	-12.4	3.40	0.240	0.889	0.676	77.0	128.8	313.2	591.2	6.63	-8.7	281.0
-6.8	341.9	160.37	14937.3	-19.2	65.4	33.1	27.3	3.14	0.511	1.361	0.666	71.5	89.0	321.4	451.0	14.99	-28.3	249.3
-9.1	331.6	133.10	25544.2	-46.6	60.5	31.9	24.3	3.60	0.438	1.215	0.683	81.1	85.5	326.5	454.5	13.09	-31.0	257.9
-13.2	316.8	98.24	29094.6	-80.9	70.5	30.9	21.6	3.87	0.378	1.123	0.698	90.7	81.8	333.3	458.2	11.47	-33.2	267.1
29.0	217.0	68.35	17026.0	61.0	95.4	32.1	24.0	2.44	0.440	1.245	0.698	100.2	88.4	27.8	91.6	13.09	-28.5	281.8
17.7	210.5	118.60	43828.0	57.8	320.4	29.4	20.2	1.88	0.346	1.011	0.662	109.7	68.8	48.5	111.2	10.42	-28.0	281.7
13.4	206.2	161.91	25753.7	13.5	292.1	27.4	15.8	1.40	0.304	0.891	0.620	119.3	47.6	67.8	132.4	8.17	-27.7	279.0
11.3	203.4	168.69	17329.3	2.4	284.4	26.0	11.2	1.02	0.293	0.829	0.586	128.8	30.2	81.2	149.8	6.51	-27.4	273.4
9.8	200.9	169.35	13939.9	-2.3	280.1	25.2	6.9	0.69	0.297	0.796	0.560	138.4	16.9	89.9	163.1	5.49	-26.5	265.1
8.5	198.4	168.95	12148.2	-5.3	276.8	24.7	3.0	0.33	0.308	0.776	0.537	148.0	6.9	96.1	173.1	5.05	-24.5	256.1
7.3	195.5	168.53	10894.7	-7.3	273.9	24.3	-0.5	0.08	0.326	0.762	0.514	337.7	179.0	101.1	181.0	5.17	-21.5	248.3
-14.3	313.5	91.39	7345.4	48.6	315.4	27.0	-0.4	9.77	0.170	0.861	0.714	347.4	177.9	342.7	542.1	5.46	33.9	265.0
6.3	192.3	168.51	9872.6	-8.3	271.0	24.0	-3.8	0.57	0.349	0.750	0.488	347.4	172.9	105.8	187.1	5.72	-18.9	244.5
-18.2	301.9	90.88	10498.6	47.2	303.2	27.2	-1.8	9.25	0.168	0.862	0.717	357.1	171.0	347.8	549.0	5.23	33.3	263.3
5.2	188.2	169.42	8612.6	-8.2	267.9	23.6	-7.2	1.22	0.387	0.734	0.450	357.1	168.3	111.7	191.7	6.73	-17.0	244.4
-24.5	286.2	89.16	14826.2	44.1	285.0	27.3	-3.0	9.23	0.168	0.864	0.719	6.9	164.7	353.7	555.3	5.30	32.4	262.2
4.3	182.7	171.52	6871.5	-6.5	263.2	22.8	-11.2	2.09	0.451	0.708	0.388	6.9	165.7	120.1	194.3	8.45	-16.3	248.1

MARS DEPART	VENUS PASS	EARTH ARRIVE	TRIP TIME	MARS SPEED	ASYMPTOTE DECL	R A	VELM	PTHM	MARS-VENUS INCL	ECC	HELIOCENTRIC SMA	PERIH	TRANSFER LAN	APF	THETM	THETV	VENUS SPEED
4-1270	4-1431	4-1600	330.	8.08	16.1	43.1	21.1	-11.3	7.82	0.344	1.097	0.720	24.8	149.4	203.5	365.6	6.94
4-1270	4-1449	4-1600	330.	8.28	-24.5	49.6	20.7	-9.3	8.15	0.350	1.075	0.699	190.9	348.6	198.2	389.4	9.65
4-1270	4-1456	4-1610	340.	7.37	-12.9	52.1	20.5	-8.1	3.23	0.355	1.063	0.685	180.2	2.2	195.3	397.0	8.59
4-1270	4-1466	4-1620	350.	7.13	-9.2	55.0	20.3	-7.1	1.94	0.360	1.054	0.674	167.6	17.1	193.0	402.3	8.91
4-1270	4-1371	4-1640	370.	10.70	-1.1	62.9	16.7	-11.6	1.30	0.579	0.909	0.383	65.9	123.2	188.7	253.8	21.39
4-1270	4-1386	4-1650	380.	8.84	0.4	53.2	19.2	-11.3	2.00	0.450	1.001	0.550	46.8	136.4	194.6	284.1	14.62
4-1270	4-1418	4-1660	390.	7.94	6.7	41.8	21.1	-11.9	4.24	0.350	1.097	0.713	30.9	142.5	204.2	345.0	6.43
4-1270	4-1425	4-1670	400.	7.94	10.1	41.9	21.2	-11.7	5.51	0.346	1.100	0.720	27.8	145.6	204.3	356.4	6.21
4-1280	4-1403	4-1480	200.	9.36	2.4	36.1	21.1	-16.2	2.88	0.393	1.104	0.670	39.8	134.9	209.0	319.5	9.32
4-1280	4-1411	4-1490	210.	9.23	3.7	34.3	21.4	-16.1	3.40	0.377	1.124	0.700	37.3	135.2	211.2	334.5	7.52
4-1280	4-1456	4-1500	220.	8.37	-14.6	43.9	20.7	-11.6	4.37	0.369	1.081	0.682	193.2	349.2	201.4	398.1	9.34
4-1280	4-1462	4-1510	230.	7.92	-8.9	46.9	20.4	-10.3	2.01	0.374	1.067	0.668	180.3	5.1	198.4	404.3	9.47
4-1280	4-1466	4-1520	240.	7.69	-6.6	49.9	20.2	-9.2	1.18	0.378	1.056	0.657	161.1	26.8	195.8	408.9	9.88
4-1280	4-1470	4-1530	250.	7.54	-5.3	52.4	20.0	-8.3	0.87	0.382	1.048	0.648	137.2	52.6	193.9	412.3	10.28
4-1280	4-1473	4-1540	260.	7.42	-4.4	54.8	19.9	-7.5	0.80	0.386	1.041	0.639	111.8	79.7	192.2	415.3	10.66
4-1280	4-1476	4-1550	270.	7.31	-3.5	57.8	19.7	-6.4	0.88	0.392	1.033	0.628	88.4	105.2	190.2	418.7	11.14
4-1280	4-1480	4-1560	280.	7.20	-2.6	61.6	19.5	-5.1	1.07	0.399	1.023	0.615	71.9	124.0	187.8	422.5	11.71
4-1280	4-1412	4-1570	290.	9.22	3.8	34.2	21.4	-16.1	3.47	0.376	1.125	0.702	37.0	135.4	211.3	336.2	7.36
4-1280	4-1485	4-1570	290.	7.11	-1.6	66.6	19.3	-3.4	1.33	0.409	1.012	0.598	60.8	138.1	184.9	427.2	12.46
4-1280	4-1417	4-1580	300.	9.14	4.9	33.9	21.5	-15.9	3.90	0.370	1.130	0.712	35.6	136.4	211.8	344.5	6.68
4-1280	4-1491	4-1580	300.	7.09	-0.6	73.7	18.9	-0.9	1.64	0.425	0.999	0.574	52.9	149.6	181.3	433.1	13.50
4-1280	4-1422	4-1590	310.	9.09	6.5	33.8	21.5	-15.7	4.57	0.366	1.133	0.719	33.8	138.0	211.9	354.1	6.28
4-1280	4-1498	4-1590	310.	7.26	0.5	83.7	18.6	2.7	2.01	0.450	0.983	0.540	47.1	159.9	176.6	440.3	14.96
4-1280	4-1430	4-1600	320.	9.01	10.2	34.9	21.5	-15.1	6.15	0.362	1.128	0.720	31.2	141.7	210.8	365.6	6.53
4-1280	4-1454	4-1610	330.	8.60	-17.4	43.3	20.7	-11.9	5.68	0.368	1.085	0.686	195.7	345.9	202.2	396.2	9.57
4-1280	4-1460	4-1620	340.	8.05	-10.5	45.7	20.5	-10.8	2.63	0.372	1.072	0.674	186.1	358.2	199.5	402.1	9.33
4-1280	4-1384	4-1650	370.	10.27	0.1	45.5	19.2	-16.7	1.88	0.485	1.011	0.521	48.9	135.2	199.6	278.9	16.19
4-1280	4-1417	4-1660	380.	9.14	4.8	33.9	21.5	-15.9	3.89	0.370	1.130	0.712	35.6	136.3	211.8	344.3	6.69
4-1280	4-1425	4-1670	390.	9.06	7.3	34.0	21.5	-15.5	4.92	0.364	1.132	0.720	33.1	138.9	211.7	357.5	6.25
4-1290	4-1412	4-1490	200.	10.75	3.1	27.1	22.1	-20.5	3.43	0.403	1.182	0.706	40.1	129.7	219.8	339.4	7.50
4-1290	4-1459	4-1500	210.	9.37	-13.9	37.8	20.8	-14.9	4.73	0.388	1.101	0.673	202.1	341.0	206.6	401.4	10.20
4-1290	4-1464	4-1510	220.	8.87	-8.5	40.3	20.5	-13.7	2.11	0.391	1.085	0.661	192.5	353.6	203.6	406.7	10.16
4-1290	4-1468	4-1520	230.	8.58	-6.1	42.8	20.3	-12.6	1.09	0.394	1.072	0.650	174.9	13.7	201.0	410.9	10.51
4-1290	4-1472	4-1530	240.	8.39	-4.8	45.0	20.1	-11.7	0.69	0.397	1.062	0.640	145.4	45.3	199.0	414.2	10.87
4-1290	4-1475	4-1540	250.	8.22	-3.8	47.2	19.9	-10.8	0.64	0.401	1.053	0.631	108.1	84.5	197.1	417.2	11.24
4-1290	4-1478	4-1550	260.	8.04	-3.0	49.9	19.7	-9.7	0.79	0.405	1.044	0.622	81.8	112.8	195.0	420.1	11.63
4-1290	4-1481	4-1560	270.	7.86	-2.2	53.1	19.5	-8.5	1.03	0.410	1.033	0.610	66.7	130.3	192.6	423.6	12.12
4-1290	4-1412	4-1570	280.	10.75	3.1	27.1	22.1	-20.5	3.43	0.403	1.181	0.706	40.1	129.7	219.8	339.3	7.52
4-1290	4-1486	4-1570	280.	7.68	-1.4	57.5	19.2	-6.9	1.32	0.418	1.021	0.594	57.7	142.2	189.7	427.7	12.76
4-1290	4-1417	4-1580	290.	10.65	3.9	26.9	22.1	-20.2	3.80	0.397	1.185	0.715	39.1	130.3	220.2	347.8	6.86
4-1290	4-1491	4-1580	290.	7.52	-0.6	63.3	18.9	-4.7	1.64	0.430	1.007	0.574	52.0	151.4	186.3	432.6	13.60
4-1290	4-1423	4-1590	300.	10.52	5.1	27.1	22.1	-19.8	4.37	0.392	1.184	0.720	37.9	131.9	219.9	357.2	6.52
4-1290	4-1498	4-1590	300.	7.45	0.4	71.4	18.5	-1.7	1.99	0.448	0.990	0.547	47.9	159.7	182.1	438.7	14.73
4-1290	4-1431	4-1600	310.	10.35	7.5	28.2	22.0	-19.1	5.51	0.388	1.175	0.719	36.2	135.0	218.5	368.0	6.74
4-1290	4-1506	4-1600	310.	7.63	1.4	83.4	18.0	3.1	2.41	0.479	0.971	0.506	44.6	168.4	176.6	446.8	16.46
4-1290	4-1440	4-1610	320.	10.32	15.1	31.0	21.7	-18.0	9.27	0.385	1.154	0.709	33.5	140.8	215.3	380.3	8.40
4-1290	4-1414	4-1660	370.	10.72	3.3	27.0	22.1	-20.4	3.53	0.401	1.183	0.709	39.8	129.8	220.0	341.7	7.30
4-1290	4-1423	4-1670	380.	10.52	5.2	27.1	22.1	-19.8	4.39	0.392	1.184	0.720	37.8	131.9	219.9	357.5	6.51
4-1300	4-1461	4-1500	200.	10.55	-13.2	32.7	21.1	-18.5	5.18	0.413	1.129	0.663	210.7	333.2	211.7	404.7	11.21
4-1300	4-1466	4-1510	210.	9.98	-7.9	34.7	20.7	-17.3	2.20	0.414	1.110	0.651	204.0	342.9	208.7	409.4	11.01
4-1300	4-1470	4-1520	220.	9.63	-5.5	36.9	20.4	-16.2	1.00	0.415	1.094	0.640	189.5	0.0	206.1	413.3	11.28
4-1300	4-1474	4-1530	230.	9.38	-4.2	38.9	20.2	-15.2	0.50	0.417	1.081	0.631	153.1	38.6	203.9	416.4	11.60
4-1300	4-1477	4-1540	240.	9.15	-3.3	41.0	20.0	-14.3	0.50	0.419	1.070	0.622	97.3	96.4	201.8	419.2	11.94
4-1300	4-1480	4-1550	250.	8.93	-2.5	43.4	19.8	-13.2	0.77	0.422	1.058	0.612	70.7	125.3	199.6	422.2	12.32
4-1300	4-1483	4-1560	260.	8.70	-1.8	46.2	19.5	-12.0	1.07	0.426	1.046	0.600	59.8	138.5	197.2	425.4	12.77
4-1300	4-1488	4-1570	270.	8.43	-1.1	50.0	19.2	-10.4	1.38	0.432	1.032	0.587	54.2	147.1	194.3	429.0	13.29
4-1300	4-1418	4-1580	280.	12.46	3.2	20.9	23.1	-24.8	3.75	0.436	1.273	0.717	42.3	124.3	229.0	352.0	7.21
4-1300	4-1492	4-1580	280.	8.18	-0.4	54.8	18.9	-8.4	1.69	0.440	1.017	0.569	50.6	154.0	190.9	433.3	13.98
4-1300	4-1424	4-1590	290.	12.25	4.2	21.4	23.0	-24.2	4.26	0.430	1.264	0.720	41.5	125.8	228.2	361.3	6.98
4-1300	4-1498	4-1590	290.	7.94	0.4	61.5	18.5	-5.7	2.02	0.453	1.000	0.546	48.1	160.5	186.9	438.5	14.90
4-1300	4-1432	4-1600	300.	11.97	5.8	22.5	22.7	-23.5	5.16	0.424	1.244	0.716	40.4	128.8	226.2	371.6	7.29
4-1300	4-1505	4-1600	300.	7.83	1.3	71.0	18.0	-1.9	2.39	0.475	0.980	0.514	46.2	167.3	182.1	445.9	16.19
4-1300	4-1440	4-1610	310.	11.66	9.6	24.7	22.3	-22.3	7.23	0.418	1.214	0.706	39.0	133.6	222.9	381.9	8.31
4-1300	4-1408	4-1660	360.	12.78	2.1	21.2	23.0	-25.6	3.11	0.450	1.268	0.697	43.7	123.6	228.2	334.4	8.74
4-1300	4-1421	4-1670	370.	12.37	3.6	21.0	23.0	-24.5	3.95	0.434	1.270	0.719	41.9	124.8	228.7	356.1	7.05

ASYMPTOTE		VENUS PASSAGE						VENUS-EARTH HELIOCENTRIC TRANSFER							EARTH ASYMPTOTE		
DECL	R A	INCL	R C A	DECL	R A	VELE	PTHE	INCL	ECC	SMA	PERIH	LAN	APF	THETV	THETE	SPEED	DECL	R A
-40.1	260.9	88.10	18015.5	34.2	258.1	27.4	-4.1	11.29	0.169	0.866	0.720	16.8	159.1	3.8	200.9	6.31	34.8	264.2
46.3	226.8	98.92	12787.8	-30.2	235.5	27.3	-4.5	11.93	0.180	0.859	0.704	196.8	338.7	33.5	201.3	6.69	-79.5	238.8
24.8	215.1	97.65	9245.8	-45.7	226.6	27.4	-5.9	9.17	0.189	0.859	0.697	206.7	333.1	39.8	206.9	5.77	-71.4	247.7
17.7	210.5	95.77	6992.4	-50.2	219.3	27.5	-7.0	9.16	0.195	0.862	0.694	216.7	328.3	42.3	211.7	6.05	-69.0	256.2
-3.2	8.2	18.18	39417.8	17.8	280.9	27.7	-34.3	0.87	0.575	0.865	0.367	56.8	136.1	250.0	583.8	16.88	-22.0	261.4
-4.9	353.1	21.52	21045.8	-21.2	265.4	28.0	-23.7	2.68	0.419	0.874	0.508	66.9	130.2	270.2	589.8	11.95	-17.7	269.6
-19.6	298.2	30.60	14181.5	-28.5	221.8	28.3	-12.5	3.40	0.241	0.888	0.675	77.0	128.8	312.7	591.2	6.66	-8.8	280.9
-28.3	278.4	35.43	8044.8	-32.0	208.8	28.5	-12.6	3.41	0.239	0.895	0.681	87.2	126.7	316.1	593.3	6.78	-8.0	289.2
-8.8	328.9	127.80	29205.6	-52.0	59.5	32.0	24.4	3.59	0.442	1.225	0.684	81.1	86.1	327.1	453.9	13.18	-31.0	258.3
-12.4	312.7	88.67	31311.1	-86.2	153.5	31.0	21.7	3.84	0.382	1.130	0.699	90.7	82.4	334.1	457.6	11.55	-33.0	267.4
29.5	213.6	73.13	14455.3	64.7	83.3	32.2	24.7	2.31	0.451	1.256	0.689	100.2	87.8	32.4	92.2	13.47	-28.1	281.4
18.4	208.6	121.58	32985.5	55.0	315.5	29.3	20.6	1.76	0.352	1.004	0.650	109.7	67.4	52.6	112.6	10.59	-27.7	280.8
13.9	205.1	160.01	21764.0	15.8	291.2	27.2	16.0	1.29	0.311	0.884	0.609	119.3	46.4	71.1	133.6	8.31	-27.3	278.0
11.7	202.6	168.06	15407.8	4.4	283.7	25.9	11.3	0.92	0.301	0.823	0.575	128.8	29.3	83.9	150.7	6.62	-26.9	272.3
10.1	200.4	169.57	12711.1	-0.6	279.5	25.1	6.9	0.60	0.304	0.791	0.550	138.4	16.3	92.1	163.7	5.60	-26.0	264.1
8.8	198.1	169.53	11301.8	-3.9	276.5	24.6	3.0	0.25	0.315	0.772	0.529	148.0	6.6	97.6	173.4	5.15	-24.0	255.5
7.6	195.6	169.16	10390.7	-6.2	273.9	24.3	-0.5	0.12	0.329	0.760	0.510	337.7	178.9	101.9	181.1	5.23	-21.3	248.1
-12.9	310.6	90.20	6739.8	49.0	310.9	27.0	-0.4	9.95	0.170	0.861	0.715	347.4	178.0	343.0	542.0	5.54	34.3	265.1
6.5	192.7	169.00	9639.9	-7.5	271.4	24.0	-3.8	0.57	0.349	0.750	0.488	347.4	172.9	105.8	187.1	5.72	-18.9	244.5
-16.1	298.6	89.53	9313.7	47.9	298.0	27.2	-1.8	9.43	0.168	0.862	0.717	357.1	171.1	348.1	548.9	5.31	33.7	263.4
5.5	189.3	169.48	8816.0	-7.9	268.7	23.8	-7.0	1.12	0.378	0.738	0.459	357.1	168.2	110.2	191.8	6.54	-17.2	244.3
-20.7	282.5	87.76	12371.6	45.7	279.4	27.3	-3.0	9.40	0.168	0.864	0.719	6.9	164.7	354.0	555.3	5.37	32.8	262.3
4.6	185.3	170.84	7813.8	-7.0	265.5	23.4	-10.4	1.78	0.419	0.724	0.421	6.9	164.9	115.5	195.1	7.77	-16.5	247.3
-29.2	261.1	86.74	14241.0	40.3	256.5	27.4	-4.1	10.55	0.169	0.867	0.720	16.8	159.0	2.6	201.0	5.99	33.5	263.6
35.0	214.8	97.63	9167.2	-38.0	226.2	27.4	-5.8	11.09	0.187	0.860	0.699	206.7	333.1	38.0	206.9	6.53	-76.1	247.1
21.4	210.4	95.94	6716.3	-47.2	219.2	27.5	-7.0	10.00	0.194	0.862	0.695	216.7	328.3	41.6	211.7	6.37	-71.3	256.5
-4.4	355.9	18.67	18076.2	-18.4	268.5	28.0	-26.1	2.58	0.456	0.873	0.475	66.9	131.1	265.1	588.9	13.12	-18.5	269.9
-16.0	299.0	25.05	13457.4	-23.4	224.8	28.3	-12.8	3.40	0.245	0.888	0.670	77.0	128.6	310.7	591.4	6.80	-9.1	280.8
-22.7	276.2	28.69	7882.7	-26.3	210.6	28.5	-12.6	3.42	0.240	0.895	0.680	87.2	126.7	315.8	593.3	6.80	-8.1	289.1
-11.8	305.9	71.84	31108.0	-71.5	209.1	31.1	21.9	3.80	0.387	1.143	0.701	90.7	83.4	335.3	456.6	11.68	-32.9	268.0
29.5	210.2	77.39	12214.1	67.7	70.4	32.3	25.5	2.18	0.465	1.265	0.677	100.2	86.9	37.3	93.1	13.91	-27.6	280.8
18.6	206.6	124.68	25537.6	52.1	310.4	29.2	21.2	1.63	0.361	0.997	0.636	109.7	65.8	57.2	114.2	10.84	-27.2	279.9
14.0	203.5	159.59	17949.6	16.4	289.1	27.0	16.4	1.14	0.322	0.875	0.593	119.3	44.7	75.5	135.2	8.50	-26.8	276.6
11.5	201.1	167.99	13171.5	5.2	282.1	25.6	11.5	0.76	0.315	0.814	0.558	128.8	28.0	88.1	152.0	6.81	-26.2	270.6
9.9	199.1	169.92	11095.8	0.0	278.1	24.8	7.0	0.42	0.319	0.782	0.533	138.4	15.5	95.8	164.4	5.82	-25.1	262.7
8.6	197.1	170.08	10063.5	-3.1	275.5	24.4	3.0	0.10	0.328	0.765	0.514	148.1	6.1	100.6	173.9	5.37	-23.1	254.4
7.5	194.9	169.79	9436.8	-5.4	273.1	24.1	-0.6	0.25	0.340	0.754	0.497	337.7	178.7	104.2	181.2	5.43	-20.7	247.5
-11.7	306.1	88.50	6050.7	49.1	304.1	27.0	-0.4	10.26	0.170	0.861	0.715	347.4	178.1	343.4	541.9	5.67	34.8	265.2
6.4	192.4	169.58	8941.0	-6.8	271.0	23.9	-3.9	0.67	0.358	0.745	0.478	347.4	172.9	107.4	187.1	5.88	-18.6	244.3
-14.2	293.1	87.59	8010.1	48.1	289.8	27.2	-1.8	9.78	0.168	0.862	0.717	357.1	171.2	348.7	548.8	5.46	34.4	263.7
5.5	189.5	169.83	8450.8	-7.4	268.9	23.7	-7.1	1.16	0.381	0.737	0.456	357.1	168.2	110.7	191.8	6.60	-17.2	244.3
-17.6	276.6	86.20	9819.8	46.3	271.4	27.3	-3.0	9.88	0.168	0.864	0.719	6.9	164.8	355.0	555.2	5.58	33.8	262.8
4.7	186.2	170.78	7855.4	-7.1	266.2	23.5	-10.2	1.72	0.413	0.727	0.427	6.9	164.8	114.6	195.2	7.64	-16.5	247.2
-23.0	256.6	85.91	10405.0	42.7	251.1	27.4	-4.1	10.90	0.169	0.866	0.720	16.8	159.0	3.2	201.0	6.14	34.1	263.9
4.0	182.0	172.70	6897.3	-5.4	262.9	23.0	-13.7	2.39	0.461	0.710	0.383	16.8	162.7	120.3	197.3	9.08	-16.6	252.9
-37.4	235.1	88.89	9772.3	34.0	233.5	27.6	-5.2	14.28	0.173	0.868	0.718	26.7	153.6	14.2	206.4	7.79	36.9	267.2
-12.4	302.6	19.96	11946.1	-18.8	229.4	28.3	-13.5	3.40	0.257	0.887	0.659	77.0	128.3	306.2	591.7	7.16	-9.9	280.4
-17.7	276.1	22.65	7227.2	-21.0	213.2	28.5	-12.9	3.45	0.244	0.895	0.676	87.2	126.5	313.6	593.4	6.95	-8.3	289.0
29.3	207.0	81.45	10234.6	70.2	56.5	32.4	26.4	2.03	0.480	1.275	0.662	100.2	85.7	42.6	94.3	14.43	-27.2	280.1
18.3	204.3	128.87	20052.6	48.1	304.7	29.1	21.9	1.46	0.374	0.988	0.618	109.7	63.8	62.7	116.2	11.18	-26.7	278.6
13.6	201.7	160.30	14550.9	15.9	286.4	26.8	16.9	0.96	0.337	0.863	0.573	119.3	42.8	80.6	137.2	8.77	-26.2	275.0
11.1	199.6	168.37	11014.1	5.2	280.0	25.3	11.9	0.57	0.331	0.803	0.537	128.8	26.5	92.7	153.5	7.07	-25.4	268.7
9.5	197.7	170.36	9460.4	0.3	276.4	24.5	7.1	0.23	0.336	0.771	0.512	138.5	14.5	100.0	165.4	6.10	-24.1	260.9
8.2	195.8	170.61	8674.3	-2.8	273.9	24.0	2.9	0.11	0.346	0.754	0.493	328.0	185.6	104.5	174.5	5.68	-22.1	253.0
7.1	193.8	170.36	8249.6	-5.0	271.8	23.8	-0.8	0.45	0.358	0.744	0.477	337.7	178.5	107.6	181.5	5.75	-19.8	246.8
6.2	191.6	170.12	7994.9	-6.4	270.0	23.6	-4.2	0.83	0.373	0.737	0.462	347.4	172.9	110.0	187.1	6.17	-18.1	244.2
-12.5	285.7	85.61	6415.1	47.8	279.9	27.2	-1.7	10.46	0.168	0.862	0.718	357.1	171.4	349.7	548.6	5.75	35.7	264.2
5.3	189.2	170.22	7762.6	-7.1	268.2	23.5	-7.3	1.27	0.392	0.731	0.445	357.1	168.4	112.4	191.6	6.82	-17.0	244.4
-14.8	268.8	85.05	7197.2	46.1	262.3	27.3	-3.0	10.74	0.167	0.864	0.720	6.9	165.0	356.5	555.0	5.95	35.3	263.4
4.6	186.3	170.93	7457.0	-6.9	266.1	23.4	-10.3	1.76	0.417	0.724	0.422	6.9	164.9	115.3	195.1	7.73	-16.5	247.3
-18.2	250.3	85.89	7053.6	44.0	245.0	27.4	-4.1	11.92	0.169	0.866	0.720	16.8	159.1	4.8	200.9	6.59	35.7	264.6
3.9	182.9	172.44	6952.1	-5.8	263.8	23.1	-13.6	2.32	0.453	0.714	0.390	16.8	162.4	119.2	197.6	8.93	-16.6	252.5
-25.5	233.7	88.29	6649.7	39.9	231.4	27.6	-5.2	14.11	0.173	0.868	0.718	26.7	153.6	14.1	206.4	7.72	36.7	267.1
-8.9	312.3	15.89	9942.5	-15.2	238.1	28.3	-15.4	3.41	0.287	0.885	0.631	77.0	127.8	297.0	592.2	8.05	-11.5	279.8
-13.5	278.3	17.70	6216.1	-16.7	216.9	28.5	-13.6	3.50	0.254	0.894	0.666	87.2	126.3	309.5	593.7	7.26	-8.8	288.8

SECTION 4
REFERENCES

1. Ross, S. (ed.), Space Flight Handbooks, Volume 3 Planetary Flight Handbook, NASA SP-35 (1963).

2. Clarke, V. C., Design Parameters for Ballistic Interplanetary Trajectories Part 1, TR 32-77, Jet Propulsion Laboratory, Pasadena, California, January 16, 1963.

3. Hollister, W. M., "The Mission for a Manned Expedition to Mars," Sc.D. Thesis, Massachusetts Institute of Technology, Cambridge, Mass. (1963).

4. Sohn, R., L., "Summary of Manned Mars Mission Study," Proceedings of the Symposium on Manned Planetary Missions, 1963/1964 Status, NASA TM-53049, Pt. 5, June 12, 1964.

5. Deerwester, J. M., "Initial Mass Savings Associated with the Venus Swingby Mode of Mars Roung Trips," AIAA Paper 65-89 (1965).

6. Sohn, R. L., "Venus Swingby Mode for Manned Mars Missions," J. Spacecraft Rockets 1, 565-567 (1964).

7. Sohn, R. K., "Manned Trips Using Venus Swingby Modes," J. Spacecraft Rockets 3, 161-169 (1966).

8. "Programmer's Manual for Quick Look Mission Analysis Program," WDL-TR2217 Philco WDL, Palo Alto, California, 24 January 1964.

9. Peabody, P. R., Scott, J. F., Orozco, E. D., "User's Description of JPL Ephemeris Tapes," TR 32-580, Jet Propulsion Laboratory, Pasadena California, 2 March 1964.

10. Sandifer, R. J., "Use of Moon Elements to Calculate the Position of the Sun, Moon, and Earth," NASA X-507-66-209, January, 1966.

TR-DA1568

TASK 2

ESTIMATION OF INERTIAL PLATFORM ERRORS

(SUMMARY)

Contract No. NAS8-20358

21 October 1967

Prepared by

John V. Brown

and

James S. Tyler, Jr.

PHILCO-FORD CORPORATION

Space & Re-Entry Systems Division

Palo Alto, California

for

National Aeronautics and Space Administration

Marshall Space Flight Center

Huntsville, Alabama

SECTION 1

INTRODUCTION

This report presents the results of one of the three parts of Contract NAS8-20358, entitled Advanced Spaceborne Tracking, Detection, and Navigation Study. The objective of this part of the contract was to evaluate the feasibility of estimating the inertial guidance platform errors from data obtained during a powered flight ascent.

One method of estimating the inertial platform errors is to combine the telemetry data, which contains information on the vehicle position-velocity state plus deviations in the trajectory caused by the platform errors, with the tracking data, which also contains information on the vehicle state, but includes errors from the tracking system.

There are three potential uses for the information contained in this combined platform-tracking system. If it is possible to estimate the platform errors during a flight, then the guidance system could be updated. Also the ability to determine platform errors would be useful in a postflight analysis where the objective is to determine whether the guidance components performed according to specification. Although the primary interest in this study is to evaluate the ability to estimate the guidance errors, a third use of this data would be to obtain a better estimate of the vehicle than could be obtained with tracking data alone.

The feasibility of estimating the platform errors has been evaluated in this study by simulating an orbit determination process that would combine the telemetry and tracking data. It is the ensemble behavior of this combined system and in particular the behavior of the covariance matrix of the errors in estimate of the position-velocity state plus the platform and tracking errors, that has been investigated. A Kalman or minimum variance filter has been assumed for the estimation process.

Platform errors as well as a nominal trajectory that are similar to a Saturn V mission have been used in the study. The equations for the platform model, the tracking model, and the minimum variance estimation are presented in Section 2. A discussion of the computer program used to generate the covariance matrix of errors, and the nominal ascent trajectory along which the covariance matrix is propagated, are included in Section 3 and Section 4, respectively. Section 5 discusses the effect of individual error sources in the platform and tracking systems on the trajectory. These results are used to define the significant error sources which should be included in the combined platform-tracking system model.

The principal results of the study are presented in Section 6. In this section the feasibility of estimating the platform errors is evaluated as a parametric function of the system error sources and tracking parameters.

SECTION 2

DERIVATION OF EQUATIONS

2.1 INERTIAL PLATFORM ERROR MODEL

The inertial platform model that has been used for this study consists of up to 30 error sources and is similar to that used by Daniels, Neighbors, and Cole, in Reference 1. The four types of accelerometer errors and the four types of gyro errors considered are:

α_i the i^{th} accelerometer bias, km/sec^2

β_{ij} the misalignment of the i^{th} accelerometer into the j^{th} axis, radians

ε_i the scale factor error of the i^{th} accelerometer, parts/part

s_i the threshold of the i^{th} accelerometer, km/sec^2

ϕ_{oi} the initial platform misalignment about the i^{th} axis, radians

$\dot{\phi}_{oi}$ the steady-state drift rate of the i^{th} gyro, rad/sec

μ_{Ii}, μ_{si} the mass unbalance drift about the input and spin axes, $(rad/sec)/(km/sec^2)$

c_i the anisoelastic drift of the i^{th} gyro, $(rad/sec)/(km/sec^2)^2$

The platform is oriented in an inertial frame fixed at launch as shown in Figure 2-1.

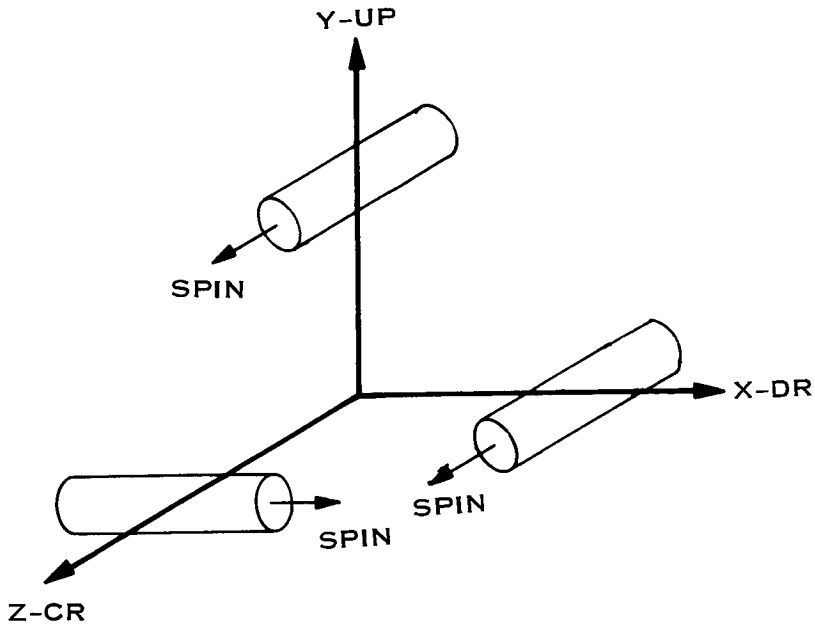

Figure 2-1 Platform Orientation

The gyro input axes are along the X, Y, and Z axes and the three accelerometers are also assumed to be mounted along these axes.

The platform error model used in this study includes the total error in acceleration caused by (1) the misalignment of the platform axes resulting from the gyro drifts and initial misalignment, and (2) the errors in the accelerometers themselves which are mounted on the drifting platform axes, for a given nominal acceleration time history. The drift rate for the i^{th} gyro is given by

$$\dot{\Phi}_i = \dot{\phi}_{oi} + \begin{bmatrix} \mu_{si} & \mu_{Ii} & 0 \end{bmatrix} \begin{bmatrix} a_{Gis} \\ a_{GiI} \\ a_{Gio} \end{bmatrix} + c_i (a_{Gis})^2, \qquad (2\text{-}1)$$

where a_{Gis}, a_{GiI}, and a_{Gio} are the accelerations along the spin, input, and output axes of the i^{th} gyro, respectively. The total platform drift, which is found by integrating (2-1), is

$$\Phi_i = \phi_{oi} + \dot{\phi}_{oi} t + \begin{bmatrix} \mu_{si} & \mu_{Ii} & 0 \end{bmatrix} T_{PI2Gi} \int_o^t a_{PIi}(\tau) d\tau + c_i \int_o^t \left(q_i \, a_{PIi}(\tau) \right)^2 d\tau, \qquad (2\text{-}2)$$

where a_{PIi} is the acceleration along the i^{th} ideal platform axis, T_{PI2Gi} is the transformation from the ideal platform axes to the i^{th} gyro axis, and q_i, is the first row of T_{PI2Gi}. For the gyro orientation in Figure 2-1, T_{PI2GI}, the transformation from the ideal platform axes to the X gyro axes, is

$$T_{PI2GI} = \begin{bmatrix} 0 & 0 & 1 \\ 1 & 0 & 0 \\ 0 & 1 & 0 \end{bmatrix}, \qquad (2\text{-}3)$$

where the order of the gyro axes is $\begin{bmatrix} s \\ I \\ o \end{bmatrix}$.

The accelerometer errors are found from the sensed acceleration along the accelerometer axes, a_{si}', which is

$$a_{si}' = \begin{bmatrix} \alpha_x + s_x \\ \alpha_y + s_y \\ \alpha_z + s_z \end{bmatrix} + \left\{ I + \begin{bmatrix} \varepsilon_x & \beta_{xy} & \beta_{xz} \\ \beta_{yx} & \varepsilon_y & \beta_{yz} \\ \beta_{zx} & \beta_{zy} & \varepsilon_z \end{bmatrix} \right\} \begin{Bmatrix} a_{PIx} \\ a_{PIy} \\ a_{PIz} \end{Bmatrix} \quad (2\text{-}4)$$

The total error in acceleration is given by the sum of the accelerometer errors plus the error in acceleration caused by the platform misalignment. The total sensed acceleration can be written as the sum of the acceleration in (2-4) plus the cross product of the platform orientation angles, Φ_i in (2-2), and the true acceleration along the ideal platform axes. This expression is

$$a_{si} = \begin{bmatrix} \alpha_x + s_x \\ \alpha_y + s_y \\ \alpha_z + s_z \end{bmatrix} + \left[I + E \right] a_{PI} + \begin{bmatrix} \Phi_x \\ \Phi_y \\ \Phi_z \end{bmatrix} \otimes a_{PI}, \quad (2\text{-}5)$$

where $\otimes$ denotes the cross product, and E is the matrix of scale factor and misalignment errors in (2-4).

2.2 DYNAMIC EQUATIONS OF THE VEHICLE

The dynamic equations of the vehicle include the effects of gravity as well as the thrusting accelerations and the acceleration errors. These equations can be expressed in an inertial frame as

$$\ddot{R} = G(R,t) + T_{A2I}\, a_{PI}(t), \quad (2\text{-}6)$$

where G(R,t) is the gravitational acceleration and T_{A2I} is the transformation from accelerometer axes to the inertial axes, and $a_{PI}(t)$ has been defined as the true value of the non-gravitational acceleration. Since $a_{PI}(t)$ can be expressed as the difference between the sensed acceleration and the acceleration errors, equation (2-6) can be written as

$$\ddot{R} = G(R,t) + T_{A2I}\left[a_s(t) - \delta_a(e,t)\right], \tag{2-7}$$

where $\delta_a(e,t)$ is a function of the platform errors and from (2-5) is given by

$$\delta_a(e,t) = \begin{bmatrix} \alpha_x + s_x \\ \alpha_y + s_y \\ \alpha_z + s_z \end{bmatrix} + E\, a_{PI} + \Phi \otimes a_{PI} \tag{2-8}$$

Representing (2-7) as

$$\ddot{R} = G(R,t) + f(e,t), \tag{2-9}$$

and considering perturbations only about the nominal values of R and a, results in the linear equations of motion that are used for the error analysis. These equations are

$$\ddot{\Delta R} = F\Delta R + B\ \Delta a, \tag{2-10}$$

where

$$F = \left.\frac{\partial\, G(R,t)}{\partial R}\right|_{R\ \text{Nominal}} \qquad B = \left.\frac{\partial f(e,t)}{\partial a}\right|_{a\ \text{Nominal}}$$

For the purpose of error propagation, the total state vector (z), in general, may consist of the 6 vector of position (R) and velocity (V) plus any number of the sensor error and tracking bias error sources (e), i.e.,

$$z = \begin{bmatrix} R \\ V \\ e \end{bmatrix} = \begin{bmatrix} x \\ e \end{bmatrix} \tag{2-11}$$

The state transition matrix for this expanded state vector is given by

$$\Phi(t,t_o) = \begin{bmatrix} \frac{\partial x}{\partial x_o} & \frac{\partial x}{\partial e} \\ 0 & I \end{bmatrix} = \begin{bmatrix} \emptyset & \emptyset_u \\ 0 & I \end{bmatrix} \tag{2-12}$$

The expression $\frac{\partial x}{\partial x_o}$ is found by solving the following equation for $\frac{\partial R}{\partial x_o}$:

$$\frac{\partial \ddot{R}}{\partial x_o} = \frac{d^2}{dt^2}\frac{\partial R}{\partial x_o} = \frac{\partial G}{\partial R}\frac{\partial R}{\partial x_o}, \tag{2-13}$$

where $\frac{\partial R}{\partial x_o}$ is a 3x6 matrix and

$$\frac{\partial G}{\partial R} = F$$

The sensitivities of the position and velocity state to the i^{th} platform error source are found by integrating the equation

$$\frac{d^2}{dt^2}\frac{\partial R}{\partial e_i} = \frac{\partial \ddot{R}}{\partial e_i} = \frac{\partial G}{\partial R}\frac{\partial R}{\partial e_i} - \frac{\partial \delta a}{\partial e_i} \tag{2-14}$$

The velocity partial $\frac{\partial V}{\partial e_i}$ in (2-12) is found by differentiating the solution for $\frac{\partial R}{\partial e_i}$ in (2-14). Detailed descriptions of the error source sensitivities $\left(\frac{\partial\, \delta a}{\partial e_i}\right)$ are given in Reference 2.

2.3 TRACKING EQUATIONS

The tracking model is obtained by assuming that the radar observations are of the form

$$Y = f(X, W, T) + q$$

where X = 6 state of position and velocity
W = tracking bias errors (2-15)

Linearization of this equation about a nominal trajectory results in the following equations for the measurement y:

$$y = \frac{\partial f}{\partial X} x + \frac{\partial f}{\partial W} W + q(t) \qquad (2\text{-}16)$$

The tracking model consists of the partials of the observation with respect to the state (H) and the partial of the observation with respect to the measurement bias parameters (G), and the random measurement error vector q(t). For each observation the model is given by

$$y = Hx + Gw + q(t), \qquad (2\text{-}17)$$

where H and G are row vectors.

The tracking that can be simulated includes range, range-rate, azimuth, elevation, right ascension, declination, and direction cosines and their rates. Each of these measurements may contain a random and a bias error, in addition to the station-location errors for the station and a station clock error.

2.4 MINIMUM VARIANCE ESTIMATION EQUATIONS

Since the equations for the minimum-variance estimator are an essential part of the error analysis of the inertial platform and tracking systems, these equations are summarized here. It is the ensemble type behavior of the inertial platform-tracking system that is to be studied and therefore the variance-covariance matrix of the error in estimate of the state (P) is processed by the filter. The nominal trajectory is used throughout to evaluate the measurement, platform, and state sensitivities, H, $\emptyset_u$, and $\emptyset$, respectively. Residuals are not determined in this analysis.

The general form of the covariance matrix which is progagated along the nominal trajectory is

$$P_e = \begin{bmatrix} \overset{6X6}{P} & C_{de} & C_{me} \\ C_{de}^T & D & C_1 \\ C_{me}^T & C_1^T & W \end{bmatrix}, \qquad (2\text{-}18)$$

where

$P_e = E(\tilde{x}_e \tilde{x}_e^T)$ - the error in estimate of the complete state vector

$x_e = \begin{bmatrix} x \\ u \\ w \end{bmatrix}$ the total state vector of estimated variables

x = vector of position and velocity

u = vector of dynamic bias errors

w = vector of measurement bias errors

$\tilde{x} = x - \hat{x}$ - the error in estimate of the state

$D = E[\, uu^T \,]$ - the covariance matrix of dynamic bias errors

$W = E[\, ww^T \,]$ - covariance matrix of measurement bias errors

C_{ij}'s - correlations between the estimated parameters.

The equations for updating the covariance matrix in time and at an observation are given by

Propagating in Time

$$x(t) = \phi(t,t_o)\, x(t_o) \tag{2-19}$$

$$P(t) = \phi(t,t_o)\, P(t_o)\, \phi(t,t_o)^T \tag{2-20}$$

After an Observation

$$\hat{x}_n = \hat{x}(t) + P_n\, H^T(HP_nH^T + Q)^{-1}(y-\hat{y}) \tag{2-21}$$

or

$$\hat{x}_n = \hat{x}(t) + K(y-\hat{y}) \tag{2-22}$$

$$P_n = P(t) - P(t)\, H^T(HP(t)H^T + Q)^{-1}HP(t), \tag{2-23}$$

where

$$\Phi = \begin{bmatrix} \phi & \phi_u & 0 \\ 0 & I & 0 \\ 0 & 0 & I \end{bmatrix}$$ the total state transition matrix

ϕ = the 6X6 transition matrix of the position-velocity state

ϕ_u = change in position and velocity errors due to the platform errors

$$H = \begin{bmatrix} H' \\ 0 \\ G \end{bmatrix}$$ - the partial of the observation with respect to the expanded state

$Q = E[\, qq^T \,]$ - the covariance matrix of the random measurement error q

$\hat{x}(t)$ = estimate of the state at time t before an observation

$\hat{x}_n(t)$ = new estimate of the state after an observation

y = the observation.

2.4.1 Equations for Determining the Effect of Neglecting Error Sources

The standard equations for the Kalman filter, which have been summarized in the previous section, are applicable when all the elements in the state vector are to be estimated. A variation on this basic estimation process has been developed which enables one to determine the effect of neglecting error sources.

The general form of the total state covariance matrix (P_{ne}), when some parameters are estimated and other parameters are neglected, is

$$P_{ne} = \begin{array}{|c|c|c|} \hline P_e & C_{dn} & C_{mn} \\ \hline & D_o & 0 \\ \hline & 0 & W_o \\ \hline \end{array} \qquad (2\text{-}24)$$

where D_o and W_o are the variances of the dynamic and measurement biases, respectively, which have been neglected. The correlation between the state and the measurement biases (C_{mn}) and the correlation between the state and the dynamic biases (C_{dn}) are computed as follows:

$$C_{dn}(t) = \phi(t,t_o)\, C_{dn}(t_o) + \phi_u D \qquad (2\text{-}25)$$

$$C_{mn}(t) = \phi(t,t_o)\, C_{mn}(t_o) \qquad (2\text{-}26)$$

$$C_{dn}^{+} = [I\text{-}KH]\, C_{dn}^{-} \qquad (2\text{-}27)$$

$$C_{mn}^{+} = [I\text{-}KH]\, C_{mn}^{-} - KGW_o\,, \qquad (2\text{-}28)$$

where (-) and (+) denote time before and after an observation, respectively.

The total covariance matrix P_T which gives the uncertainty of having neglected measurement and dynamic bias errors, in addition to the uncertainties given by P_n and P(t) in (2-23) and (2-20), is

$$P_T = P_e + C_{dn} D_o^{-1} C_{dn}^{T} + C_{mn} W_o^{-1} C_{mn}^{T} \qquad (2\text{-}29)$$

where P_e is the m x n matrix in (2-18) which includes P, D and W. Since the last two terms in (2-29) can be written with C_{dn} and C_{mn} as column vectors and D and W as scalars, or with C_{dn}, C_{mn}, D, and W as matrices, equation (2-29) may be used to obtain the effect of neglecting individual error sources or groups of error sources.

2.4.2 Equations for an Equivalent Observation. In a conventional error analysis, where for example one element of P may be the variance of an inertial guidance error and a number of observations are made of the vehicle (range, range-rate, etc.), the effect of changing the initial variance on the final uncertainty of the vehicle state, would be determined by simulating the mission with a new value of this particular variance. This would correspond to changing the initial variance of the parameter (P_o) by a factor of k, i.e.,

$$P'_o = kP_o \quad , \tag{2-30}$$

as shown in Fig. 2-2.

However, this same value of the initial variance (P'_o) can be found by taking a direct observation of the parameter whose variance is to be changed (h = 1), with a measurement error variance (q) that is specified such that the state variance after the observation is P'_o.

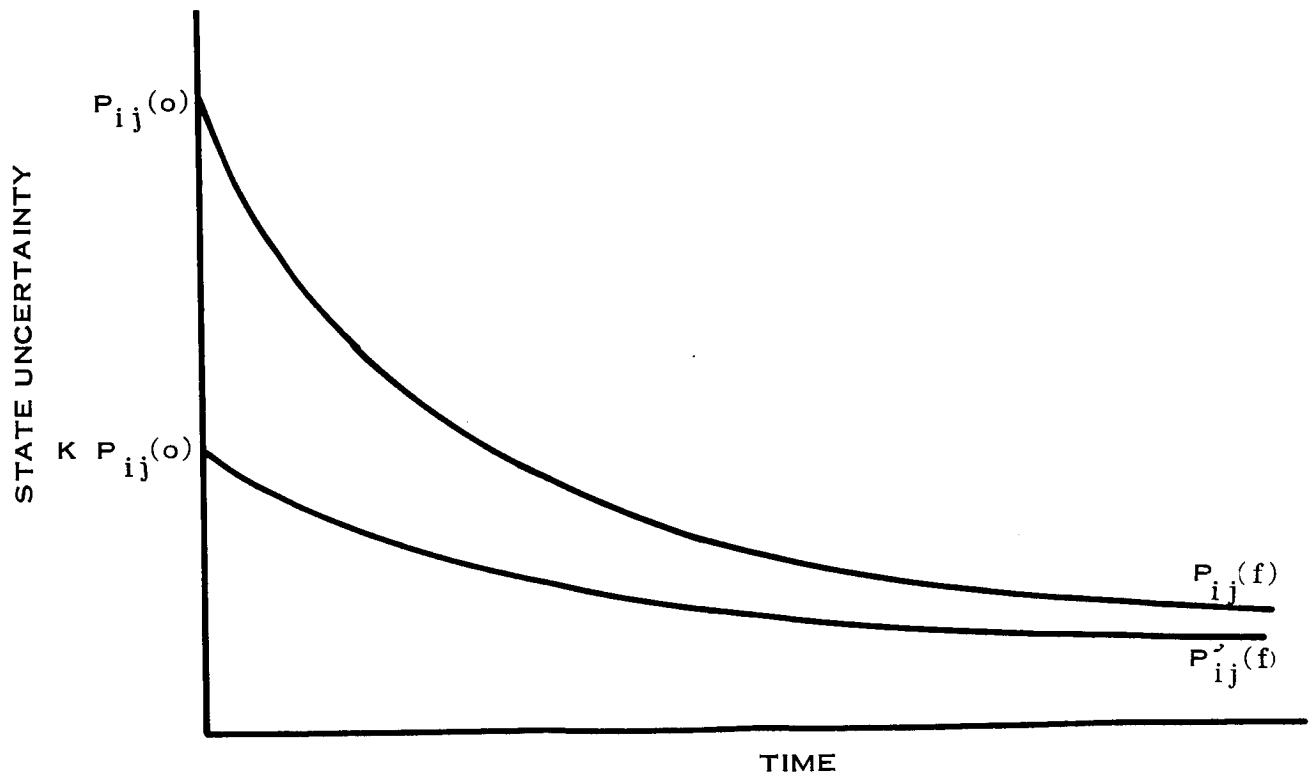

Figure 2-2 Effect of an Equivalent Observation

Since the final value of the state uncertainty $P'_{ij}(f)$ can be shown to be independent of the order of the observations, the equivalent observation can be made at the end of a run. This final value of the total state uncertainty P'(f) that would be obtained with the new value of the initial state uncertainty kP(0), is given by

$$P'(f) = P(f) - P(f)\, H^T \left[H\, P(f) H^T + P_{ij}(0) \frac{k}{1-k} \right]^{-1} HP(f) \qquad (2\text{-}31)$$

where

$$H = [0 \cdots 1 \cdots 0], \qquad (2\text{-}32)$$

and the location of the 1 in (2-32) corresponds to the parameter that is being observed.

In this manner any number of changes can be made in one or more of the initial variances by adding equivalent observations at the end of a run. Thus the results of a number of computer runs can be obtained in one run.

2.4.3 The Equations For a Perfect Observation. A special case of the equivalent observation concept is where a perfect observation is made of a parameter. An observation of this type has the H of (2-32), where the element in H which is 1 corresponds to the element of the state which is being observed, but there is no measurement error variance Q. The effect of a perfect observation of a measurement bias error on the covariance matrix P is given by

$$P' = P - C_m W^{-1} C_m^T \tag{2-33}$$

where C_m is the column vector of correlations between the state and the measurement bias which is being observed. The effect on P of a perfect observation of a dynamic bias error is given by

$$P' = P - C_d D^{-1} C_d^T \tag{2-34}$$

SECTION 3

POWERED FLIGHT ERROR PROPAGATION PROGRAM

The computer program that has been used to obtain the numerical results for this study is the Powered Flight Error Propagation Program. The original version of this program was written by Philco-Ford for NASA Goddard under Contract NAS-5-9700, and is described in Reference 2.

The program simulates an actual orbit determination that would combine the tracking data from the ETR radars with the telemetry data from the vehicle, and would be used to estimate the position and velocity of the vehicle plus any additional parameters such as the inertial platform errors or the tracking bias errors. As a result, it is a useful tool for studying the ensemble behavior of the combined inertial platform-tracking system under a wide variety of conditions.

The essential output from the program is a variance-covariance matrix of errors in estimate of the position and velocity state, and the estimated error parameters. The covariance matrix is propagated along a nominal powered flight trajectory. A general flow diagram of the program functions are shown in Figure 3-1.

The program reads an input tape of the nominal trajectory position X(t) and acceleration A(t) that is generated by the Philco Ford Powered Flight Optimization Program. (Ref. 2) The gravity partials (F) are evaluated for the nominal values of X(t) and the platform error partials are evaluated for the nominal values of acceleration A(t). These partials define the differential equations for the deviations about the nominal trajectory. These equations are integrated for short time intervals in order to obtain the transition matrices $\emptyset$ and $\emptyset_u$. The matrix $\emptyset_u$ defines the perturbation of the trajectory resulting from the guidance errors.

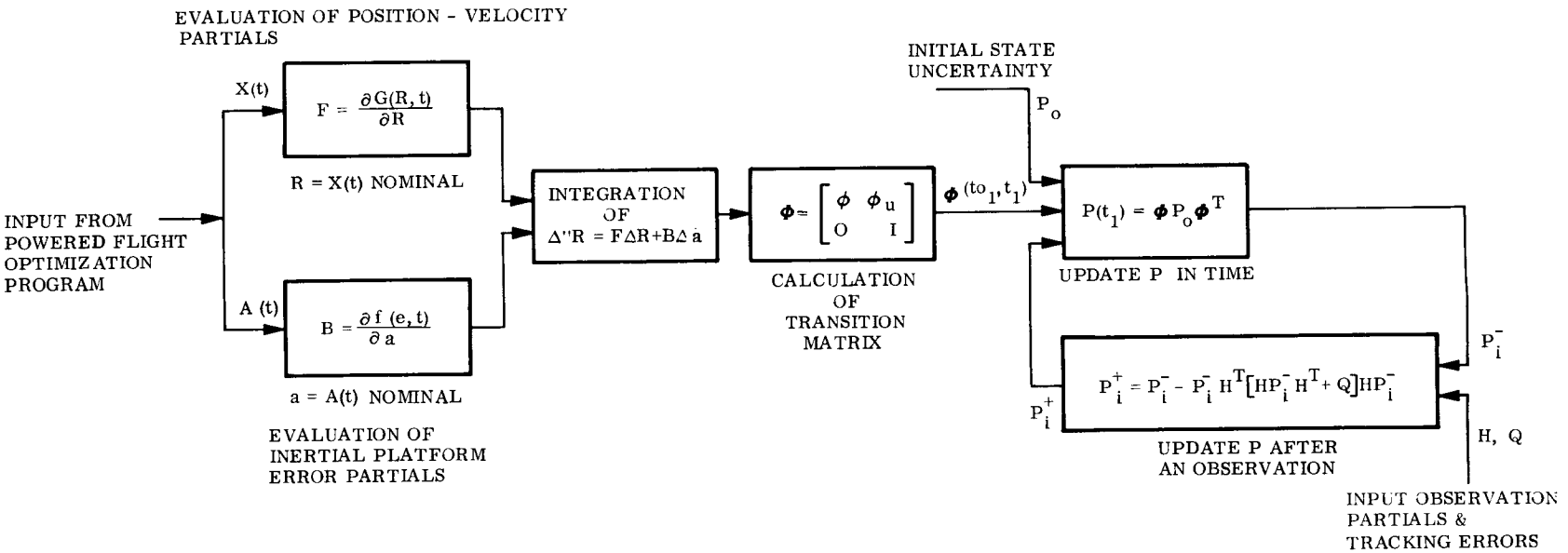

Figure 3-1 Functional Diagram of Powered Flight Error Analysis Program

The transition matrices are used to update the covariance matrix (P) in time. There is no modification made to the trajectory in the sense that the actual perturbed trajectory is calculated.

The essential part of the estimation process which simulates an orbit determination is the updating of the covariance matrix P. As shown in Figure 3-1 P is propagated between two points in time based in the previous value of P and the total transition matrix Φ. This propagation in time accounts for the fact that the guidance errors will in general increase the state uncertainty P as the time along the trajectory increases.

The data from the trackers is incorporated into the estimation by updating the state uncertainty at each observation. Observations are processed one at a time, that is the partial of the observation with respect to the state (H) is a vector and the random tracking error q is a scalar.

The program has a capability of handling a 60 x 60 covarinace matrix. It's elements include the uncertainty in the three coordinates of position and the three coordinates of velocity, which are initially zero, plus the uncertainly in any inertial guidance error, or tracking bias error. Up to 30 guidance errors may be included in the guidance model.

SECTION 4

THE ASCENT TRAJECTORY

The ascent trajectory which has been used as the nominal trajectory for this study is similar to a Saturn V trajectory. This trajectory was generated by the Philco-Ford Powered Flight Optimization Program. The output of the program is a trajectory tape which contains the vehicle position and acceleration at discrete time points. An altitude profile of the nominal trajectory is shown in Figure 4-1. The ground track for this trajectory (latitude vs. longitude) is shown in Figure 4-2. The locations of the tracking stations are also shown in this figure.

Variations of this basic trajectory have also been used. However, it was determined the results presented in the succeeding sections are not sensitive to small variations in the trajectory. In particular, one trajectory whose final altitude was about twice the value in Figure 4-1 caused no significant changes in the ability to estimate the guidance errors. Acceleration levels in the DR, CR, UP coordinate system are shown in Figure 4-3.

The total time for the ascent trajectory is 9 minutes, 26 seconds.

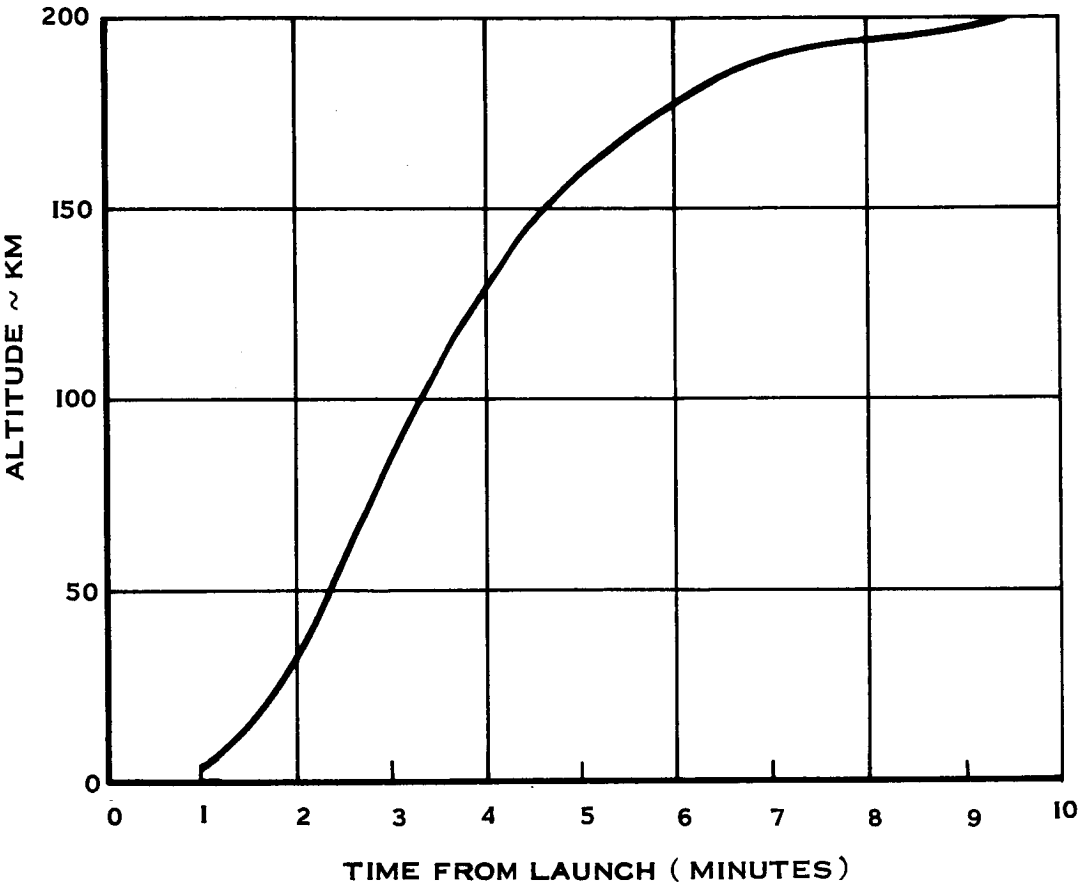

Figure 4-1 Trajectory Altitude vs Time

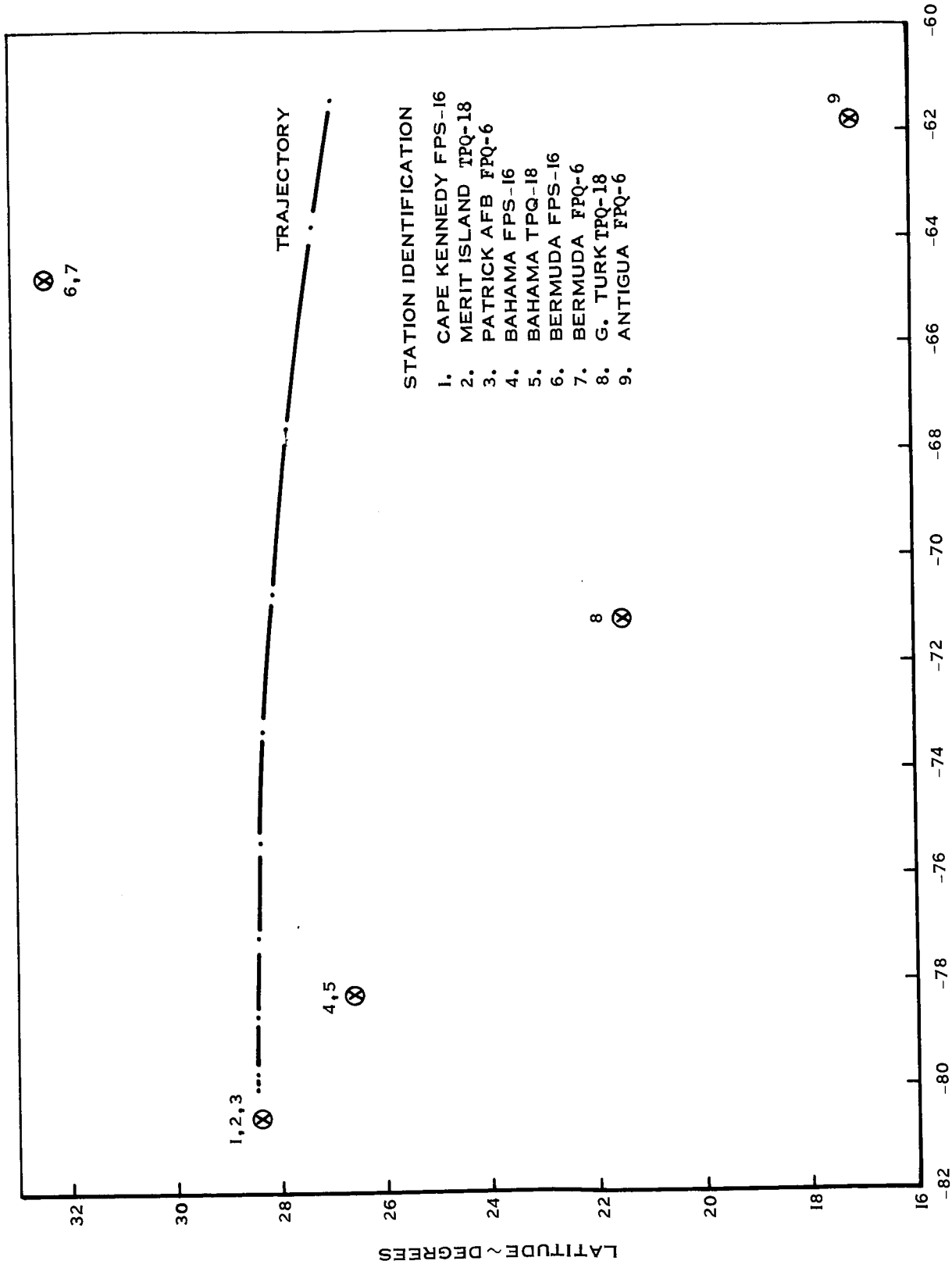

Figure 4-2 Trajectory and Tracking Station Location

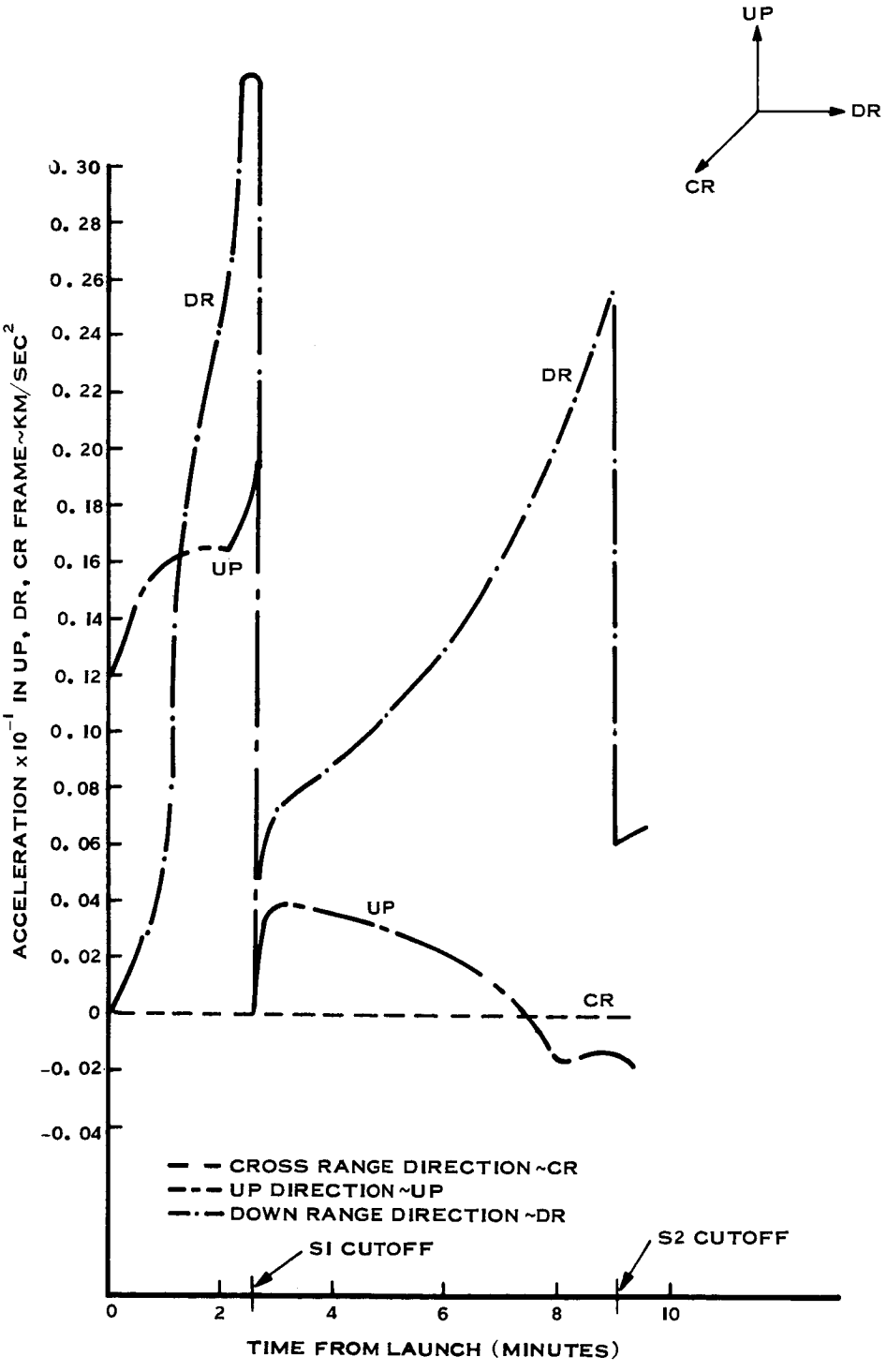

Figure 4-3 Acceleration Levels for Nominal Trajectory

SECTION 5

SELECTION OF COMBINED PLATFORM-TRACKING

Prior to determining the feasibility of estimating the inertial platform errors, an analysis was made to evaluate the effect of individual errors, both from the tracking and the inertial platform. This analysis shows (1) the effect of the inertial platform errors on the trajectory dispersions, (2) the effect of varying the numerical values of the platform errors, and (3) the effect of the tracking bias errors.

5.1 DISPERSIONS FROM THE PLATFORM ERRORS WITHOUT TRACKING

The dispersions resulting from the inertial platform errors have been determined by propagating an initial covariance matrix (P_o), consisting of the 30 platform errors, along the nominal trajectory according to (2-19). The RMSP and the RMSV of these errors are shown in Figures 5-1 and 5-2 where the RMSP and RMSV are defined as

$$RMSP = \sqrt{P_{11} + P_{22} + P_{33}}$$

$$RMSV = \sqrt{P_{44} + P_{55} + P_{66}}$$

The total uncertainty in position and velocity at the end of the trajectory is seen to be 0.5 km and 2 m/sec, respectively. Although the three components of errors do not differ significantly, the largest error in both position and velocity is an altitude, and the smallest is in the down range direction.

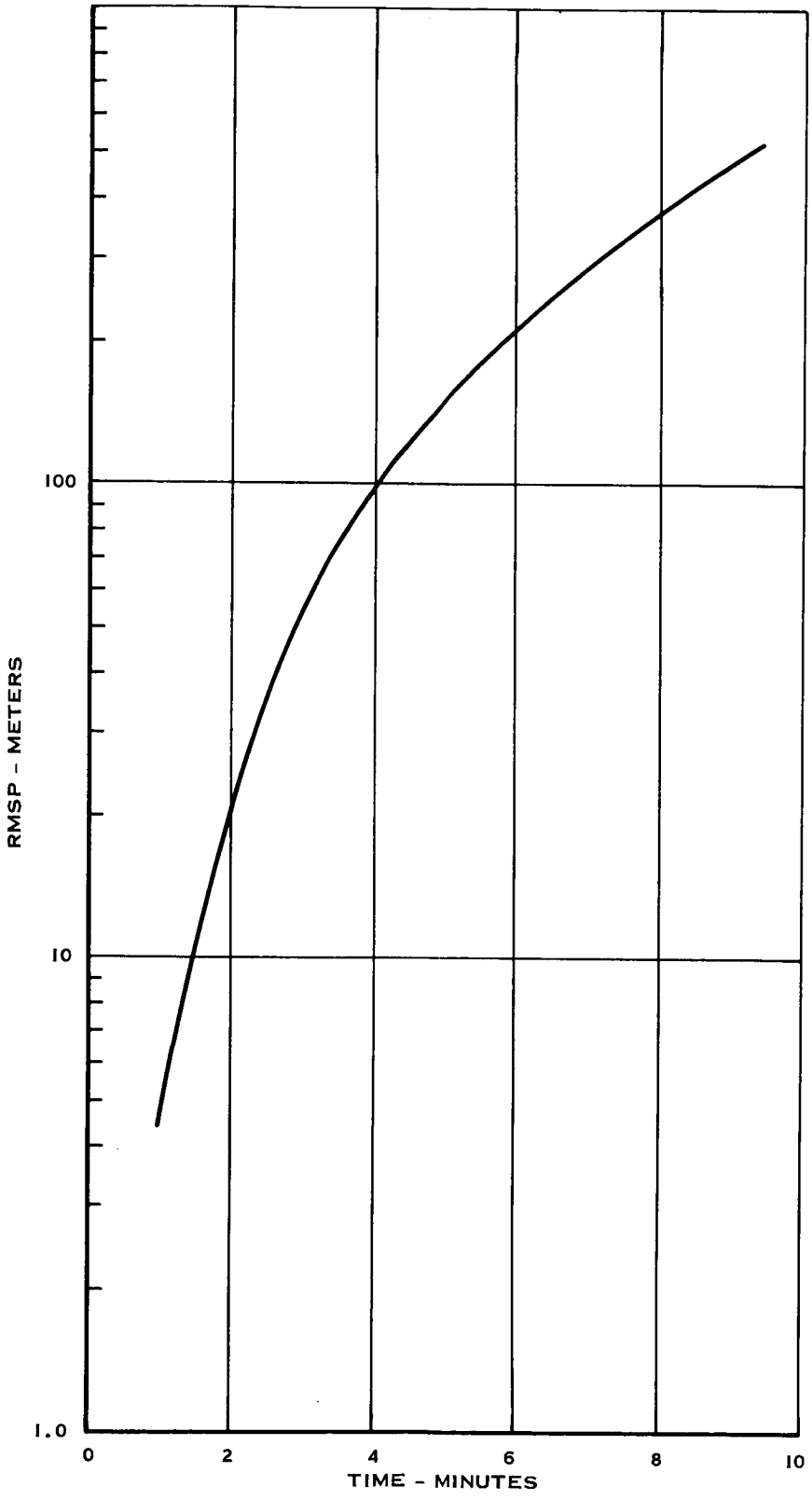

Figure 5-1 RMS Uncertainty in Position State From the 30 Platform Error Sources (No Tracking)

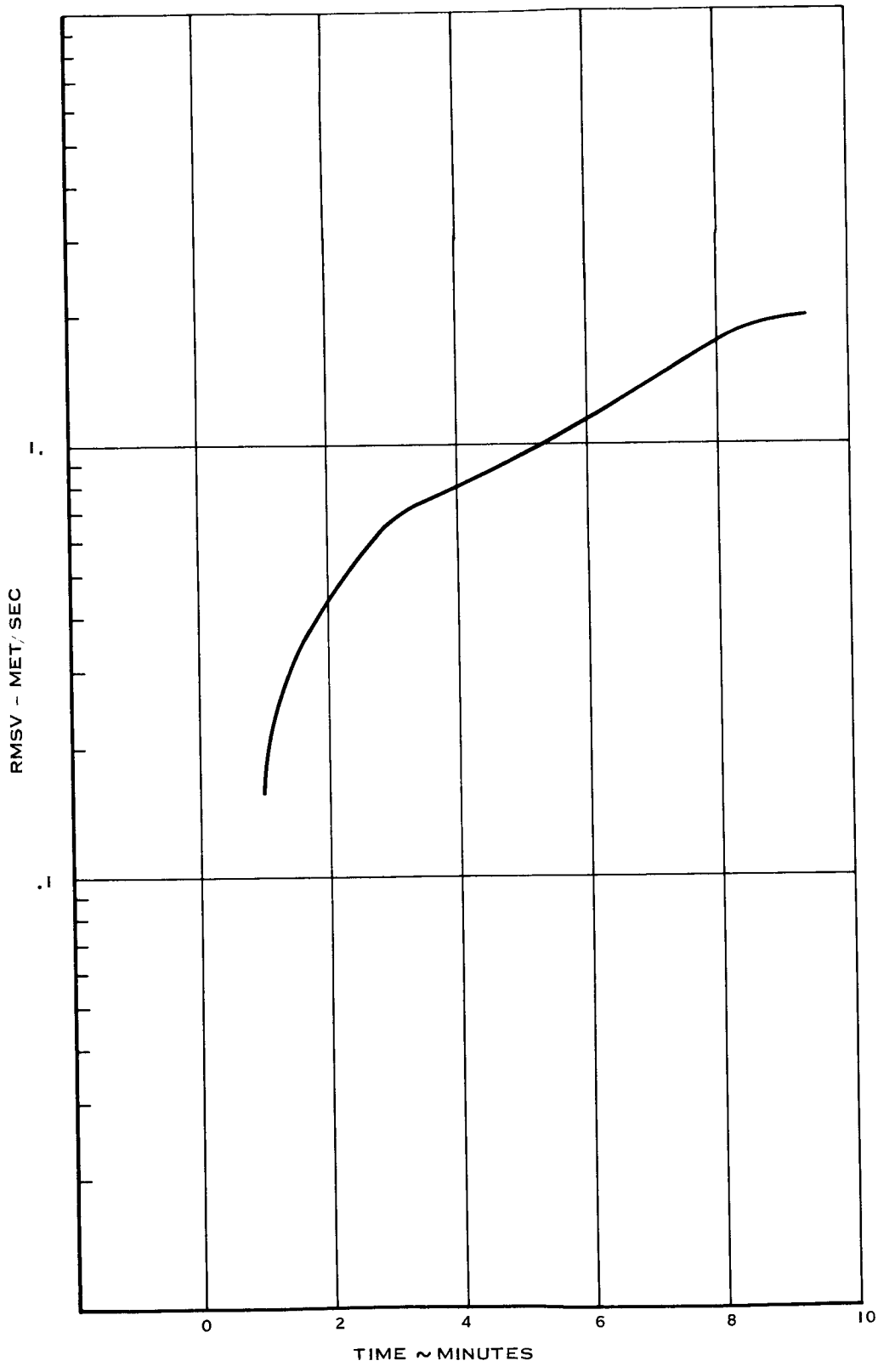

Figure 5-2 RMS Uncertainty in Velocity State from the 30 Platform Error Sources

In order to determine the relative effect of individual error sources on the total position and velocity dispersions, the effect of neglecting each of the 30 error sources has been evaluated. The effect of each error source on the position uncertainty is given by

$$\text{RMSPP} = \sqrt{\sum_{i=1}^{3} C_i \frac{1}{d} C_i^T} \quad ,$$

where each C_i is the correlation between one inertial error source and one of the three coordinates of position. Since the total position uncertainty is only from the platform error sources, the square root of the sum of the RMSPP's squared from all the error sources is equal to the 0.5 km in Figure 5-1. The relative importance of the individual error sources is shown in Table 5-1. The most significant error sources are seen to be the initial platform misalignments. The first 20 error sources listed in Table 5-1 were selected for the final error model of the inertial platform. The last 10 error sources in this table clearly have a negligible effect on the trajectory, and therefore were omitted from the final model.

TABLE 5-1 ORDER OF IMPORTANCE OF THE INERTIAL PLATFORM ERRORS

PROGRAM NO.	RANK	SOURCE		RMSPP IN METERS
17	1.	ϕ_{oy}	Initial platform misalignment about Y-axis	316
18	2.	ϕ_{oz}	Initial platform misalignment about Z-axis	213
2	3.	β_{yx}	Y Accelerometer misalignment into X-axis	146
3	4.	β_{zx}	Z Accelerometer misalignment into X-axis	134
16	5.	ϕ_{ox}	Initial platform misalignment about X-axis	129
21	6.	$\dot{\phi}_z$	Steady-state drift of Z gyro	112
4	7.	β_{xy}	X Accelerometer misalignment into Y-axis	110
6	8.	β_{zy}	Z Accelerometer misalignment into Y-axis	110
20	9.	$\dot{\phi}_y$	Steady-state drift of Y gyro	100
11	10.	α_y	Y Accelerometer bias	85
10	11.	α_x	X Accelerometer bias	77
12	12.	α_z	Z Accelerometer bias	77
1	13.	ϵ_x	X Accelerometer scale factor	65
5	14.	ϵ_y	Y Accelerometer scale factor	62
19	15.	$\dot{\phi}_x$	Steady-state drift of X gyro	38
27	16.	μ_{sz}	Spin axis mass unbalance of Z gyro	33
30	17.	C_z	Anisoelastic drift of Z gyro	32
23	18.	μ_{Iy}	Input axis mass unbalance of Y gyro	7.9

TABLE 5-1 ORDER OF IMPORTANCE OF THE INERTIAL PLATFORM ERRORS (Cont)

PROGRAM NO.	RANK	SOURCE		RMSPP IN METERS
22	19.	μ_{Ix}	Input axis mass unbalance of X gyro	6.1
15	20.	S_z	Z Accelerometer threshold	1.7
13	21.	S_x	X Accelerometer threshold	.009
8	22.	β_{yz}	Y Accelerometer misalignment into Z axis	.006
7	23.	β_{xz}	X Accelerometer misalignment into Z axis	.005
9	24.	ϵ_z	Z Accelerometer scale factor	.003
25	25.	μ_{sx}	Spin axis mass unbalance of X gyro	.002
26	26.	μ_{sy}	Spin axis mass unbalance of Y gyro	.001
24	27.	μ_{Iz}	Input axis mass unbalance of Z gyro	.0008
29	28.	E_y	Anisoelastic drift of Y gyro	$.2 \times 10^{-9}$
28	29.	C_x	Anisoelastic drift of X gyro	$.2 \times 10^{-9}$
14	30.	S_y	Y Accelerometer threshold	0

5.2 THE TRACKING MODEL

The tracking model that was used for this study consisted of significant error sources from the C-band radars. Up to nine trackers were considered. Ascension Island could not observe the vehicle until near the very end of the trajectory, and therefore the two radars at this site were not considered. The error sources at each radar consisted of random and bias errors in range, azimuth and elevation. Station location errors (latitude, longitude, and altitude) were also considered.

The numerical values of the tracking errors as well as the location of the C-band radars are listed in Table 5-2. These values were obtained from Reference 5, with the exception of the station location errors and the accuracy of the NASA tracker at Bermuda.

Since the total number of bias errors from the nine trackers could be as many as 54, a study was first made to determine the importance of these errors in order to eliminate any errors that do not significantly affect the system. This was accomplished by making two runs; first, with the measurement biases neglected, and second, with the station location errors neglected from the model. In both cases the combined inertial platform-tracking system was simulated with 20 guidance errors included in the model. The effect of neglecting the station location and measurement bias is shown in Table 5-3.

The values shown represent the effect of neglecting the individual tracking errors on both the position uncertainty and the velocity uncertainty. Since the total size of the covariance matrix (P) could be up to 60 x 60, and this number must include the 20 guidance errors and the six coordinates of position and velocity, up to 34 tracking biases could be included in the model. The tracking bias errors that were omitted from the final model are indicated in Table 5-3.

TABLE 5-2 C-BAND RADAR ACCURACIES

STATION NUMBER	STATION NAME	LAT (Deg)	LON (Deg)	ALT (ft)	RANDOM ERRORS			STATION LOCATION ERRORS*			BIAS ERRORS		
					$3\sigma_R$ (ft)	$3\sigma_A$ (mr)	$3\sigma_E$ (mr)	$3\sigma_{LAT}$ (ft)	$3\sigma_{LON}$ (ft)	$3\sigma_{ALT}$ (ft)	$3\sigma_R$ (ft)	$3\sigma_A$ (mr)	$3\sigma_A$ (mr)
	TPQ-18 RADARS												
19.18	MERRITT IS.	28.417	80.667	36.9	60	0.45	0.45	4.46	4.46	0	150	0.3	0.3
3.18	GRAND BAHAMA	26.633	78.267	39.0	60	0.45	0.45	22.3	22.3	13.4	150	0.3	0.3
7.18	GRAND TURK	21.467	71.133	118.9	60	0.45	0.45	325	325	107	150	0.3	0.3
	FPQ-6 RADARS												
91.18	ANTIQUA	17.15	61.8	138.8	60	0.45	0.45	475	475	147	150	0.3	0.3
0.18	PATRICK	28.233	80.6	48.9	60	0.45	0.45	18	18	0	150	0.3	0.3
NASA**	BERMUDA	32.348	64.654	0.0984	60	0.45	0.45	1050	1050	151	150	0.3	0.3
	FPS-16 RADARS												
1.16	CAPE KENNEDY	28.483	80.583	44.8	60	0.6	0.6	8.92	8.92	0	150	0.3	0.3
3.16	GRAND BAHAMA	26.617	78.35	45.5	60	0.6	0.6	22.3	22.3	13.4	150	0.3	0.3
NASA	BERMUDA	32.348	64.654	0.0984	60	0.6	0.6	1050	1050	151	150	0.3	0.3

*Station Location Errors, except for Bermuda, obtained from: "The accuracy of AMR instrumentation," H. P. Mann, AD #432034, Systems Analysis RCA Service Co., Patrick Air Force Base, Florida, 13 December 1963.

**NASA Tracking Station Accuracies at Bermuda obtained from: APOLLO Navigation Working Group TR No. AN-1.1- NASA Goddard, Greenbelt, Md., April 4, 1966.

TABLE 5-3

STATION	ERROR	POSITION UNCERTAINTY (RMSPP) (km)	VELOCITY UNCERTAINTY (RMSVP) (km/sec)
BERMUDA 1	La	.164	$.527 \times 10^{-3}$
BERMUDA 2	La	.163	$.524 \times 10^{-3}$
ANTIGUA	La	.134	$.889 \times 10^{-3}$
BERMUDA 1	Lo	$.548 \times 10^{-1}$	$.261 \times 10^{-2}$
BERMUDA 2	Lo	$.546 \times 10^{-1}$	$.261 \times 10^{-2}$
ANTIGUA	R	$.518 \times 10^{-1}$	$.306 \times 10^{-3}$
ANTIGUA	Lo	$.461 \times 10^{-1}$	$.330 \times 10^{-3}$
G. TURK	Lo	$.451 \times 10^{-1}$	$.569 \times 10^{-3}$
G. TURK	La	$.288 \times 10^{-1}$	$.453 \times 10^{-3}$
BERMUDA 1	R	$.212 \times 10^{-1}$	$.146 \times 10^{-3}$
BERMUDA 2	R	$.212 \times 10^{-1}$	$.146 \times 10^{-3}$
BAHAMA 1	R	$.171 \times 10^{-1}$	$.282 \times 10^{-3}$
BAHAMA 2	R	$.171 \times 10^{-1}$	$.282 \times 10^{-3}$
G. TURK	R	$.163 \times 10^{-1}$	$.189 \times 10^{-3}$
BERMUDA 2	Aℓ	$.155 \times 10^{-1}$	$.795 \times 10^{-4}$
BERMUDA 1	Aℓ	$.154 \times 10^{-2}$	$.793 \times 10^{-4}$
CAPE 5	R	$.993 \times 10^{-2}$	$.724 \times 10^{-4}$
MERIT IS.	R	$.942 \times 10^{-2}$	$.770 \times 10^{-4}$
PATRICK	R	$.920 \times 10^{-2}$	$.108 \times 10^{-4}$
ANTIGUA	Aℓ	$.842 \times 10^{-2}$	$.728 \times 10^{-4}$
G. TURK	Aℓ	$.527 \times 10^{-2}$	$.377 \times 10^{-4}$
BAHAMA 1	Lo	$.110 \times 10^{-2}$	$.259 \times 10^{-4}$
BAHAMA 2	Lo	$.109 \times 10^{-2}$	$.254 \times 10^{-4}$
BAHAMA 1	La	$.982 \times 10^{-3}$	$.229 \times 10^{-4}$
PATRICK	Lo	$.973 \times 10^{-3}$	$.108 \times 10^{-4}$
BAHAMA 2	La	$.961 \times 10^{-3}$	$.227 \times 10^{-4}$
PATRICK	E	$.925 \times 10^{-3}$	$.135 \times 10^{-4}$
MERIT IS	E	$.859 \times 10^{-3}$	$.124 \times 10^{-4}$
BERMUDA 2	E	$.828 \times 10^{-3}$	$.256 \times 10^{-5}$

TABLE 5-3 (Cont)

STATION	ERROR	POSITION UNCERTAINTY (RMSPP) (km)	VELOCITY UNCERTAINTY (RMSVP) (km/sec)
MERIT IS	A	$.764 \times 10^{-3}$	$.203 \times 10^{-4}$
PATRICK	A	$.633 \times 10^{-3}$	$.195 \times 10^{-4}$
ANTIGUA	E	$.531 \times 10^{-3}$	$.272 \times 10^{-5}$
CAPE 5	E	$.516 \times 10^{-3}$	$.720 \times 10^{-4}$
G. TURK	E	$.503 \times 10^{-3}$	$.161 \times 10^{-5}$
BERMUDA 2	A	$.498 \times 10^{-3}$	$.555 \times 10^{-5}$*
CAPE 5	A	$.482 \times 10^{-3}$	$.125 \times 10^{-4}$*
CAPE 5	Lo	$.481 \times 10^{-3}$	$.373 \times 10^{-5}$*
BAHAMA 2	Aℓ	$.477 \times 10^{-3}$	$.103 \times 10^{-4}$ *
BAHAMA 2	E	$.476 \times 10^{-3}$	$.108 \times 10^{-4}$ *
BERMUDA 1	E	$.466 \times 10^{-3}$	$.144 \times 10^{-5}$ *
BAHAMA 1	Aℓ	$.462 \times 10^{-3}$	$.101 \times 10^{-4}$ *
BAHAMA 2	A	$.445 \times 10^{-3}$	$.117 \times 10^{-4}$ *
BERMUDA 1	A	$.280 \times 10^{-3}$	$.312 \times 10^{-5}$ *
BAHAMA 1	E	$.268 \times 10^{-3}$	$.611 \times 10^{-5}$ *
G. TURK	A	$.265 \times 10^{-3}$	$.154 \times 10^{-5}$ *
BAHAMA 1	A	$.250 \times 10^{-3}$	$.656 \times 10^{-5}$ *
ANTIGUA	A	$.250 \times 10^{-3}$	$.182 \times 10^{-5}$ *
MERIT IS	Lo	$.226 \times 10^{-3}$	$.191 \times 10^{-5}$ *
PATRICK	La	$.218 \times 10^{-3}$	$.629 \times 10^{-5}$ *
CAPE 5	La	$.320 \times 10^{-4}$	$.131 \times 10^{-5}$ *
MERIT IS	La	$.274 \times 10^{-4}$	$.946 \times 10^{-6}$ *

* Denotes those error sources eliminated

The tracking model therefore consists of thirty-four tracking station error sources.

Although the selection of the tracking model has been made on the basis of the position and velocity uncertainties, the effect of neglecting tracking biases on the guidance errors has also been evaluated. Table 5-4 shows these results. The initial values of the guidance error uncertainties and the final values for the nominal model are shown. Also the final values of the guidance error standard deviations are shown for the cases where (1) all the measurement biases are neglected and (2) all the station location errors are neglected. Clearly both of these classes of error sources are too important to be neglected from the model, if the guidance errors are to be estimated.

The tracking radars that have been used for this study are in general the same ones that have been used for preliminary Saturn test flights (Reference 6).

TABLE 5-4

EFFECT OF NEGLECTING TRACKING BIASES ON THE ESTIMATION OF PLATFORM ERRORS

ERROR* SOURCE	INITIAL 3σ VALUE	FINAL 3σ VALUES		
		For Nominal Model	With Measurement Biases Neglected	With Station Location Biases Neglected
17	0.174×10^{-3}	0.632×10^{-4}	0.566×10^{-3}	0.309×10^{-3}
18	0.873×10^{-4}	0.394×10^{-4}	0.218×10^{-3}	0.474×10^{-3}
16	0.873×10^{-4}	0.312×10^{-4}	0.191×10^{-3}	0.474×10^{-3}
21	0.242×10^{-6}	0.127×10^{-6}	0.107×10^{-5}	0.351×10^{-5}
4	0.739×10^{-4}	0.352×10^{-4}	0.176×10^{-3}	0.208×10^{-3}
20	0.242×10^{-6}	0.156×10^{-6}	0.139×10^{-5}	0.122×10^{-5}
11	0.5×10^{-6}	0.396×10^{-6}	0.167×10^{-5}	0.240×10^{-5}
10	0.5×10^{-6}	0.333×10^{-6}	0.271×10^{-5}	0.660×10^{-5}
12	0.5×10^{-6}	0.448×10^{-6}	0.310×10^{-5}	0.653×10^{-5}
1	0.36×10^{-4}	0.203×10^{-4}	0.141×10^{-3}	0.310×10^{-3}
5	0.36×10^{-4}	0.197×10^{-4}	0.207×10^{-3}	0.355×10^{-3}
19	0.242×10^{-6}	0.229×10^{-6}	0.560×10^{-6}	0.126×10^{-5}
27	0.371×10^{-4}	0.370×10^{-4}	0.570×10^{-4}	0.429×10^{-4}
30	0.201×10^{-2}	0.201×10^{-4}	0.386×10^{-2}	0.231×10^{-2}
23	0.148×10^{-4}	0.148×10^{-4}	0.151×10^{-4}	0.154×10^{-4}
22	0.148×10^{-4}	0.148×10^{-4}		
15	0.2×10^{-7}	0.200×10^{-7}		

*These numbers refer to program number assigned to each error source in Table 5.1

SECTION 6

THE ESTIMATION OF INERTIAL PLATFORM ERRORS

The principal results of the study are presented in this section. These results show the feasibility of estimating the inertial platform errors during a powered flight ascent by combining the telemetry and tracking data.

The general method that has been used is to examine the behavior of a covariance matrix of error dispersions along the nominal trajectory. In particular, the amount by which the standard deviations of the guidance errors reduced, was used as a criterion. Although no absolute figure of merit has been defined for the amount by which these standard deviations decrease, it has been assumed that a decrease in the 3σ value of an error source by an order of magnitude, would be significant; conversely, if the standard deviation of a particular error was reduced by a small percentage, it has been assumed that this error source could not be estimated very well in an actual fitting process using real telemetry and tracking data.

In addition to the results for the nominal platform-tracking model, the results of a number of parametric variations of the error sources are presented. The objective for studying the error sources parametrically was twofold. First, it was desired to determine whether the ability to estimate each of the error sources depended on the relative accuracies of the guidance error compared to the tracking accuracies, or whether there are certain error sources that cannot be estimated regardless of the relative accuracies. The second reason for presenting parametric data was simply to show how the results changed for changes in significant parameters of the model.

6.1 ESTIMATION OF PLATFORM ERRORS WITH NOMINAL TRACKING

A simulation of the combined platform-tracking system has been made with an error model that includes (1) the first 20 guidance errors in Table 5-1, (2) the first 34 tracking errors in Table 5-3, and (3) the uncertainties in the six components of position and velocity. Although the primary objective was to evaluate the behavior of the standard deviations of the guidance errors, the uncertainty in the vehicle position (RMSP) and velocity (RMSV) have also been included in the results.

The uncertainties in the vehicle position and velocity are about 30 meters and 0.2 meters/sec as shown in Figures 6-1 and 6-2.* A breakdown of these uncertainties into the DR, CR, and UP directions is also shown in the figures. Although the magnitude of the dispersions has been reduced considerably from the case where there was no tracking (Section 5.1), the largest uncertainty is still the UP direction and the smallest is in the DR direction.

As a point of interest, the ability to estimate the vehicle position and velocity with the combined platform-tracking model was compared with an estimate of the vehicle state with tracking only. In the complete version of this summary report, the RMSP and RMSV were shown for large initial uncertainties and no guidance errors in the model (Fig. 6-3, Philco-Ford SRS TR-DA1569.) The position errors were less for the case where the tracking and telemetry data were used; however, the velocity errors were actually worse for this case. Upon closer examination of these results, it has been concluded that the assumption of a large initial uncertainty and no guidance errors in the model is not a fair evaluation of the value of the tracking and telemetry data, compared to the tracking data alone. An additional run was, therefore, made where the guidance errors were included in the model, but they were not estimated. This is the "consider" mode for error propagation (see Reference 3), and enables the estimation process to account for the effect of guidance errors without reducing their uncertainties. The results of this simulation are shown in Figures 6-3(a) and 6-3(b).

*Figures appear at end of Section 6.

A comparison of Figures 6-1 and 6-3(a), as well as 6-2 and 6-3(b), shows that the estimate of the position-velocity state would improve if the telemetry data were included in an actual estimation of the state. This effect is more pronounced for the velocity (.18 m/sec in Figure 6-2 vs .34 m/sec in Figure 6-3(b). The position state is also improved with telemetry and tracking data (31 m in 6-1 vs 34 in 6-3(a)); however, the improvement seems to be limited by the uncertainties in the CR and UP directions. The uncertainty in the DR direction improves by almost a factor of 2 (3.7 m in Figure 6-1 vs 7 m in 6-3(a)).

The behavior of the guidance error standard deviations for nominal tracking may be summarized with the aid of Table 6-1. The initial and final values of the standard deviations are shown as well as the percentage decrease. Five error sources showed no improvement along the trajectory for the nominal case. These sources are:

1. Spin axis mass unbalance of the Z gyro
2. Anisoelastic drift Z gyro
3. Input axis mass unbalance of the Y gyro
4. Input axis mass unbalance of the X gyro
5. Threshold of the Z accelerometer

Typical time histories of the standard deviations of guidance errors which did reduce are shown in Figures 6-4 through 6-7. Curve No. 1 pertains to the nominal case.

In general, the greatest improvement in the standard deviations occurred for those error sources which caused the largest dispersion in the trajectory as shown in Table 5-1. An additional explanation for some specific component errors may be found in terms of the acceleration levels. As shown in Figure 4-3, the acceleration in the Z direction (CR) is very small. As a result, the components that cause errors in this direction have less effect and, therefore, their deviations do no improve significantly.

TABLE 6-1

PERCENTAGE DECREASE IN GUIDANCE ERROR UNCERTAINTIES FOR NOMINAL TRACKING

ERROR SOURCE*	INITIAL 3σ VALUE	FINAL 3σ VALUE	PERCENT CHANGE
17	0.174-3	0.869-4	50
18	0.873-4	0.492-4	44
2	0.739-4	0.52-4	30
3	0.739-4	0.688-4	7
16	0.873-4	0.594-4	32
21	0.242-6	0.132-6	45
4	0.739-4	0.474-4	36
6	0.739-4	0.579-4	22
20	0.242-6	0.158-6	35
11	0.5-6	0.418-6	16
10	0.5-6	0.334-6	33
12	0.5-6	0.448-6	10
1	0.36-4	0.203-4	43
5	0.36-4	0.198-4	45
19	0.242-6	0.229-6	5
27	0.371-4	0.371-4	No Change
30	0.202-2	0.202-2	No Change
23	0.148-4	0.148-4	No Change
22	0.148-4	0.148-4	No Change
15	0.2-7	0.2-7	No Change

*The numbers in this column are program numbers. See Table 5-1 for the corresponding error source.

For example, the improvement in the knowledge of the Z accelerometer misalignments in the X (No. 3), or Y (No. 6) direction is less than that of the X accelerometer misalignment in the Y direction (No. 4), or the Y accelerometer in the X direction (No. 2). Also the improvement in the Z accelerometer bias (No. 12) was smaller than the improvement in the X or Y accelerometer biases (Numbers 10 and 11). (See Table 6-1 for these comparisons.)

The results of simulating the combined platform-tracking system indicate that it would not be possible, at least for the values of the tracking accuracies that have been assumed, to significantly improve the uncertainty of the platform error sources. Therefore if the only objective is to update the guidance system during a flight, this method would not be feasible, assuming the guidance errors were equal or less than their 3σ values. However, if the objective is a postflight analysis, or if the tracking is improved, the conclusion may be considerably different.

6.2 ESTIMATION OF GUIDANCE ERRORS WITH ADDITIONAL KNOWLEDGE OF PLATFORM

In the previous section, the results were presented for the estimation of the guidance errors with nominal tracking. In succeeding sections, the estimation of these errors for improved tracking and degraded guidance errors will be presented. However, before discussing the results for parametric variations of the platform-tracking system, an important point concerning the correlation between the initial platform errors (errors in the accelerometer misalignments and the gyro misalignments) should be noted.

Preliminary results for estimating the guidance errors with improved tracking showed that there was little improvement in the uncertainty of the gyro misalignments or the accelerometer misalignments regardless of how good the tracking was. This indicated that there was not enough information in the combined platform-tracking system to distinguish between

platform misalignments and accelerometer misalignments. The complete covariance matrix for the nominal simulation is included in Appendix A, and can be used to explain this result. It shows that the normalized correlations between (1) the Y accelerometer misalignment to the X axis and the platform misalignment about the Z axis ($C_{2/18}$), (2) Z accelerometer misalignment to the X axis and the platform misalignment about the Y axis ($C_{3/17}$), and (3) the Z accelerometer misalignment about the Y axis and the platform misalignment about the X axis, ($C_{6/16}$), are almost unity. As a result a large uncertainty in these three accelerometer misalignments prevents an improvement in the knowledge of the initial platform misalignments.

In order to see the effect of additional knowledge of the platform on the estimation of the initial gyro misalignments, an additional simulation was made assuming no errors in (1) the Z accelerometer misalignment about the Y axis, (2) the Z accelerometer misalignment about the X axis and (3) the misalignment of the Y accelerometer about the X axis. For the nominal tracking with these three errors omitted the uncertainties in the three initial gyro misalignments and the misalignment of the X accelerometer about the Y axis reduces as shown in Figures 6-4 through 6-7, curve (2).

There is additional justification for omitting these three platform error sources. As stated in Reference 1 the misalignments of the Z accelerometers would be eliminated before the flight by aligning the X-Y plane. In addition some calibration on either the X accelerometer or Y accelerometer would be necessary in order to be able to predict excessive variations in the initial gyro drift about the Z axis. This was evident from runs that were made with all five accelerometer misalignments. The result was that for very large values of the initial variances of the gyro misalignments, or very good tracking, no significant improvement was found in the uncertainty of the gyro misalignments at the end of the trajectory.

For the parametric results that are presented in the following sections, the following accelerometer errors were omitted from the model:

1. Z accelerometer misalignment in the direction of the X axis
2. Z accelerometer misalignment in the direction of the Y axis
3. Y accelerometer misalignment in the direction of the X axis.

6.3 ESTIMATION OF GUIDANCE ERRORS WITH IMPROVED TRACKING

Due to the fact that the ability to estimate the guidance errors with nominal tracking has been found to be somewhat marginal, a number of studies were made to investigate the system parametrically. The first parametric study involved the tracking accuracies. Runs were made with all the tracking error standard deviations (random and bias measurement errors, and station location errors) reduced by factors of 10, 100, 1000, and finally, with random errors reduced by a factor of 1000 and no bias errors. These results are shown in Table 6-2. Typical time history for the behavior of the guidance error standard deviations with improved tracking are shwon in Figures 6-4 through 6-7. As shown in Table 6-2, all of the significant guidance error uncertainties can be improved with better tracking. Again, in general, the amount by which the guidance errors improve depends on their relative effect on the trajectory. Of the total 17 guidance error sources, the three errors which have the least effect on the trajectory are:

(1) The input mass unbalance of the Y gyro
(2) The input mass unbalance of the X gyro
(3) The Z accelerometer threshold error

The uncertainty in these error sources does not improve significantly even with good tracking.

TABLE 6-2

DECREASE IN GUIDANCE ERROR UNCERTAINTIES WITH IMPROVED TRACKING

ERROR* SOURCE	INITIAL 3σ VALUE	3σ VALUE AT END OF TRAJECTORY				
		NOMINAL TRACKING	Q/10	Q/100	Q/1000	Q/1000 NO TRACKING BIASES
17	.174-3	.632-4	.226-4	.622-5	.385-5	.143-5
18	.873-4	.394-3	.932-5	.134-5	.102-5	.749-7
16	.873-4	.312-4	.655-5	.185-5	.178-5	.139-5
21	.242-6	.127-6	.241-7	.414-8	.208-8	.194-9
4	.739-4	.352-4	.816-5	.932-6	.774-6	.763-7
20	.242-6	.156-6	.544-7	.127-7	.809-8	.295-8
11	.5-6	.396-6	.144-6	.213-7	.143-7	.146-8
10	.5-6	.332-6	.85-7	.136-7	.725-8	.637-9
12	.5-6	.448-6	.14-6	.31-7	.267-7	.198-7
1	.36-4	.203-4	.5-5	.9-6	.416-6	.384-7
5	.36-4	.197-4	.648-5	.107-5	.730-6	.644-7
19	.242-6	.229-6	.148-6	.42-7	.152-7	.249-8
27	.371-4	.370-4	.354-4	.304-4	.255-4	.391-5
30	.202-2	.201-2	.175-2	.1-2	.884-3	.139-3
23	.148-4	--	--	--	--	--
22	.148-4	--	--	--	--	--
15	.2-7	--	--	--	--	--

*The numbers in this Column are program numbers. See Table 5-1 for the corresponding error source.

From the results presented in this section it may be concluded that, in general, the feasibility of estimating the guidance errors does depend on the relative accuracies of the guidance errors and the tracking errors.

Approximately one order of magnitude improvement in the tracking accuracies would be required to obtain a significant improvement in the guidance error uncertainties during an actual flight. In addition this improvement would be contingent on a preflight calibration of three of the accelerometer misalignments.

6.4 ESTIMATION OF GUIDANCE ERRORS WITH PERFECT KNOWLEDGE OF THE TRAJECTORY END POINT

One method that was considered for improving the estimate of the guidance errors was to track the vehicle in a parking orbit. That is, the telemetry data and the tracking data would be combined in the same manner, only for a parking orbit rather than a powered flight ascent. The end result of this simulation would be an improvement in the knowledge of the end point of the powered flight trajectory.

Before simulating the system for a parking orbit, a check was made to determine the effect of perfect knowledge of the trajectory end point.

This would show the maximum decrease in the uncertainty of the guidance errors and would represent the results for perfect tracking. Six equivalent observations were made of the position and velocity states with zero error variance. The results are summarized in Table 6-3. As shown in the table there is very little improvement in the uncertainty of the guidance errors by a perfect knowledge of the trajectory end point. This indicates that there is even less knowledge that would be added to the guidance error uncertainties as a result of tracking the vehicle in a parking orbit. The parking orbit simulation was therefore not implemented.

TABLE 6-3

THE EFFECT OF A PERFECT KNOWLEDGE OF THE TRAJECTORY END-POINT ON THE GUIDANCE ERROR UNCERTAINTIES

ITEM		NOMINAL @ t=9.5 MIN.	PERFECT OBSERVATION OF POSITION VELOCITY STATE @ t=9.5 MIN.
RMSP		0.938×10^{-2}	0.754×10^{-6}
RMSV		0.695×10^{-4}	0.697×10^{-8}
ERROR* SOURCE	17	0.874×10^{-4}	0.847×10^{-4}
	18	0.489×10^{-4}	0.473×10^{-4}
	16	0.599×10^{-4}	0.586×10^{-4}
	21	0.100×10^{-6}	0.599×10^{-7}
	4	0.478×10^{-4}	0.464×10^{-4}
	20	0.146×10^{-6}	0.127×10^{-6}
	11	0.423×10^{-6}	0.418×10^{-6}
	10	0.350×10^{-6}	0.319×10^{-6}
	12	0.457×10^{-6}	0.435×10^{-6}
	1	0.211×10^{-4}	0.206×10^{-4}
	5	0.221×10^{-4}	0.182×10^{-4}
	19	0.228×10^{-6}	0.208×10^{-6}

*The numbers in this Column are program numbers. See Table 5-1 for the corresponding error source.

6.5 ESTIMATION OF GUIDANCE ERROR WITH LARGE INITIAL UNCERTAINTIES

In addition to using the combined platform-tracking system to improve the knowledge of the vehicle state, or to update the guidance system during a flight, a third and perhaps more useful application would be in a post-flight analysis. For this latter objective it would be desirable to determine whether the guidance components performed normally, or whether there was a malfunction.

To evaluate the feasibility of estimating the guidance errors in a post-flight analysis, the combined platform-tracking system has been simulated for parametric variations in the guidance errors themselves. Large initial values of the guidance error standard deviations have been assumed to simulate a malfunction or a component error that was larger than predicted by the 3σ nominal value.

A typical time history of the standard deviation of a guidance error with a large initial uncertainty is shown in Fig. 6-8. A summary of these results for all the guidance errors in the model, is given in Table 6-4. Again, results are not included for the three accelerometer errors Z to X, Z to Y, and Y to X. It was found that with these error sources in the model, the standard deviations of the gyro misalignments did not decrease, even for large initial values of guidance errors. However, with the assumption of a perfect knowledge of these errors, it is possible to reduce the uncertainty in the gyro misalignments. The results in Table 6-4 indicate that the uncertainties in the most important guidance errors reduce significantly for large initial values of these uncertainties. The uncertainties in the four least significant error sources (30, 23, 22, and 15) do not decrease. However, this is because even with initial values of 1000 times the nominal initial values, these error sources do not have a significant effect on the trajectory.

TABLE 6-4

BEHAVIOR OF GUIDANCE ERROR UNCERTAINTIES
WITH
LARGE INITIAL VALUES OF THE ERROR SOURCES

ERROR SOURCE*	3σ VALUE AT END OF TRAJECTORY			
	FOR NOMINAL VALUE OF INITIAL STANDARD DEV	FOR LARGE INITIAL UNCERTAINTIES		
		σ_g X 10	σ_g X 100	σ_g X 1000
17	.632-4	.206-3	.379-3	.151-6
18	.394-3	.914-4	.109-3	.130-3
16	.312-4	.624-4	.177-3	.141-2
21	.127-6	.217-6	.299-6	.407-6
4	.352-4	.797-4	.837-4	.884-4
20	.150-6	.486-6	.799-6	.309-5
11	.396-6	.139-5	.175-5	.179-5
10	.332-6	.832-6	.977-6	.109-5
12	.448-6	.130-5	.278-5	.2-4
1	.203-4	.448-4	.569-4	.628-4
5	.197-4	.617-4	.871-4	.891-4
19	.229-6	.125-5	.160-5	.262-5
27	.370-4	.354-3	.287-2	.63-2
30	.201-2	.174-1	.942-1	.202
23	.148-4	.148-3	.146-2	.112-1
22	.148-4	.148-3	.146-2	.116-1
15	.2-7	.2-6	.2-5	.185-4

*The numbers in this Column are program numbers. See Table 5-1 for the corresponding error source.

Based on the results in Table 6-4, it may be concluded that it would be feasible to estimate the guidance errors in a post-flight analysis. That is, it would be possible to distinguish between those guidance errors which performed nominally, and any error source whose numerical value on a particular flight was considerably greater than its 3 σ value.

6.6 ESTIMATION OF GUIDANCE ERRORS WITH INCREASED OBSERVATION RATE

For the nominal tracking model an observation rate of one per second was used. One additional run was made to determine the effect of a reduced observation rate on the guidance error uncertainties. Table 6-5 shows a comparison of the guidance error uncertainties for 1 observation per second and 10 observations per second at 7 minutes along the trajectory. A decrease in the observation rate by an order of magnitude is seen to reduce the guidance error uncertainties by at most a factor of 2. The RMSP and RMSV are also shown in the table for the two observation rates.

TABLE 6-5

VARIATION OF GUIDANCE ERRORS, POSITION AND VELOCITY WITH OBSERVATION RATE

		STATES AT 7 MIN.	
		NOMINAL CASE OBS ~ 1 SEC	OBS ~ 0.1 SEC
RMSP		0.193×10^{-1}	0.808×10^{-2}
RMSV		0.160×10^{-3}	0.775×10^{-4}
GUIDANCE ERROR* SOURCE	17	0.653×10^{-4}	0.439×10^{-4}
	18	0.415×10^{-4}	0.287×10^{-4}
	16	0.336×10^{-4}	0.245×10^{-4}
	21	0.179×10^{-6}	0.130×10^{-6}
	4	0.401×10^{-4}	0.250×10^{-4}
	20	0.200×10^{-6}	0.156×10^{-6}
	11	0.410×10^{-6}	0.337×10^{-6}
	10	0.340×10^{-6}	0.233×10^{-6}
	12	0.460×10^{-6}	0.366×10^{-6}
	1	0.254×10^{-4}	0.189×10^{-4}
	5	0.232×10^{-4}	0.175×10^{-4}
	19	0.239×10^{-6}	0.237×10^{-6}
	27	0.370×10^{-4}	0.371×10^{-4}
	30	0.201×10^{-2}	0.202×10^{-2}
	23	0.148×10^{-4}	0.148×10^{-4}
	22	0.148×10^{-4}	0.148×10^{-4}
	15	0.200×10^{-7}	0.200×10^{-4}

*The numbers in this Column are program numbers. See Table 5-1 for the corresponding error source.

6.7 ESTIMATION OF GUIDANCE ERRORS WITH DIFFERENT KINDS OF TRACKING

In order to determine which type of tracking is the most effective for reducing the guidance error uncertainties, two runs were made; one with range observations only, and a second run with azimuth and elevation measurements only.

Position uncertainty (RMSP) and velocity uncertainty (RMSV) for these two cases are shown in Figures 6-9 and 6-10, respectively. The uncertainty in the guidance errors at the end of each of these runs is shown in Table 6-6.

The results of this study show very little difference between the effectiveness of range measurements and azimuth and elvation measurements.

TABLE 6-6

VARIATION OF GUIDANCE ERRORS FOR DIFFERENT TRACKING @ t=9.5 MIN.

		RANGE ONLY	AZ&EL ONLY
RMSP		0.944×10^{-1}	0.853×10^{-1}
RMSV		0.485×10^{-3}	0.421×10^{-3}
GUIDANCE ERROR* SOURCE	17	0.751×10^{-4}	0.705×10^{-4}
	18	0.417×10^{-4}	0.480×10^{-4}
	16	0.369×10^{-4}	0.414×10^{-4}
	21	0.195×10^{-6}	0.178×10^{-6}
	4	0.370×10^{-4}	0.486×10^{-4}
	20	0.170×10^{-6}	0.210×10^{-6}
	11	0.409×10^{-6}	0.432×10^{-6}
	10	0.357×10^{-6}	0.459×10^{-6}
	12	0.467×10^{-6}	0.475×10^{-6}
	1	0.222×10^{-4}	0.336×10^{-4}
	5	0.207×10^{-4}	0.300×10^{-4}
	19	0.231×10^{-6}	0.239×10^{-6}
	27	0.370×10^{-4}	0.371×10^{-4}
	30	0.201×10^{-2}	0.201×10^{-2}
	23	0.148×10^{-4}	0.148×10^{-4}
	22	0.148×10^{-4}	0.148×10^{-4}
	15	0.200×10^{-7}	0.200×10^{-7}

*The numbers in this Column are program numbers. See Table 5-1 for the corresponding error source.

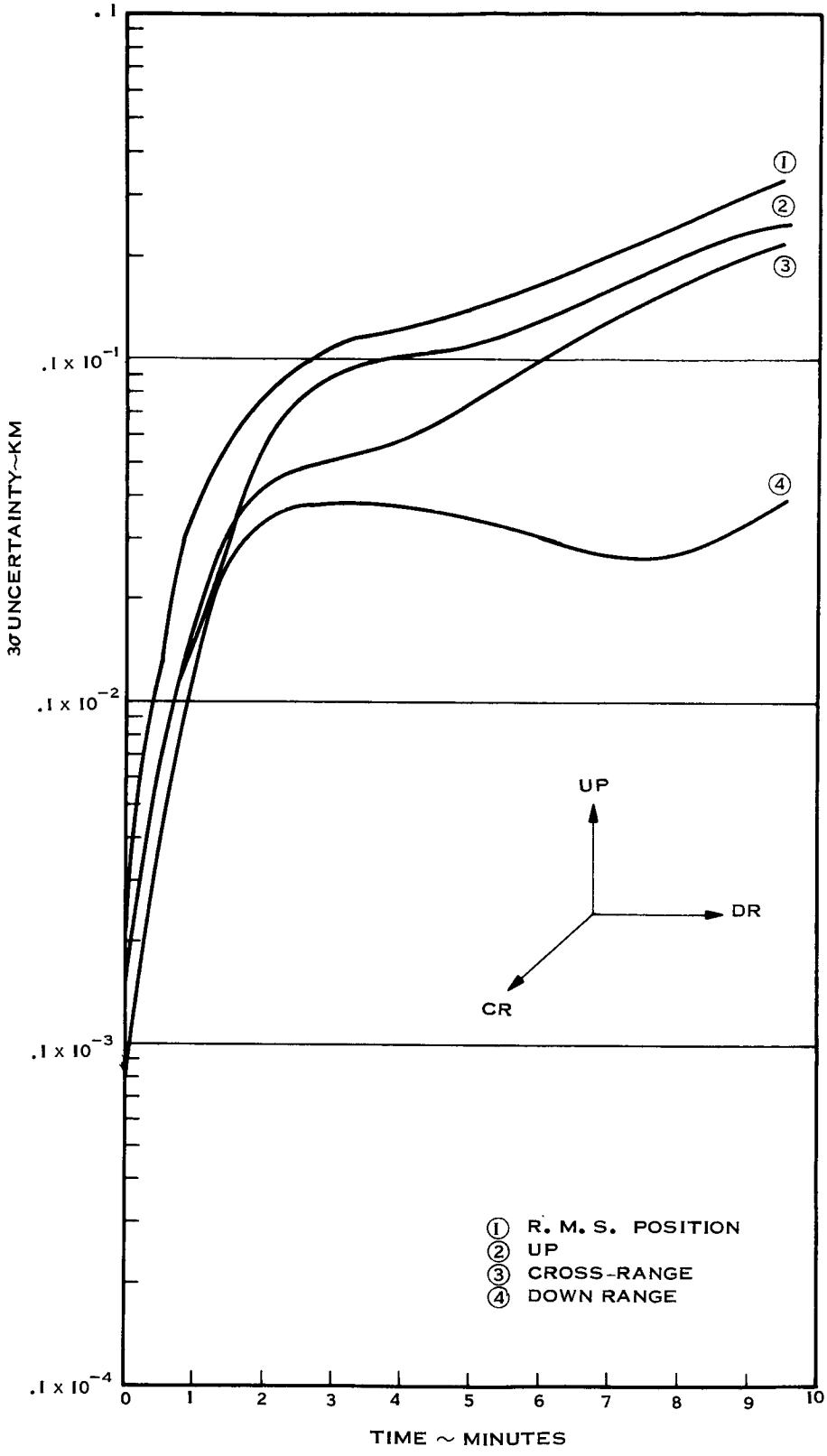

Figure 6-1 Variation in Position Uncertainties ~ Nominal Case

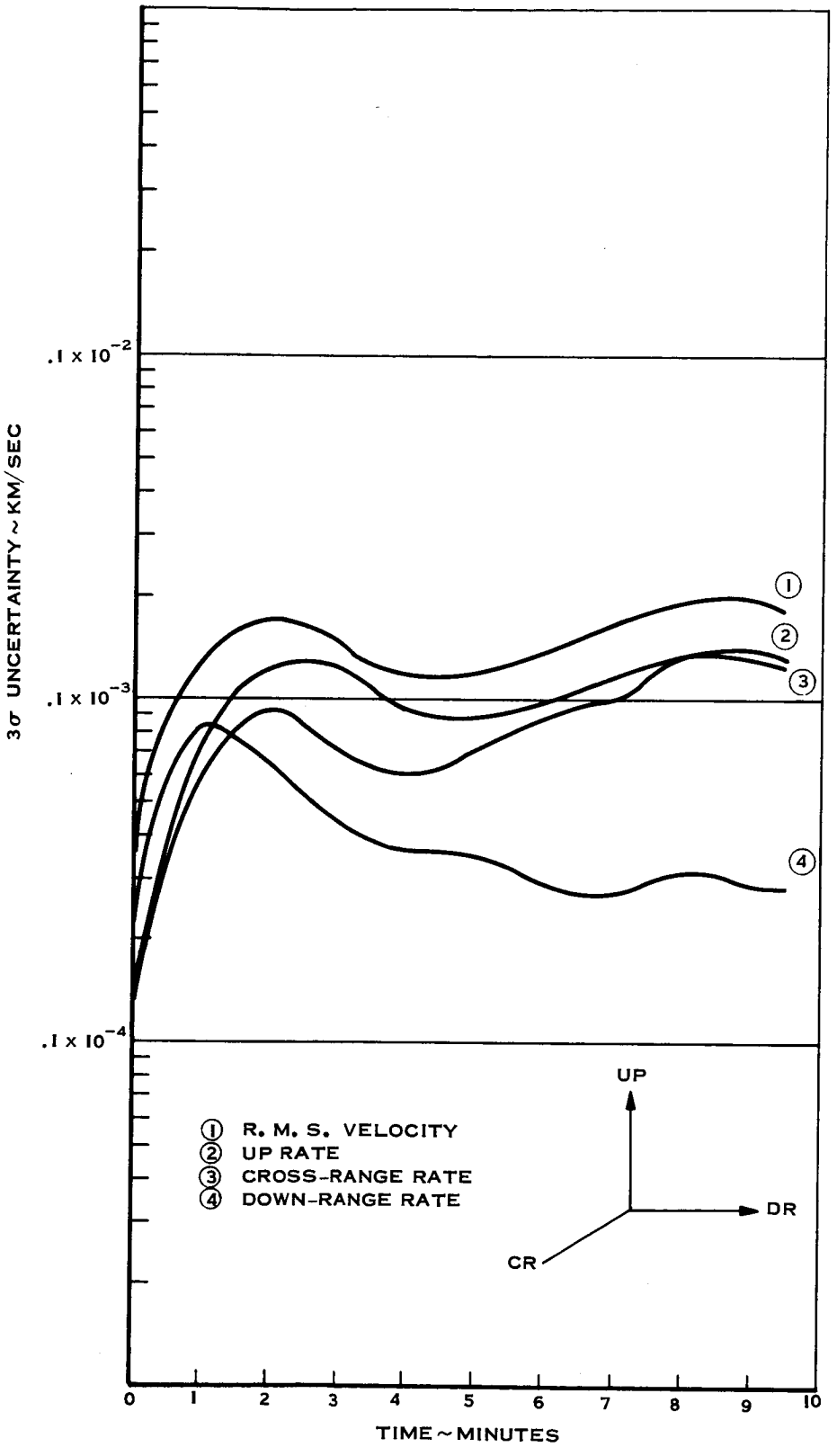

Figure 6-2 Variation in Velocity Uncertainties ~ Nominal Case

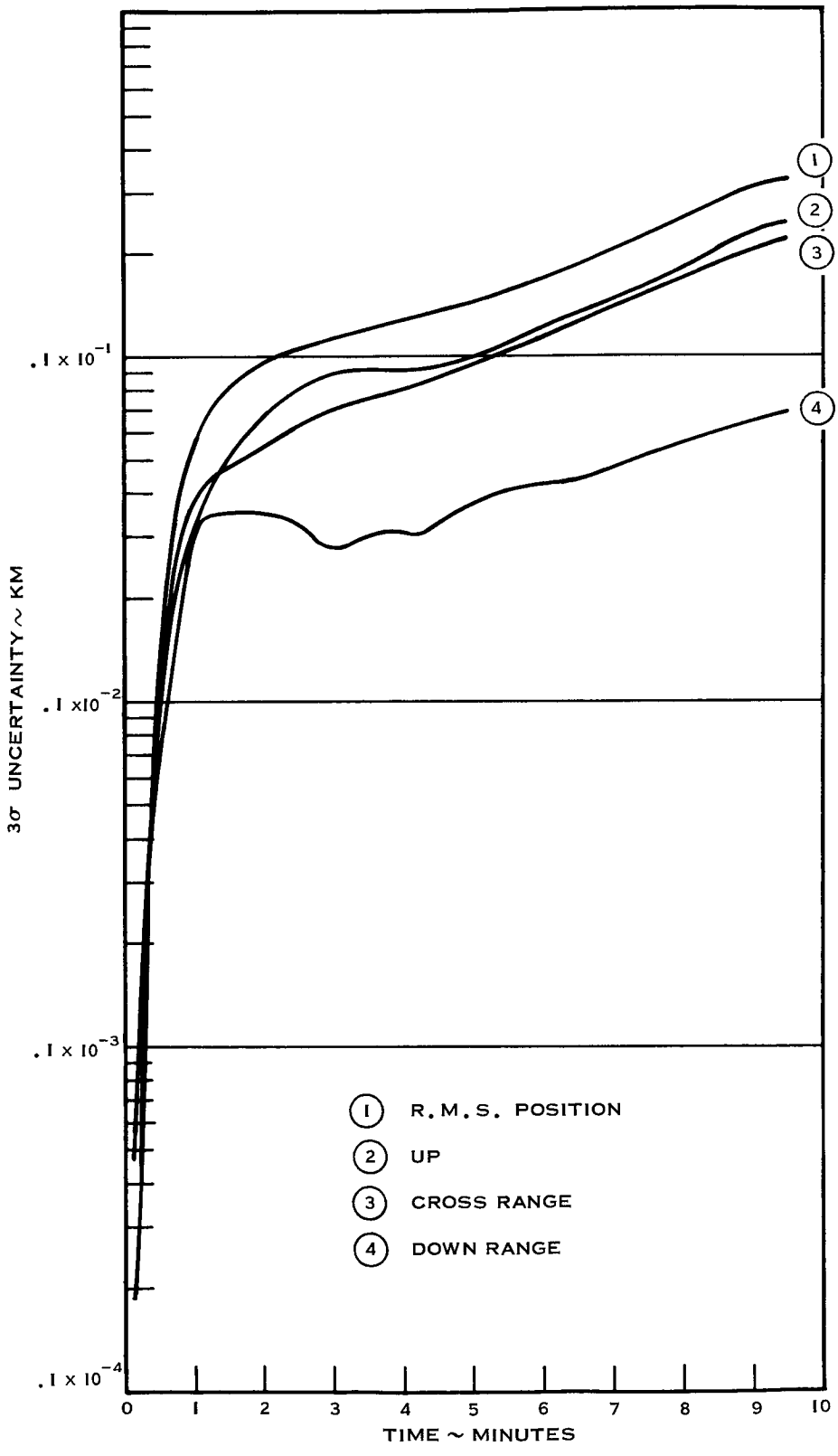

Figure 6-3a Variation in Position Uncertainties ~ Tracking Only (Guidance Errors Not Estimated.)

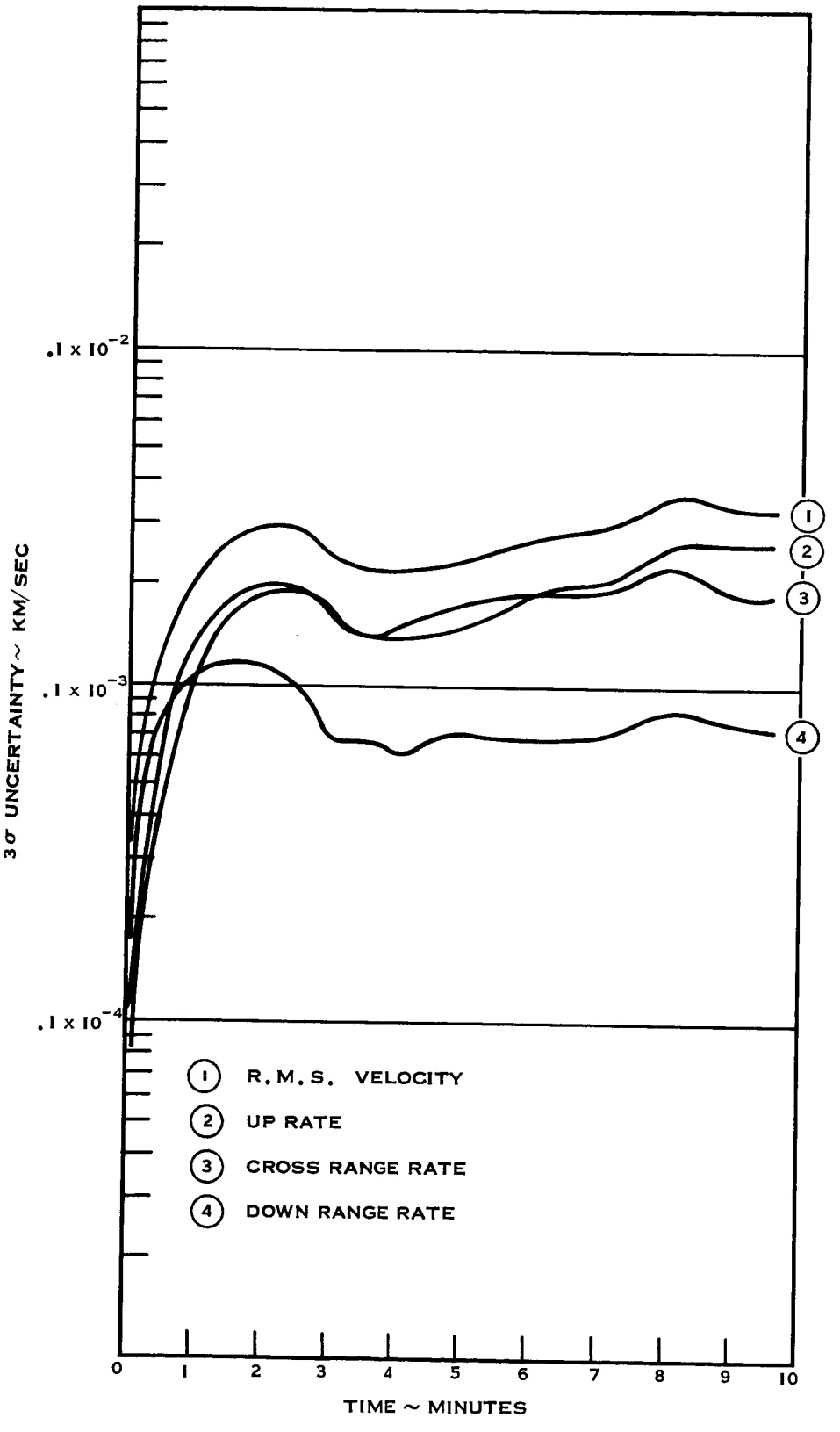

Figure 6-3b Variation in Velocity Uncertainties ~ Tracking Only (Guidance Errors Not Estimated.)

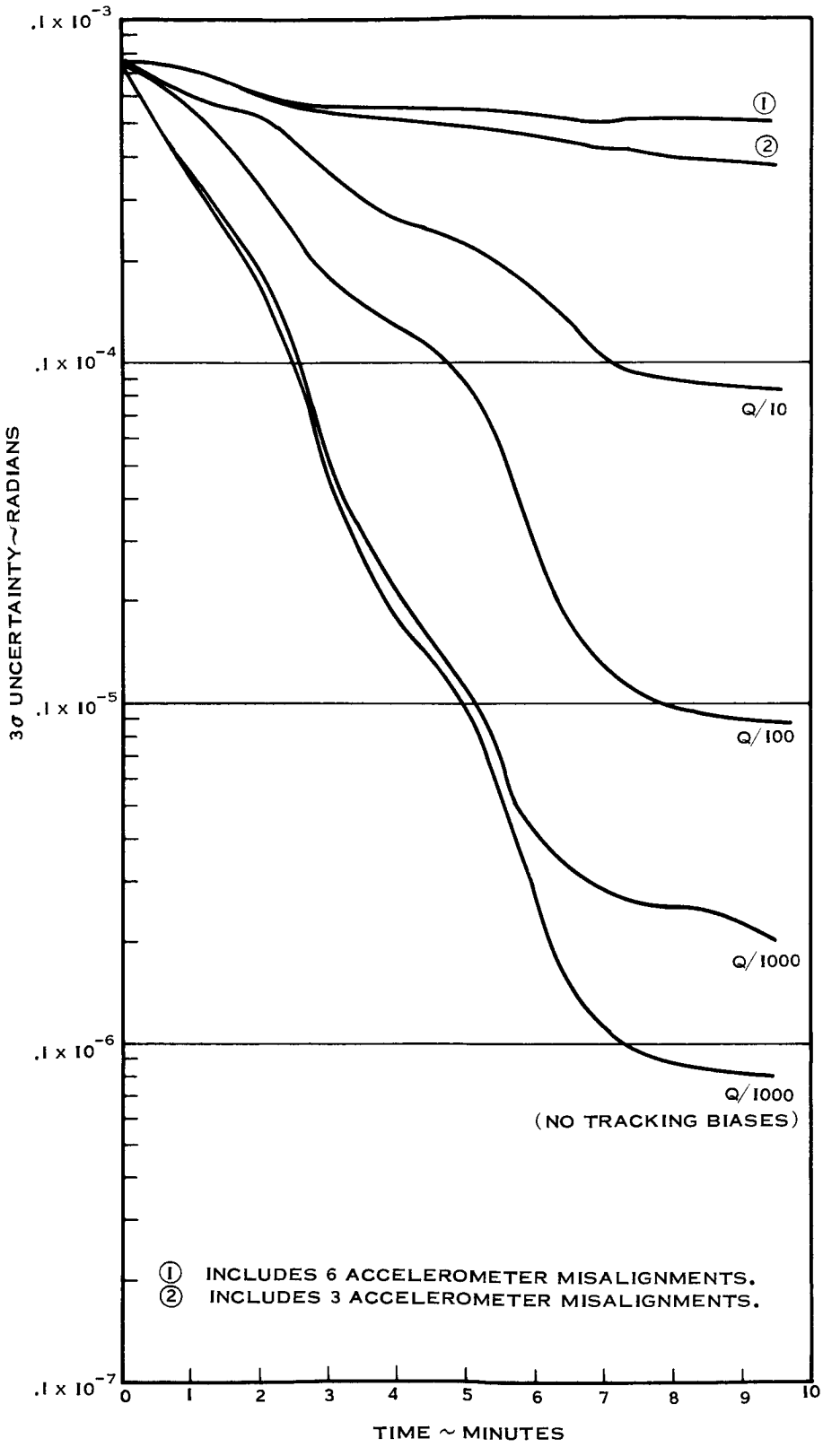

Figure 6-4 3σ Uncertainty in X-Accelerometer Misalignment Into Y-Axis

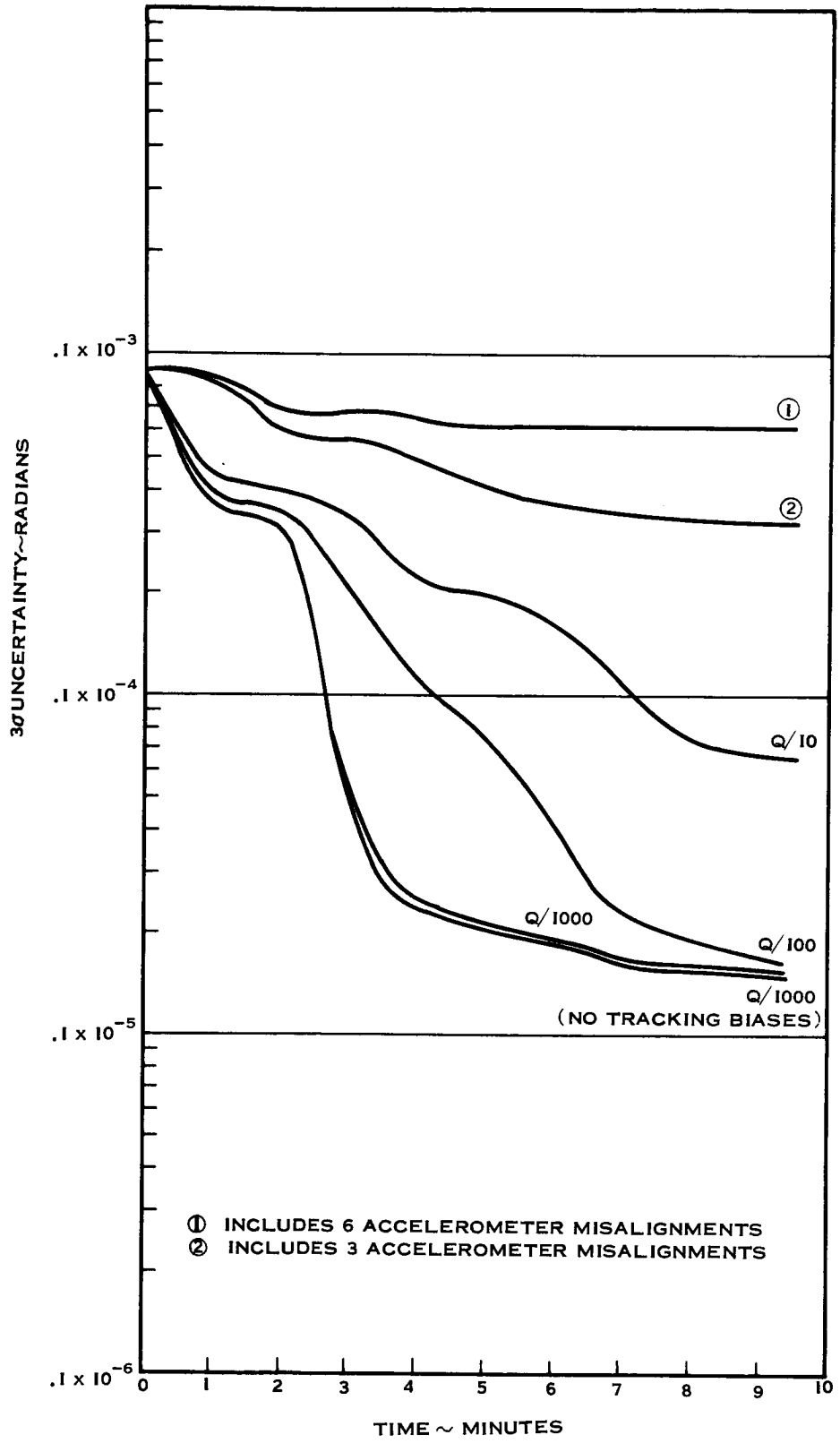

Figure 6-5 3σ Uncertainty in Initial Platform Misalignment About X-Axis

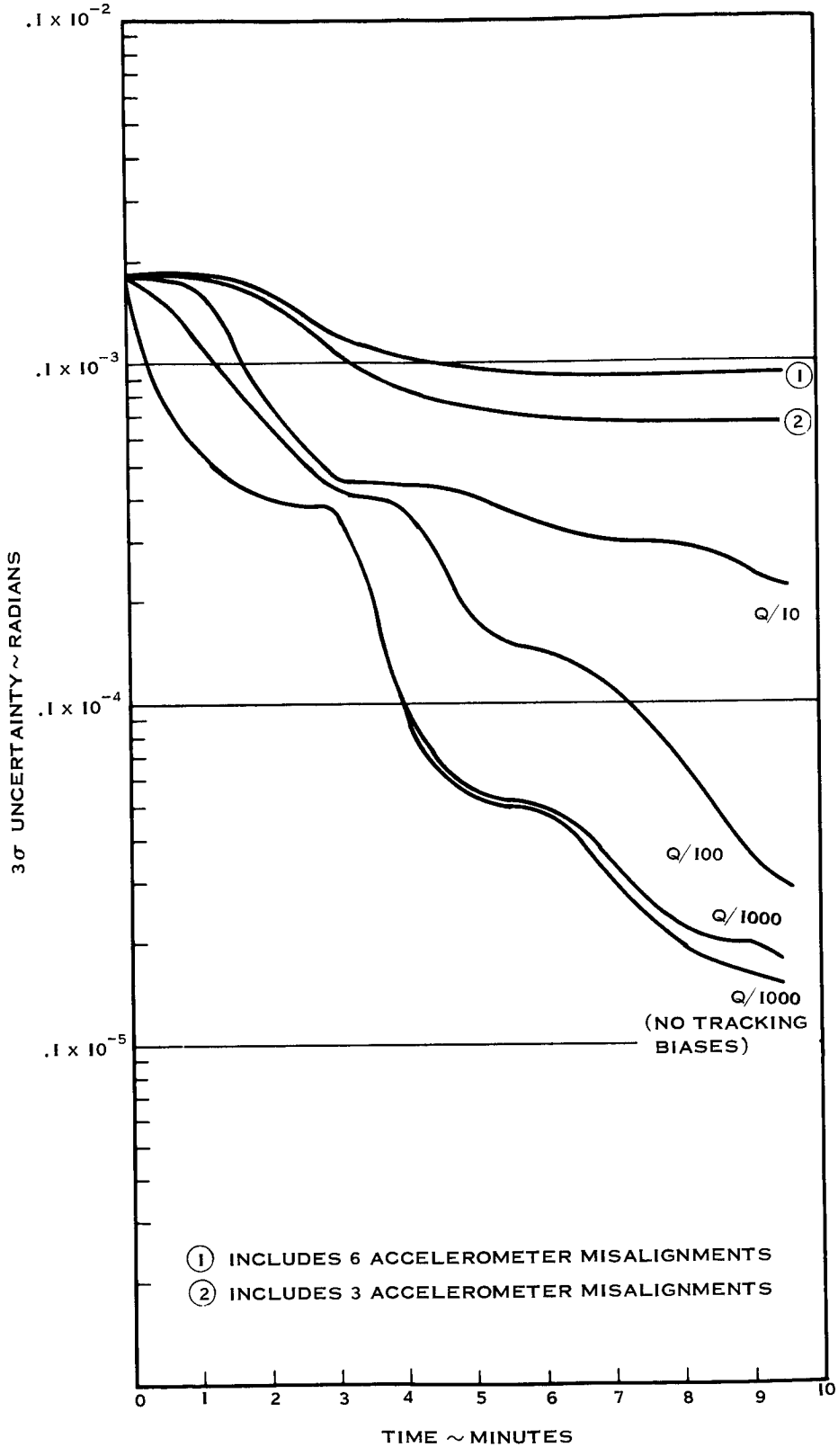

Figure 6-6 3σ Uncertainty in Initial Platform Misalignment About Y-Axis

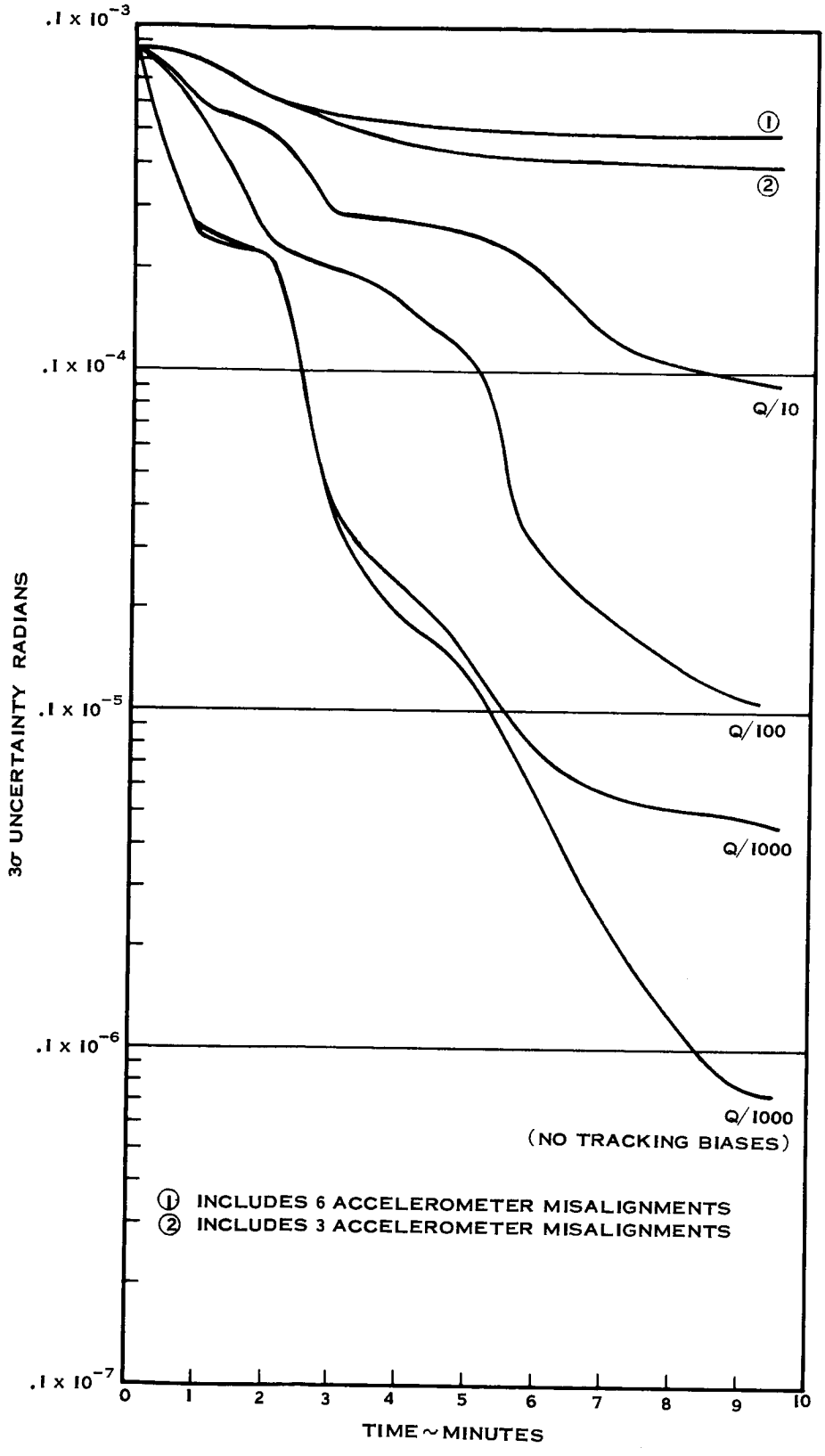

Figure 6-7 3σ Uncertainty in Initial Platform Misalignment About Z-Axis

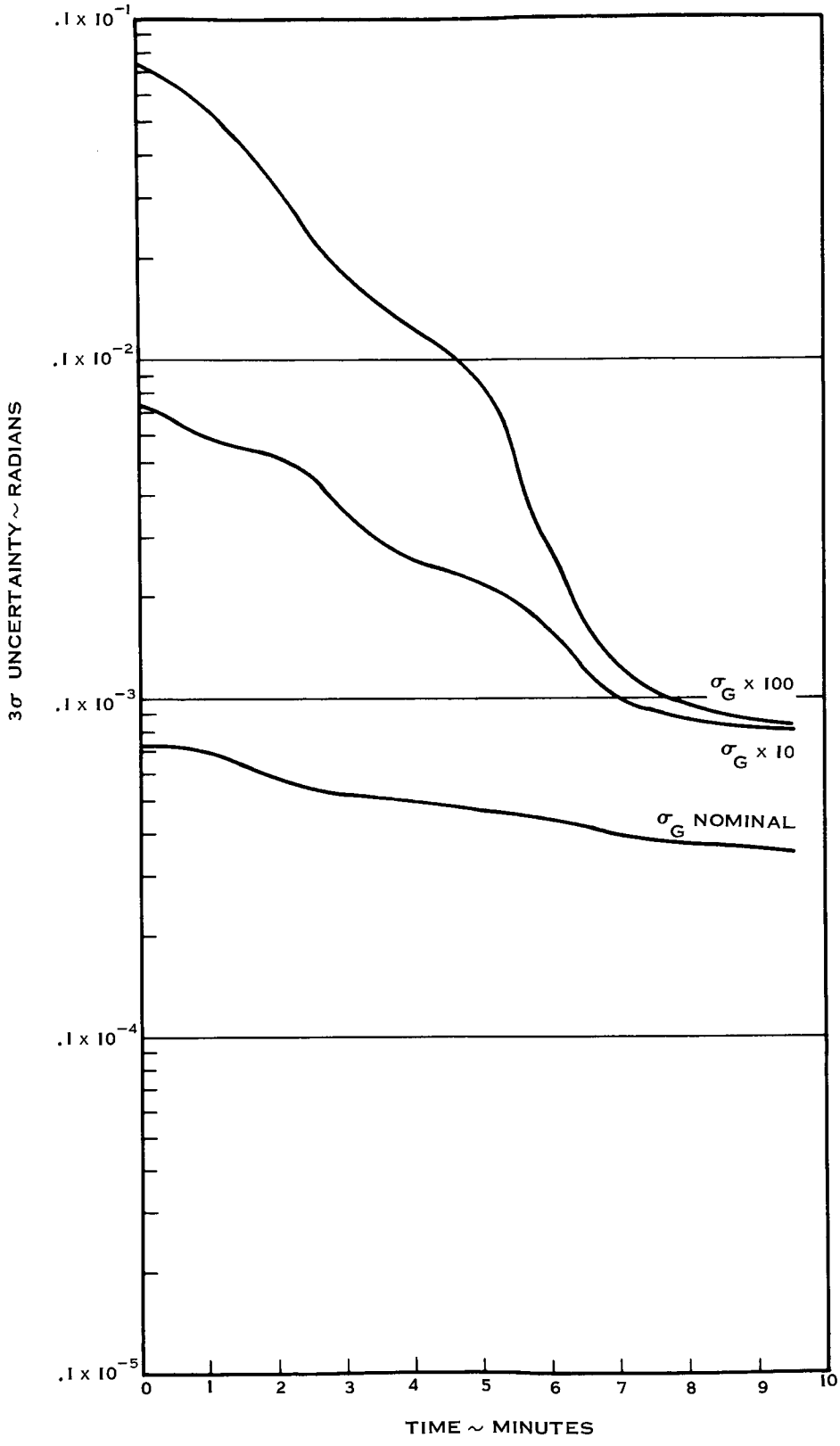

Figure 6-8 3σ Uncertainty in X-Accelerometer Misalignment Into Y-Axis for High Initial Uncertainties

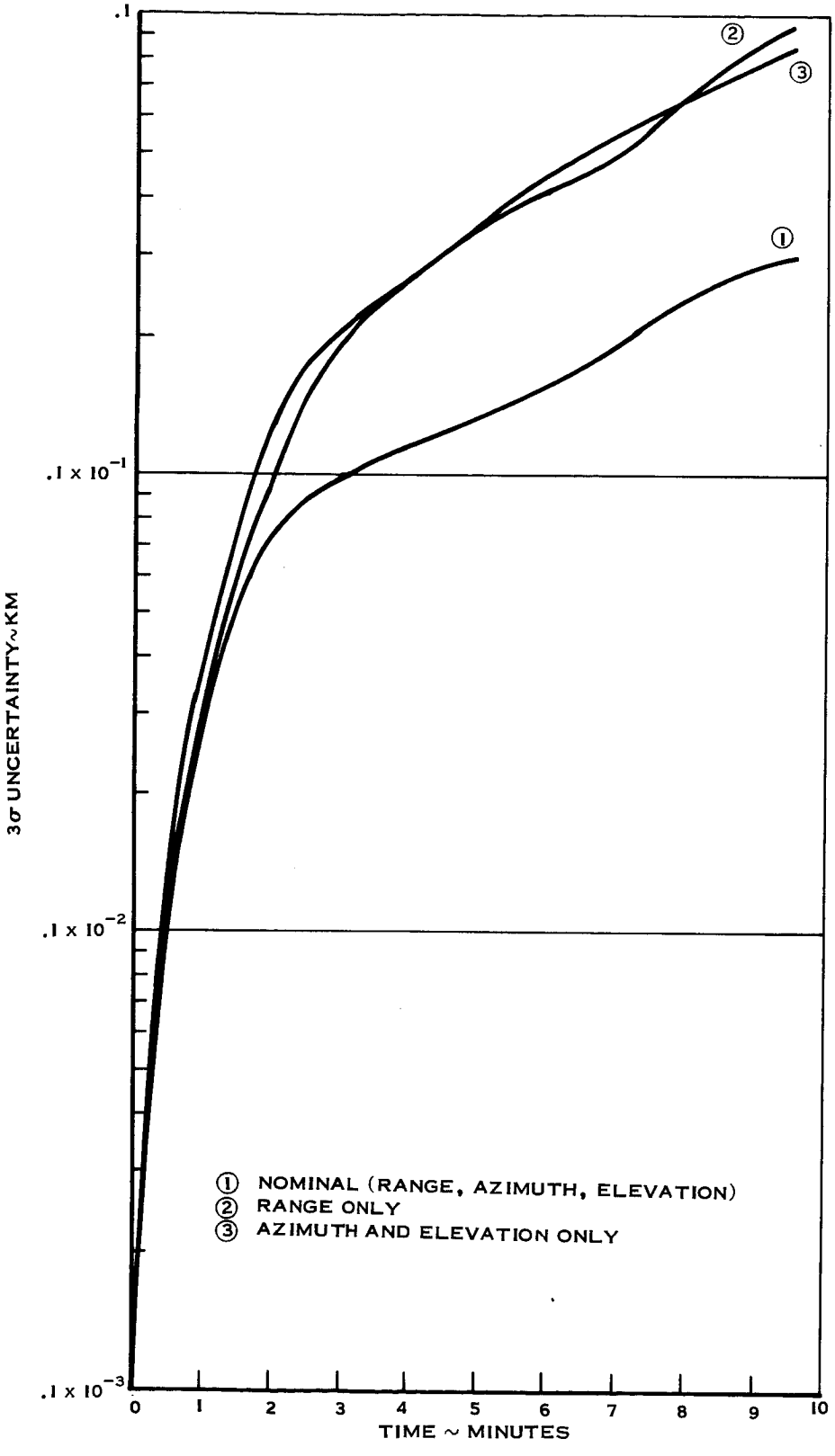

Figure 6-9 Variation in Position Uncertainty for Different Kinds of Tracking

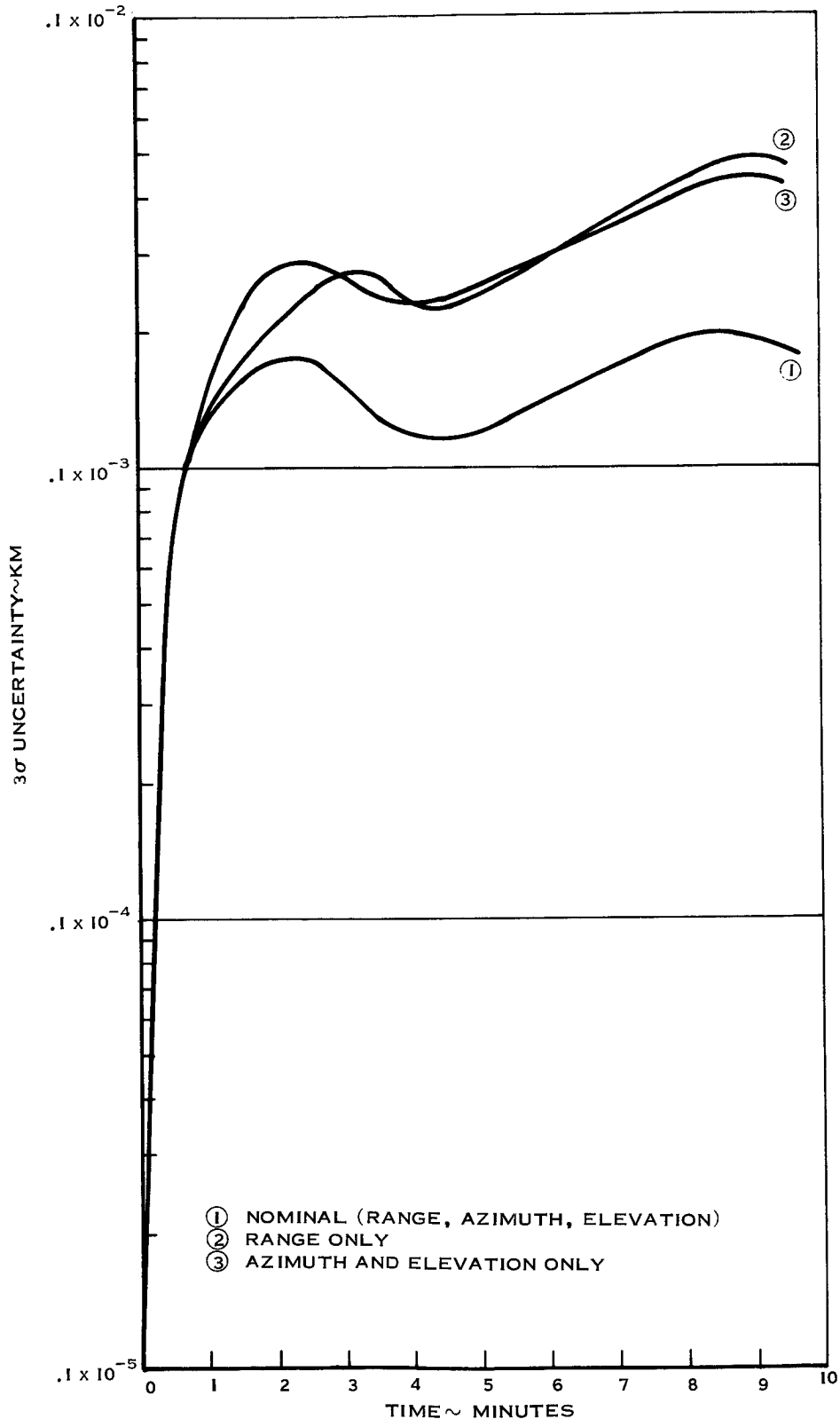

Figure 6-10 Variation in Velocity Uncertainty For Different Kinds of Tracking

SECTION 7
CONCLUSIONS

The over-all concept of combining telemetry and tracking data to estimate either the trajectory or error parameters that affect the trajectory has been found to be effective. However, the specific numerical results that can be obtained are highly dependent on the accuracy of the guidance system relative to that of the tracking system. As a result, the concept is, at the present time, more useful for some of the applications that were considered than it is for others.

The preliminary results presented in this report are mainly concerned with the importance of individual error sources in both the guidance and tracking systems. The effect of the guidance errors alone on the trajectory uncertainty is about 0.5 km in position and 2 meters/second in velocity. The most important error sources are the platform misalignments, the gyro drifts, the accelerometer biases, and some of the accelerometer misalignments and scale-factor errors. Some of the error sources, such as the Z accelerometer scale factor and the X and Y accelerometer misalignments in the Z direction, do not have a significant effect on the trajectory due to the low acceleration levels in the cross range direction. Other error sources, such as most of the mass unbalances, anisoelastic drifts, and accelerometer thresholds, do not cause any noticeable deviations in the trajectory. The final guidance model included twenty significant error sources.

The significant errors in the C-band radars included random and measurement bias errors in range, azimuth and elevation, as well as the station location errors. It was found that some of the station location errors and some of the azimuth and elevation biases could be omitted from the model. In addition to the random tracking errors, thirty-four bias errors were included in the final model.

The principal results of the report show the feasibility of estimating the platform error sources, both for the purpose of updating the guidance system during a flight and for a post-flight analysis. Although the primary interest for this investigation was in estimating the platform errors, results are also presented for estimating the trajectory.

With both the guidance and tracking errors estimated, the uncertainty in the vehicle state was better than when the guidance errors were not estimated. This improvement was about a factor of 2 in the velocity uncertainty. Therefore, it may be concluded that the combination of telemetry and tracking data improves the estimate of the state compared to the use of tracking data alone.

For the tracking model used in this study, it may be concluded that the Saturn V type inertial platform errors are so small that it is not possible to significantly reduce the uncertainties in these error sources during a powered flight. The uncertainties in these error sources have been found to be reduced by about 20 to 50 percent. With an order of magnitude improvement in the present tracking accuracies, the significant guidance errors could be updated, i.e., these uncertainties could be reduced by about an order of magnitude. The general conclusion, therefore, is that the extent to which the guidance error uncertainties can be reduced does depend on the relative accuracies of the guidance components and the tracking system.

A notable exception to the above conclusions is that the ability to estimate the platform misalignments (orthogonal rotations), depends on a good **initial calibration of the accelerometer misalignments. It was found** that there is not enough information obtained from the telemetry-tracking system to distinguish between platform misalignments and accelerometer misalignments. However, if the Z accelerometer misalignments are eliminated, as well as either the X accelerometer misalignment in the Y direction, or the Y accelerometer misalignment in the X direction, then the three initial platform misalignments can be tied down.

The most effective use of the telemetry-tracking system is perhaps for a post-flight analysis. For this type of analysis, it would be possible to distinguish error sources that caused a malfunction, or more than normal error, from those components whose errors were less than the 3σ value. This result has been obtained by assuming large initial values for the guidance error standard deviations, and noting that there is a significant decrease in the uncertainty of these errors along the trajectory.

Additional results have been presented which show that:

(1) a perfect knowledge of the trajectory end point has little effect on reducing the guidance error uncertainties,

(2) the effectiveness of range tracking alone is about the same as the effectiveness of azimuth and elevation angle measurements, and

(3) the effect of increasing the tracking rate by a factor of 10 decreases the guidance error uncertainties by, at most, a factor of 2.

APPENDIX A

COVARIANCE MATRIX DESCRIPTION

A complete covariance matrix as defined in (2-26) is presented in this section. It is taken from the Powered Flight Error Propagation Program (Reference 2) and lists values from the nominal tracking-guidance model at the end of an ascent trajectory. The off-diagonal numbers are normalized in UP, DR, CR coordinates with standard deviations on the diagonal, where

$$\text{Standard Deviation} = \sqrt{P_{ij}} \qquad i=j$$

$$\text{Normalized Correlations} = \frac{P_{ij}}{\sqrt{P_{ii}\, P_{jj}}} \qquad i \neq j$$

and P_{ij} is computed by equations (2-19) and (2-22).

The output format can be broken into three sections.

1. Time of printout. In this case time is that from launch until the end of the ascent trajectory

2. RMS position and velocity, where

$$RMSP = \sqrt{P_{11} + P_{22} + P_{33}}$$

$$RMSV = \sqrt{P_{44} + P_{55} + P_{66}}$$

and standard deviations of bias errors being estimated.

3. Covariance Matrix. Since the covariance matrix is symmetrical only half of it is outputed. The format is as follows:

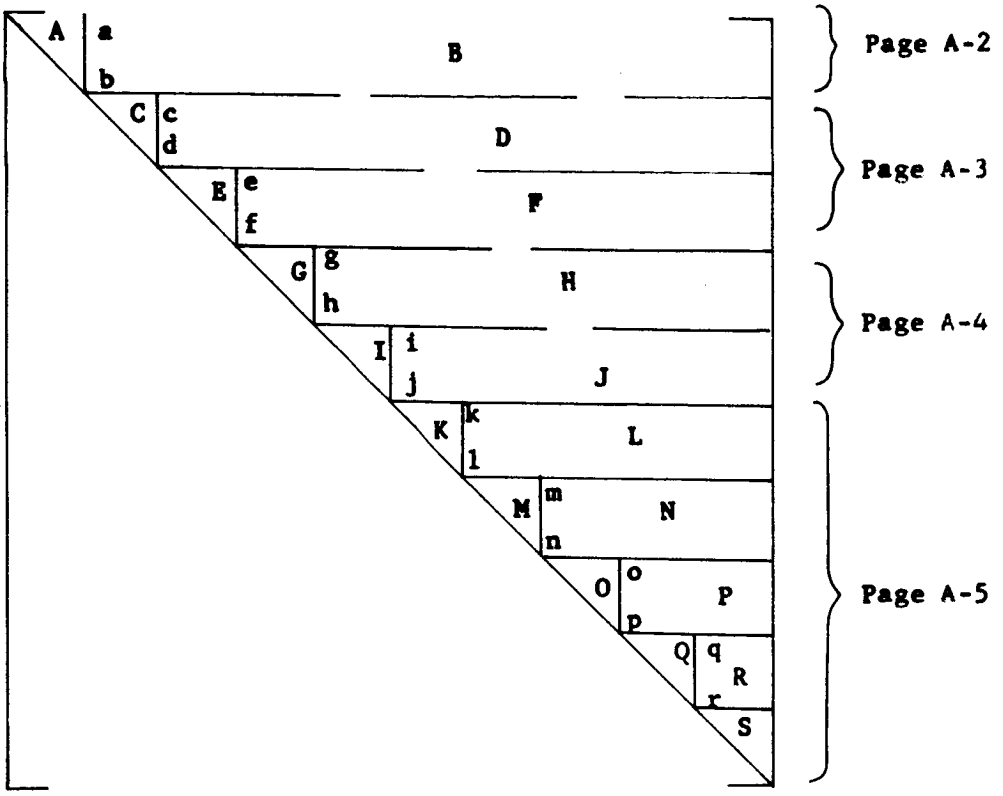

The format for the covariance matrix as defined above has been divided into pages as follows:

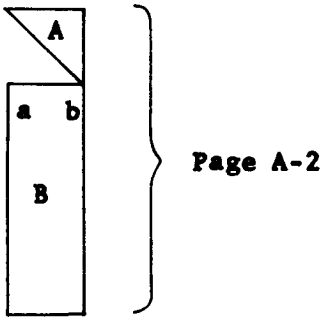

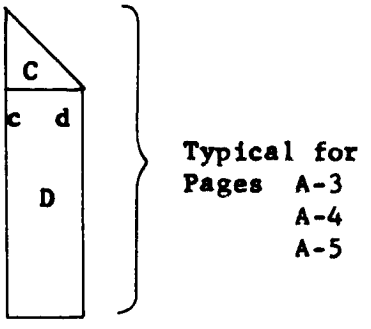

To identify the standard deviation of specific error sources (diagonal terms) or the correlation between the bias error sources from the numbers printed out on the left and top of each page, the following code is used.

Guidance Errors ~ Numbers 1 through 30 . Only 20 errors were included in the model. The specific guidance errors defined by these numbers are shown in page 3-3 and Table 5-1.

Tracking Errors ~ The first digit denotes the station. The second and third digits specify the type of tracking error.

Stations:

1	Cape Kennedy	FPS-16
2	Merit Island	FPS-16
3	Patrick A.F.B.	FPS-16
4	G. Bahama	FPS-16
5	G. Bahama	TPQ-18
6	Bermuda	FPS-16
7	Bermuda	FPQ-16
8	G. Turk	FPS-16
9	Antigua	FPS-16

Errors:

01 Range ~ meters
02 Range rate ~ meters/sec
03 Azimuth ~ millirad
04 Elevation ~ millirad
05 Azimuth rate ~ millirad/sec
06 Elevation rate ~ millirad/sec
07 Station latitude ~ degrees
08 Station longitude ~ degrees
09 Station altitude ~ meters
10 Station clock ~ seconds

The following examples illustrate the use of this numbering system:

1. 308 ~ Patrick AFB ~ longitude
   10 ~ Accelerometer bias X-axis

   The number in column 10 and row 308 (page A-3) is the correlation between Patrick AFB longitude error and accelerometer bias error in the X axis.

2. The value in the DR column and row 5 (page A-2) specifies the correlation between the Y-accelerometer scale factor error and the uncertainty in the downrange coordinate.

3. The number in column 3 and row 22 (page A-3) gives the correlation between Z accelerometer error into X-axis and X-gyro input axis mass unbalance.

4. The item at column 11 and row 11 is the standard deviation of accelerometer bias error on the Y-axis.

END CONDITIONS

0 DAY 0 HRS 9 MIN 25.985 SEC CASE 3 REC. 10 EVENT 8

CURRENT RMS VALUES

RMSP= 0.2856899E-01 RMSV= 0.1747118E-03 1= 0.2033137E-04 2= 0.5203584E-04 3= 0.6876384E-04 4= 0.4735066E-04

5= 0.1983611E-04	6= 0.5794824E-04	10= 0.3340303E-06	11= 0.4181578E-06	12= 0.4485762E-06	15= 0.1999510E-07		
16= 0.5936066E-04	17= 0.8694120E-04	18= 0.4917875E-04	19= 0.2294555E-06	20= 0.1577291E-06	21= 0.1315124E-06		
22= 0.1482978E-04	23= 0.1482969E-04	27= 0.3701221E-04	30= 0.2006918E-02	101= 0.1293153E-02	104= 0.2660293E-04		
201= 0.1290303E-02	203= 0.2203202E-04	204= 0.2064433E-04	301= 0.4830693E-02	303= 0.2261715E-04	304= 0.2158076E-04		
308= 0.4959798E-02	401= 0.3155088E-02	407= 0.4882960E-02	408= 0.2713148E-02	501= 0.3007574E-02	507= 0.4666228E-02		
508= 0.2639081E-02	601= 0.1197393E-01	607= 0.2311298E-01	608= 0.1061544E-01	609= 0.2156260E-01	701= 0.1239769E-01		
704= 0.4026404E-04	707= 0.2460006E-01	708= 0.1059291E-01	709= 0.2821349E-01	801= 0.1204296E-01	804= 0.3909360E-04		
807= 0.2049557E-01	808= 0.9650091E-02	809= 0.2542227E-01	901= 0.3463467E-01	904= 0.4252512E-04	907= 0.3890744E-01		
908= 0.2497937E-01	909= 0.4055488E-01						

P MATRIX. STD DEV. ON DIAGONAL

	UP	DR	CR	UPD	DRD	CRD
UP	0.20048940E-01	-0.72755066E 00	-0.13398790E 00	0.82198008E 00	0.62302793E-01	-0.18234316E 00
DR		0.33592640E-02	-0.34594461E 00	-0.53763217E 00	0.46907973E 00	-0.25564921E 00
CR			0.20073430E-01	-0.16917249E 00	-0.73116932E 00	0.90566488E 00
UPD				0.11693026E-03	-0.81705669E-01	-0.24253006E 00
DRD					0.29480641E-04	-0.62105574E 00
CRD						0.12642160E-03
1	0.91231061E-01	-0.32064452E-01	-0.14935736E 00	0.14909848E 00	-0.25194991E-01	-0.15599953E 00
2	-0.31743747E-01	-0.10336913E 00	0.24144885E-01	-0.87517311E-01	-0.14850257E 00	0.86882852E-01
3	0.63290792E-02	-0.67216609E-02	-0.38867944E-03	-0.87547291E-02	0.24423477E-02	-0.11494868E-01
4	-0.33068204E-01	-0.52873698E-01	0.17000173E-01	-0.24118848E-01	-0.14103926E 00	0.15750782E-01
5	0.36261865E-01	0.18392624E 00	0.20936755E-01	0.11761894E-01	0.31634574E 00	-0.12132836E-01
6	0.92594163E-02	0.13775016E-02	-0.61100669E-02	0.52652875E-02	0.27914936E-01	0.23413349E-01
10	0.57764896E-01	0.54461265E-01	-0.19381994E-01	-0.21791579E-01	0.27908096E 00	0.22833622E-01
11	0.26094338E-01	0.25884537E-01	-0.21347065E-01	0.17192540E-01	0.47877736E-01	-0.16825024E-01
12	0.50592117E-01	-0.90050353E-01	0.50763714E-01	0.92941022E-01	-0.13063518E 00	0.10225735E-01
15	0.13347085E-02	-0.31883261E-02	0.14651212E-02	0.10588128E-02	-0.42325672E-02	-0.19595403E-02
16	0.12598020E-01	0.18951957E-02	-0.83067231E-02	0.71805618E-02	0.37998983E-01	0.31820817E-01
17	-0.27896034E-01	0.29614850E-01	0.17515309E-02	0.38540602E-01	-0.10968542E-01	0.50698912E-01
18	-0.24368947E-02	-0.81457169E-01	0.12789325E-01	-0.96662469E-01	-0.29722160E-01	0.10695265E 00
19	-0.38469599E-01	0.30290373E-01	-0.31353784E-01	-0.17247277E 00	0.10118328E 00	-0.11564036E 00
20	-0.91257966E-01	0.88611831E-01	-0.12528340E 00	-0.26824580E 00	0.14521143E 00	-0.23311961E 00
21	0.23858515E 00	0.14113449E 00	-0.36250129E 00	0.49898253E 00	0.29741040E 00	-0.60257231E 00
22	-0.71957074E-03	0.13321728E-02	-0.14491146E-02	-0.52062195E-03	0.10105911E-02	-0.34278661E-03
23	0.72451828E-03	-0.13734814E-02	0.14921265E-02	0.45310488E-03	-0.10186034E-02	0.28433008E-03
27	0.46699094E-02	0.11044154E-01	-0.22162350E-03	0.28959971E-02	-0.29899794E-02	-0.11657893E-02
30	0.80615882E-02	0.15524325E-01	-0.17468233E-02	0.94192744E-02	-0.50578968E-02	-0.77576293E-02
101	0.28689031E-01	0.22127054E 00	0.72170274E-01	0.16218127E-01	0.24059656E-01	-0.12559606E-01
104	0.13846909E 00	-0.14907918E-01	-0.15431532E 00	0.38457969E-01	0.20710264E 00	-0.78573697E-01
201	-0.55262423E-02	0.25125632E 00	0.67472512E-01	0.39227199E-02	0.16128408E-01	-0.19274487E-01
203	0.25918534E 00	-0.26406754E 00	0.10222542E 00	0.11232743E 00	-0.21271355E-01	0.77499805E-01
204	0.17827739E 00	-0.21501845E-01	-0.19654651E 00	0.50911494E-01	0.26204798E 00	-0.10110217E 00
301	0.20926240E-03	0.20629991E-01	0.67575242E-01	-0.16787910E-01	-0.13195222E-01	0.23985856E-01
303	0.25616890E 00	-0.26993509E 00	0.11732608E 00	0.11150236E 00	-0.30200236E-01	0.80913138E-01
304	0.17112139E 00	-0.55680295E-02	-0.20572191E 00	0.52749346E-01	0.26140123E 00	-0.10580005E 00
308	0.25327264E-01	-0.73312926E-01	0.62668495E-01	-0.78863024E-02	-0.22153402E-01	0.37946350E-01
401	-0.16629288E 00	0.31832735E 00	-0.19364304E 00	-0.15716302E 00	0.20022125E 00	-0.17315564E 00
407	0.46470044E-01	-0.39728430E-02	-0.18811714E-01	-0.41034572E-01	0.67213189E-01	-0.88960845E-01
408	0.30281117E 00	-0.44903222E 00	0.21892686E 00	0.98585642E-01	-0.11390346E 00	0.11886989E 00
501	-0.14338370E 00	0.31505682E 00	-0.21089155E 00	-0.15546971E 00	0.23086473E 00	-0.17118684E 00
507	0.80335412E-01	-0.24762694E-01	-0.25274959E-01	-0.33080983E-01	0.89228955E-01	-0.81926209E-01
508	0.33263674E 00	-0.47195243E 00	0.21511480E 00	0.10733914E 00	-0.98163224E-01	0.12834586E 00
601	0.11023329E 00	-0.33417249E-01	0.12334604E 00	0.38617338E 00	-0.17143103E 00	0.12984199E 00
607	0.55316677E 00	-0.51090577E 00	0.48640841E-01	0.28678795E 00	-0.15375272E-01	-0.25698951E-01
608	-0.35311820E 00	0.26709825E 00	-0.20606870E 00	-0.67136344E 00	0.36232410E 00	-0.86781039E-01
609	0.32326900E 00	-0.12389681E 00	-0.34525391E 00	0.11998919E 00	0.32895731E 00	-0.27896765E 00
701	0.19886422E 00	-0.10378596E 00	0.99989117E-01	0.43647229E 00	-0.15323203E 00	0.99989112E-01
704	-0.20387676E 00	0.17017608E 00	0.13787527E-01	-0.14106087E 00	-0.99071576E-02	0.29999827E-01
707	0.35681957E 00	-0.35320872E 00	0.77683095E-01	0.14836934E 00	-0.31712322E-01	0.19642737E-01
708	-0.37378172E 00	0.28361762E 00	-0.20162018E 00	-0.68267053E 00	0.35822675E 00	-0.81036389E-01
709	0.40905381E 00	-0.21908864E 00	-0.29418463E 00	0.21351676E 00	0.26649199E 00	-0.25535588E 00
801	-0.15565760E 00	0.23062857E 00	-0.17340777E 00	-0.29151884E 00	0.28601842E 00	-0.27050570E 00
804	0.15335818E 00	-0.92463849E-01	-0.68457761E-01	0.94418038E-01	0.53651639E-01	-0.81068354E-01
807	0.11852083E 00	-0.14842042E 00	0.12681832E 00	-0.71113870E-01	0.23954914E-01	-0.19299357E-02
808	0.49932774E 00	-0.68294381E 00	0.54866196E 00	0.32375256E 00	-0.39142656E 00	0.50504562E 00
809	0.93645363E-03	0.51056808E-01	-0.97273146E-01	0.23903791E-01	0.82902117E-01	-0.43833013E-02
901	-0.69598460E-01	0.10285743E 00	-0.93541984E-01	-0.12727913E 00	0.12941284E 00	-0.14161520E 00
904	0.12663237E 00	-0.89335711E-01	-0.93658289E-02	0.83975865E-01	0.21204894E-01	0.99069613E-02
907	0.14515272E 00	-0.25202802E 00	0.30908509E 00	0.29923384E-01	-0.18182857E 00	0.21492740E 00
908	0.32385404E 00	-0.49890124E 00	0.52864938E 00	0.28522425E 00	-0.42133666E 00	0.57661249E 00
909	0.15861816E-01	0.67281840E-01	-0.19059390E 00	0.39849909E-01	0.12185946E 00	-0.16244000E 00

DETERMINISTIC ERRORS

	1	2	3	4	5	6
1	0.20331372E-04					
2	0.44148847E-01	0.52035842E-04				
3	-0.21672424E-02	0.16681603E-02	0.68763840E-04			
4	0.10762037E 00	-0.67063317E 00	0.19109780E-02	0.47350657E-04		
5	-0.13041863E 00	-0.12311295E 00	-0.30164280E-02	-0.66478305E-01	0.19836109E-04	
6	-0.96963818E-03	-0.66027091E-02	-0.15713352E-01	-0.10337043E-01	0.38623158E-01	0.57948236E-04
10	-0.95026130E 00	-0.10299002E 00	-0.60572501E-03	-0.15667539E 00	0.24797986E 00	0.16148224E-01
11	0.87032021E-01	-0.31933244E 00	-0.10032831E-02	-0.20291715E 00	-0.53683719E 00	-0.23728974E-02
12	0.44975948E-02	0.13476016E-01	-0.50643934E-01	0.19649995E-01	-0.95576903E-01	-0.99763983E-01
15	0.12169724E-04	0.82176804E-03	-0.26526007E-02	0.11129258E-02	-0.50082944E-02	0.55729675E-02
16	-0.13492103E-02	-0.89851721E-02	-0.21372384E-01	-0.14061016E-01	0.52218121E-01	-0.85375673E 00
17	0.95989052E-02	-0.72818338E-02	0.68739876E 00	-0.81629292E-02	0.13524723E-01	0.69274211E-01
18	-0.79283624E-01	-0.60202479E 00	-0.10430522E-03	0.94018696E 00	-0.92313653E-01	0.41330006E-02
19	-0.11740905E-01	0.93877175E-02	-0.50734961E-01	0.69926976E-02	-0.37466879E-01	-0.30939276E-01
20	-0.29694742E-01	0.22683673E-01	0.12030392E 00	0.20963862E-01	-0.51734319E-01	-0.15914860E 00
21	0.83286678E-01	-0.32012010E 00	0.13149878E-02	-0.11563309E 00	0.47448581E 00	-0.10916508E-01
22	-0.34068913E-03	-0.39174873E-04	-0.16032746E-02	-0.12416677E-03	0.13436067E-02	-0.28191473E-02
23	0.34712108E-03	0.49687926E-04	0.16481895E-02	0.13913808E-03	-0.14447516E-02	0.30429261E-02
27	0.20384581E-02	-0.31461415E-02	0.67636988E-03	0.11866794E-01	-0.36717330E-01	0.20528529E-03
30	-0.73206585E-03	0.69225515E-04	0.11821526E-02	0.14978350E-01	-0.65387649E-01	0.32633687E-03
101	-0.22249033E 00	-0.20591723E 00	0.33146577E-02	-0.10020725E 00	0.36426173E 00	0.13368372E-02
104	0.22987319E-01	-0.28987565E-01	-0.26181834E-03	-0.42405804E-01	0.34481358E-01	0.16624886E-01
201	-0.22226564E 00	-0.20479004E 00	0.54698228E-02	-0.96533433E-01	0.35678575E 00	-0.41333025E-02
203	-0.15111883E-01	-0.50688263E-02	-0.17413181E-01	-0.16343407E-01	0.53629482E-01	0.38359239E-01
204	0.27445049E-01	-0.35125177E-01	-0.77795957E-03	-0.52773969E-01	0.44800223E-01	0.21651714E-01
301	-0.43600721E-01	-0.92098136E-01	0.11972042E-01	-0.44855956E-01	0.14132886E 00	-0.83706097E-02
303	-0.26810271E-01	-0.18836214E-01	-0.15220766E-01	-0.22542309E-01	0.72003838E-01	0.36186678E-01
304	0.22507855E-01	-0.23942212E-01	-0.47014391E-02	-0.46409800E-01	0.30615513E-01	0.24439164E-01
308	0.14042196E-01	-0.39472780E-01	0.91616673E-02	-0.21152466E-01	0.53115409E-01	-0.38878481E-02
401	0.19394848E-01	-0.22932307E-01	0.79600154E-02	-0.11085727E-01	-0.12731354E-01	0.15597419E-01
407	-0.13817852E-01	-0.53211963E-02	-0.17776586E-01	-0.48191764E-03	-0.13551067E-01	0.62512431E-01
408	0.10086498E 00	0.52032230E-01	0.21462746E-01	0.23046252E-01	-0.10911387E 00	0.58641850E-02
501	0.19298299E-01	-0.24923485E-01	0.71098447E-02	-0.17728613E-01	0.37037128E-02	0.18538662E-01
507	-0.15543900E-01	-0.66759310E-02	-0.19706314E-01	-0.64996839E-02	0.28856702E-02	0.67486029E-01
508	0.10301203E 00	0.53365273E-01	0.20898052E-01	0.19075786E-01	-0.99880809E-01	0.78095509E-02
601	0.92144925E-03	-0.53033293E-01	-0.19724887E-01	-0.13359453E-01	0.10018950E 00	0.36376788E-01
607	0.18629192E-01	0.78704526E-02	0.14670915E-01	-0.97135404E-02	-0.15478560E-01	-0.16184014E-01
608	-0.33237319E-01	0.81047426E-01	0.78557580E-02	-0.12839320E-02	-0.71154070E-01	0.48610171E-02
609	0.64089153E-01	0.11855021E-01	0.85632314E-02	-0.22591878E-01	-0.18383618E-01	0.25335854E-02
701	0.17274407E-01	-0.50335536E-01	-0.16467096E-01	-0.14052588E-01	0.87593473E-01	0.31333366E-01
704	-0.38235364E-01	-0.14447713E-02	-0.55615064E-02	0.28469179E-02	0.15969740E-01	0.69593388E-02
707	-0.11845287E-01	0.71669419E-02	0.96540597E-02	-0.70689924E-02	-0.48716352E-03	-0.92348987E-02
708	-0.36877095E-01	0.80372820E-01	0.70835656E-02	-0.10305501E-02	-0.68258323E-01	0.60473141E-02
709	0.77938135E-01	0.87766815E-02	0.10419647E-01	-0.19299319E-01	-0.26940043E-01	-0.35892440E-02
801	-0.25808310E-01	-0.21891185E-01	0.20353150E-01	-0.72779093E-02	0.89212431E-01	-0.45365115E-01
804	0.12462991E-01	-0.87349656E-02	0.57528248E-02	-0.76522044E-02	0.10042663E-01	0.27857865E-02
807	-0.42190103E-01	-0.15265569E-01	0.13740321E-01	-0.75596971E-02	0.87887845E-01	-0.26824635E-01
808	-0.39620473E-01	0.33350176E-01	0.97347648E-02	-0.34188232E-02	-0.51249518E-02	-0.18692710E-01
809	0.14106110E-01	0.13466442E-01	-0.10785928E-01	-0.79546667E-02	-0.13754833E-01	0.15529323E-01
901	-0.22415594E-01	-0.70364753E-02	0.94676890E-02	-0.72777609E-03	0.33290759E-01	-0.27636508E-01
904	0.30789238E-02	0.16907083E-02	0.72112309E-03	-0.83116903E-02	0.39364459E-02	0.30347650F-02
907	-0.56311807E-01	-0.35852308E-02	0.97478011E-02	-0.20048290E-02	0.44645865E-01	-0.23049316E-01
908	-0.11290808E-01	0.27081520E-01	-0.68646174E-02	-0.67152802E-02	-0.31271364E-01	0.25688287E-01
909	0.37814016E-01	-0.33414209E-02	-0.31461933E-02	-0.16458451E-02	-0.14342183E-01	0.11418185E-01

DETERMINISTIC ERRORS

	10	11	12	15	16	17
10	0.33403033E-06					
11	-0.67950388E-01	0.41815781E-06				
12	-0.33664738E-01	0.17203711E-01	0.44857615E-06			
15	-0.16920141E-02	0.82352698E-03	-0.85679367E-02	0.19995096E-07		
16	0.22003570E-01	-0.32688851E-02	-0.13570403E 00	0.75788262E-02	0.59360658E-04	
17	0.24976317E-02	0.44527947E-02	0.22321171E 00	0.11691035E-01	0.94222743E-01	0.86941200E-04
18	0.58346219E-01	-0.19854958E 00	-0.64933473E-02	-0.28149586E-03	0.56163375E-02	0.21538485E-03
19	-0.18390341E-02	0.11350349E-01	-0.52709797E-01	-0.35996815E-02	-0.42088108E-01	0.22362234E 00
20	-0.45536782E-02	0.14044464E-02	0.57132550E-01	-0.99522424E-03	-0.21646845E 00	-0.53027890E 00
21	0.43474130E-01	-0.60265867E-02	0.17320353E-01	0.76644037E-03	-0.14790007E-01	-0.56914284E-02
22	0.54532520E-03	-0.47574694E-03	0.25551676E-02	0.94462946E-04	-0.38340835E-02	0.70665993E-02
23	-0.57641705E-03	0.50615624E-03	-0.26947891E-02	-0.10275664E-03	0.41384236E-02	-0.72645692E-02
27	-0.62964420E-03	0.90487893E-03	-0.52201395E-02	-0.21247343E-03	0.27295406E-03	-0.29771687E-02
30	0.55102360E-03	0.46916245E-02	-0.92065607E-02	-0.37882873E-03	0.43264179E-03	-0.52008930E-02
101	0.20894830E 00	0.80832150E-01	0.23517546E-02	0.22479314E-03	0.18624721E-02	-0.14451822E-01
104	0.46989395E-01	0.84024936E-01	-0.35737423E-01	-0.17513347E-02	0.22600456E-01	0.11876276E-02
201	0.20262337E 00	0.76751014E-01	-0.58294376E-02	0.57522339E-04	-0.55780003E-02	-0.23956304E-01
203	0.39125550E-01	0.50320139E-02	0.87956867E-01	0.23453652E-02	0.52179781E-01	0.76784384E-01
204	0.61176684E-01	0.10226776E 00	-0.42993705E-01	-0.21494755E-02	0.29435756E-01	0.34717803E-02
301	0.38000748E-01	0.58315897E-01	-0.52450573E-01	-0.16296975E-02	-0.11370259E-01	-0.52739669E-01
303	0.48330395E-01	0.10588135E-01	0.79570760E-01	0.21055031E-02	0.49226953E-01	0.67128818E-01
304	0.64136127E-01	0.90075326E-01	-0.24561329E-01	-0.15641230E-02	0.33226117E-01	0.20768113F-01
308	-0.12812304E-01	0.39021031E-01	-0.43798367E-01	-0.14605073E-02	-0.52839776E-02	-0.40390373E-01
401	-0.79168828E-02	0.55695711E-01	-0.14856143E 00	-0.59991800E-02	0.21204689E-01	-0.35090139E-01
407	0.14007439E-01	0.96815411E-02	-0.26830624E-01	-0.27366383E-02	0.85018620E-01	0.78361614E-01
408	-0.96548979E-01	0.12349262E-01	-0.78810285E-01	-0.26615320E-02	0.79592090E-02	-0.94655698F-01
501	0.33254054E-02	0.62402488E-01	-0.14820190E 00	-0.60628616E-02	0.25206765E-01	-0.31335595E-01
507	0.25843069E-01	0.14040517E-01	-0.20640153E-01	-0.26355138E-02	0.91785111E-01	0.86876904E-01
508	-0.89935512E-01	0.15703361E-01	-0.75061010E-01	-0.25641468E-02	0.10606159E-01	-0.92160851E-01
601	0.27059263E-01	-0.73907318E-01	-0.78407586E-01	-0.63281370E-02	0.49509755E-01	0.86959038E-01
607	0.24400723E-01	0.41352144E-01	0.86562953E-01	0.47979602E-02	-0.22023524E-01	-0.64659777E-01
608	0.26910213E-01	0.70856011E-01	-0.12046895E-02	0.18943710E-02	0.65831287E-02	-0.34605911E-01
609	0.36559887E-01	0.62348023E-01	0.70689287E-02	0.99369301E-03	0.34312170E-02	-0.37753052F-01
701	0.22822527E-01	-0.62963787E-01	-0.63579197E-01	-0.54381441E-02	0.42646022E-01	0.72591177E-01
704	0.11068241E-01	-0.17006539E-01	-0.26927563E-01	-0.13732070E-02	0.94706889E-02	0.24533771F-01
707	0.28937076E-01	0.26025739E-01	0.61408105E-01	0.34491340E-02	-0.12566869E-01	-0.42533304E-01
708	0.27709330E-01	0.68129603E-01	-0.46750144E-02	0.16858986E-02	0.81976334E-02	-0.31200598F-01
709	0.21923295E-01	0.59423184E-01	0.24307496E-01	0.17433275E-02	-0.48969758E-02	-0.45947336F-01
801	0.34604023E-01	-0.40865392E-01	0.96774256E-01	0.70240033E-02	-0.61680857E-01	-0.89682031E-01
804	0.12156949E-01	0.15197273E-01	-0.11178334E-01	-0.36300281E-03	0.37888672E-02	-0.25344286E-01
807	0.36320993E-01	-0.36277352E-01	0.11382794E 00	0.65562900E-02	-0.36465327E-01	-0.60532378E-01
808	0.30456480E-01	-0.20390262E-02	0.75485395E-01	0.32262348E-02	-0.25424329E-01	-0.42885578E-01
809	0.19323525E-01	0.14125028E-01	-0.23428109E-01	-0.17604649E-02	0.21115703F-01	0.47529462F-01
901	0.24067353E-01	-0.24170110E-01	0.41239360E-01	0.35181582E-02	-0.37575966E-01	-0.41709360F-01
904	0.20376445E-01	0.12641403E-01	-0.18057255E-02	-0.21354142E-03	0.41259642E-02	-0.31715766E-02
907	0.24986804E-01	-0.20581882E-01	0.66241663E-01	0.38536300E-02	-0.31336493E-01	-0.42931279F-01
908	-0.55769101E-02	0.37467457E-01	-0.26557157E-01	-0.33089057E-02	0.34925103E-01	0.30257096E-01
909	-0.83386090E-02	0.10824267E-01	-0.23397668E-01	-0.13624071E-02	0.15525042E-01	0.13851198F-01

DETERMINISTIC ERRORS

	18	19	20	21	22	23
18	0.49178747E-04					
19	0.44588808E-02	0.22945548E-06				
20	0.53179587E-02	-0.24157364E 00	0.15772911E-06			
21	-0.31679782E 00	-0.14966369E-01	-0.40095346E-02	0.13151242E-06		
22	0.10881236E-03	-0.17891611E-02	-0.91192784E-02	-0.63671602E-04	0.14829781E-04	
23	-0.11339728E-03	0.17863653E-02	0.93393839E-02	0.62820530E-04	0.16391056E-03	0.14829688E-04
27	-0.20556642E-01	-0.11962564E-02	0.19626084E-02	-0.28591614E-01	0.13591201E-03	-0.14320402E-03
30	-0.19990589E-01	-0.26186033E-02	0.31797156E-02	-0.31522340E-01	0.24365586E-03	-0.25701522E-03
101	-0.16913622E 00	0.11811105E-02	0.31078967E-01	0.32289154E 00	0.38927900E-03	-0.40362724E-03
104	0.14152196E-01	-0.34072642E-02	-0.21379834E-03	-0.22571802E-01	0.55940678E-03	-0.59249602E-03
201	-0.17240272E 00	0.39773605E-02	0.43828425E-01	0.33033522E 00	0.60673687E-03	-0.62714433E-03
203	0.14451424E-01	-0.21305660E-01	-0.10398806E 00	-0.31678751E-01	-0.20787349E-02	0.21451558E-02
204	0.19012582E-01	-0.47361160E-02	-0.24504486E-02	-0.28067676E-01	0.65536731E-03	-0.69532068E-03
301	-0.75597276E-01	0.11852757E-01	0.64738858E-01	0.11909977E 00	0.13585404E-02	-0.14066419E-02
303	0.24713361E-02	-0.18964838E-01	-0.92511336E-01	-0.94344388E-02	-0.18556241E-02	0.19147723E-02
304	0.26961137E-01	-0.87053685E-02	-0.22535051E-01	-0.37354790E-01	0.20477405E-03	-0.22846730E-03
308	-0.29815107E-01	0.91093234E-02	0.44687105E-01	0.30267738E-01	0.10294807E-02	-0.10667989E-02
401	-0.18935468E-01	0.12907300E-02	0.69193666E-01	0.36495471E-01	0.28537991E-02	-0.29868276E-02
407	-0.71979293E-02	-0.26130683E-01	-0.82110941E-01	0.31747820E-01	-0.29019435E-03	0.26639238E-03
408	0.45789407E-01	0.16768443E-01	0.98378601E-01	-0.12231930E 00	0.23893328E-02	-0.24867233E-02
501	-0.12959730E-01	0.13897770E-03	0.64465873E-01	0.21792694E-01	0.28059501E-02	-0.29385875E-02
507	-0.11225325E-02	-0.28433953E-01	-0.93345589E-01	0.17576155E-01	-0.48005392E-03	0.46168032E-03
508	0.53080764E-01	0.16114242E-01	0.93872282E-01	-0.13939250E 00	0.22975969E-02	-0.23919450E-02
601	-0.60260002E-01	-0.15747116E 00	-0.35128143E 00	0.21557608E 00	-0.80806317E-03	0.71752789E-03
607	0.24632786E-01	0.68667808E-01	0.11249068E 00	-0.48645909E-02	-0.52789204E-03	0.60606422E-03
608	0.12120111E 00	0.12128846E 00	0.30189659E 00	-0.40409049E 00	0.16612523E-02	-0.16473460E-02
609	0.47782360E-01	0.34223555E-01	0.11806233E 00	-0.75114334E-02	0.87206015E-03	-0.88386992E-03
701	-0.55353342E-01	-0.14686758E 00	-0.32320721E 00	0.21987972E 00	-0.79254570E-03	0.71127103E-03
704	-0.59489508E-02	-0.15697368E-02	-0.28015480E-01	-0.18282049E-01	-0.25122033E-04	0.20299465E-04
707	0.20048164E-01	0.58986623E-01	0.84803133E-01	-0.31910749E-01	-0.45935284E-03	0.52409304E-03
708	0.11986678E 00	0.11878436E 00	0.29536283E 00	-0.40416368E 00	0.16580692E-02	-0.16463644E-02
709	0.38827629E-01	0.29972096E-01	0.10776109E 00	0.23425010E-01	0.62681612E-03	-0.62836549E-03
801	-0.22508742E-01	0.12764296E 00	0.35629819E 00	0.95749692E-01	0.10344081E-02	-0.96603946E-03
804	-0.26119117E-02	-0.10758585E-01	0.36103545E-01	0.45451042E-01	0.74889843E-03	-0.78897685E-03
807	-0.12363333E-01	0.91326128E-01	0.20669686E 00	0.28188420E-01	-0.25861097E-03	0.34998589E-03
808	0.53750376E-01	0.88648150E-02	-0.73267215E-01	-0.20531893E 00	-0.15729698E-02	0.16521694E-02
809	0.30522767E-01	-0.82488758E-02	-0.10043706E 00	-0.58170497E-01	-0.73970822E-03	0.75804233E-03
901	-0.93969752E-02	0.10161996E 00	0.16557723E 00	0.51543077E-01	-0.85514450E-04	0.16724801E-03
904	0.13642115E-01	-0.41676300E-02	-0.16385264E-01	-0.16893054E-01	-0.30719923E-04	0.27867669E-04
907	-0.25960130E-02	0.65788666E-01	0.66134796E-01	-0.50794738E-01	-0.89027757E-03	0.99051410E-03
908	0.48931493E-01	-0.11081789E 00	-0.26822856E 00	-0.24717717E 00	-0.94632697E-03	0.89899473E-03
909	-0.27180054E-02	-0.23582131E-01	-0.12861368E-01	0.63410123E-01	0.41641915E-03	-0.45356660E-03

DETERMINISTIC ERRORS

	27	30	101	104	201	203
27	0.37012210E-04					
30	-0.57288621E-02	0.20069184E-02				
101	0.33559951E-01	0.47073985E-01	0.12931531E-02			
104	-0.81563873E-02	-0.13398374E-01	0.52637889E-02	0.26602928E-04		
201	0.34100379E-01	0.47987554E-01	0.63893925E 00	-0.41290768E-02	0.12903034E-02	
203	0.33857766E-03	0.13297088E-03	0.34172095E-01	0.40653244E-01	0.12345773E-01	0.22032021E-04
204	-0.97524833E-02	-0.16080132E-01	0.66269994E-02	0.12003319E 00	-0.54784701E-02	0.53414065E-01
301	0.54935538E-02	0.70738267E-02	0.17537995E 00	0.19482914E-02	0.17566899E 00	0.16029110E-02
303	0.19146442E-02	0.22586599E-02	0.48630609E-01	0.36744180E-01	0.27225877E-01	0.17405884E 00
304	-0.87116262E-02	-0.14409230E-01	0.51706948E-02	0.11640891E 00	-0.68441314E-02	0.53905362E-01
308	-0.35335844E-02	-0.56674336E-02	0.88984530E-02	0.60253463E-02	0.69865630E-02	0.14927853E-01
401	-0.56342939E-02	-0.96333198E-02	0.10179331E 00	0.16035009E-01	0.10853327E 00	-0.65647753E-01
407	0.10533616E-02	0.10419616E-02	0.63547255E-01	-0.26030951E-02	0.49739212E-01	0.12377102E 00
408	-0.20350902E-01	-0.30582403E-01	-0.17691021E 00	0.65764979E-02	-0.19557297E 00	0.16189211E 00
501	-0.65232168E-02	-0.11128319E-01	0.10943235E 00	0.34160274E-01	0.11422437E 00	-0.56805363E-01
507	0.51637743E-03	0.10649703E-03	0.69628212E-01	0.13940168E-01	0.52877303E-01	0.14213573E 00
508	-0.21416437E-01	-0.32254133E-01	-0.18094891E 00	0.20676719E-01	-0.20174179E 00	0.17408137E 00
601	0.31277246E-02	0.10258019E-01	0.38852477E-01	-0.57412187E-01	0.46452445E-01	-0.37997976E-01
607	0.94951787E-03	-0.14257648E-02	0.30265771E-01	0.79774524E-01	0.36489800E-02	0.20904676E 00
608	-0.85749171E-02	-0.16964941E-01	-0.12082794E 00	0.10196704E 00	-0.12857097E 00	0.78405418E-02
609	0.16094788E-02	0.11706013E-02	-0.35769423E-01	0.14338487E 00	-0.52315612E-01	0.85967445E-01
701	0.37850384E-02	0.10902865E-01	0.30880908E-01	-0.40270875E-01	0.34924724E-01	-0.12681640E-01
704	-0.25951391E-02	-0.41290626E-02	0.18132950E-01	-0.30060316E-01	0.25798327E-01	-0.57577224E-01
707	-0.55762659E-03	-0.33944395E-02	0.39312909E-01	0.49996616E-01	0.19878076E-01	0.15524650E 00
708	-0.87365248E-02	-0.17122807E-01	-0.11905301E 00	0.97885047E-01	-0.12594096E 00	0.17673635E-02
709	0.27059730E-02	0.30583378E-02	-0.37774033E-01	0.13328842E 00	-0.55787574E-01	0.10558114E 00
801	-0.29361026E-05	0.11179547E-02	0.68534938E-01	0.39297216E-02	0.69408420E-01	-0.74433035E-02
804	-0.22880482E-02	-0.47686307E-02	0.26652886E-01	0.32873212E-01	0.20190350E-01	0.46128486E-01
807	0.30258293E-02	0.58586806E-02	0.75499682E-01	-0.41770063E-02	0.62652586E-01	0.11914784E 00
808	-0.19205235E-02	-0.15952530E-02	-0.40073527E-01	0.75453831E-02	-0.62847784E-01	0.20023784E 00
809	0.31689029E-02	0.60516195E-02	-0.53488567E-01	0.40550825E-01	-0.53036897E-01	-0.25308881E-01
901	0.24570184E-02	0.68716942E-02	0.27714940E-01	-0.42929743E-03	0.29641671E-01	-0.15233466E-01
904	0.37645230E-03	0.49468331E-03	0.95236457E-03	0.31144690E-01	-0.44340112E-02	0.34904290E-01
907	0.29453068E-02	0.67466211E-02	0.58719895E-01	-0.28661575E-01	0.49164988E-01	0.99889070E-01
908	-0.29642973E-02	-0.69790923E-02	-0.42291795E-01	-0.13573754E-02	-0.57496600E-01	0.13223609E 00
909	-0.89302746E-03	-0.24005877E-02	-0.20919788E-01	0.28072445E-01	-0.20031221E-01	-0.19536604E-01

DETERMINISTIC ERRORS

	204	301	303	304	308	401
204	0.20644332E-04					
301	0.16762875E-02	0.48306935E-02				
303	0.48353119E-01	0.19930514E 00	0.22617145E-04			
304	0.14755737E 00	-0.27185266E 00	-0.81741145E-02	0.21580761E-04		
308	0.70717709E-02	0.96342453E 00	0.21606643E 00	-0.27652250E 00	0.49597982E-02	
401	0.19717232E-01	0.34827173E-02	-0.70805715E-01	0.26974183E-01	-0.32858950E-01	0.31550878E-02
407	-0.10632964E-02	-0.19377489E-01	0.11880585E 00	0.10607022E-01	-0.21469989E-01	0.81586210E 00
408	0.91970861E-02	-0.21173254E-01	0.16384399E 00	-0.91866025E-03	0.47598779E-01	0.52165691E 00
501	0.42656852E-01	0.55307504E-02	-0.62740105E-01	0.49267567E-01	-0.31671097E-01	0.16046181E 00
507	0.20009556E-01	-0.18053776E-01	0.13651138E 00	0.31168983E-01	-0.19373181E-01	0.63692180E-01
508	0.27080866E-01	-0.21113845E-01	0.17551623E 00	0.16057745E-01	0.50368633E-01	-0.10882157E 00
601	-0.72662815E-01	-0.93449084E-02	-0.37736065E-01	-0.64597767E-01	-0.25560000E-01	-0.47448454E-01
607	0.10280386E 00	0.22508267E-01	0.21083590E 00	0.92621664E-01	0.41665423E-01	-0.11423416E 00
608	0.12860131E 00	-0.22846764E-01	0.56561094E-03	0.12396851E 00	0.11430154E-01	0.11637505E 00
609	0.18252858E 00	-0.17995016E-01	0.78035614E-31	0.17870968E 00	0.25315078E-02	0.17867377E-01
701	-0.50736187E-01	-0.99573176E-02	-0.12783455E-01	-0.44225511E-01	-0.20759917E-01	-0.61263516E-01
704	-0.38528484E-01	0.14416451E-02	-0.57132129E-01	-0.35385936E-01	-0.10841833E-01	0.41173748E-01
707	0.64589785E-01	0.22907451E-01	0.15748368E 00	0.57107076E-01	0.32733919E-01	-0.79052362E-01
708	0.12338467E 00	-0.22725752E-01	-0.54096984E-02	0.11911795E 00	0.10290095E-01	0.11967449E 00
709	0.16990916E 00	-0.15533659E-01	0.99002225E-01	0.16501384E 00	0.80386010E-02	-0.14466339E-01
801	0.52036570E-02	0.21371258E-01	-0.47351868E-32	0.41182243E-02	0.24120926E-02	0.10148551E 00
804	0.42176676E-01	0.70309074E-02	0.45909881E-01	0.40308697E-01	0.58620630E-02	-0.36246187E-02
807	-0.42520338E-02	0.35325767E-01	0.12526323E 00	-0.98183848E-02	0.31016669E-01	-0.28753243E-01
808	0.99629032E-02	0.26158959E-01	0.20653904E 00	-0.44389364E-02	0.63396418E-01	-0.24995926E 00
809	0.51072866E-01	-0.25056206E-01	-0.30963170E-01	0.53337114E-01	-0.14318151E-01	0.66483218E-02
901	-0.50478047E-03	0.10829040E-01	-0.13363982E-01	-0.17006815E-02	0.16484903E-02	0.42774275E-01
904	0.39641852E-01	-0.84560957E-03	0.33398651E-01	0.38322085E-01	0.33296749E-02	-0.21112423E-01
907	-0.35976257E-01	0.37896001E-01	0.10714690E 00	-0.43015013E-01	0.35620543E-01	-0.88965690E-01
908	-0.19863349E-02	0.85240884E-02	0.13379221E 00	-0.92439216E-02	0.37130675E-01	-0.19826090E 00
909	0.35823298E-01	-0.16983005E-01	-0.23030490E-01	0.38525667E-01	-0.14190413E-01	0.38187159E-01

DETERMINISTIC ERRORS

	407	408	501	507	508	601
407	0.48829602E-02					
408	0.65517434E 00	0.27131480E-02				
501	0.63712795E-01	-0.10472117E 00	0.30075738E-02			
507	0.25401746E 00	0.12116215E 00	0.79678147E 00	0.46662277E-02		
508	0.10862803E 00	0.38660315E 00	0.49280422E 00	0.63627663E 00	0.26390810E-02	
601	-0.60972943E-01	-0.90312834E-01	-0.57394538E-01	-0.71379299E-01	-0.98444702E-01	0.11973926E-01
607	0.74196056E-01	0.29065203E 00	-0.99915429E-01	0.98527077E-01	0.31137325E 00	-0.58641667E 00
608	0.76192143E-01	0.11311134E-01	0.13644785E 00	0.93031425E-01	0.24117927E-01	-0.84083000E 00
609	0.31518006E-01	0.74765906E-01	0.42458398E-01	0.55948306E-01	0.95571741E-01	0.55400575E-01
701	-0.55813468E-01	-0.50955336E-01	-0.68504879E-31	-0.62532980E-01	-0.55651254E-01	0.37255092E 00
704	-0.69954026E-02	-0.89101503E-01	0.36355407E-01	-0.14362794E-01	-0.96169306E-01	0.11597725E-01
707	0.65456387E-01	0.21142835E 00	-0.69406863E-01	0.82802081E-01	0.22562883E 00	-0.10408732E 00
708	0.75047882E-01	0.18648687E-02	0.13907991E 00	0.90989664E-01	0.13833349E-01	-0.46768695E 00
709	0.27846149E-01	0.11669880E 00	0.79129806E-02	0.51778552E-01	0.13764241E 00	-0.12974928E 00
801	0.10067967E 00	0.26086450E-01	0.97847254E-01	0.97084207E-01	0.19876181E-01	-0.26292939E 00
804	0.30231457E-01	0.51675564E-01	0.13167752E-02	0.36861106E-01	0.56636694E-01	-0.28025350E-01
807	0.11576164E 00	0.19317642E 00	-0.30720672E-01	0.12178771E 00	0.19579400E 00	-0.16596057E 00
808	-0.52083180E-01	0.33630805E 00	-0.24179763E 00	-0.32679523E-01	0.35779190E 00	0.90314162E-01
809	-0.51489218E-01	-0.71276795E-01	0.15792706E-01	-0.45901255E-01	-0.65213552E-01	0.36653608E-01
901	0.29106450E-01	0.31534759E-02	0.40621301E-01	0.26338949E-01	-0.10385303E-03	-0.12239670E 00
904	-0.56555513E-02	0.34595675E-01	-0.14589496E-01	0.15585012E-02	0.41218040E-01	0.57760999E-02
907	0.31352400E-01	0.17904869E 00	-0.92049289E-01	0.35295588E-01	0.18260366E 00	-0.28320336E-01
908	-0.75565605E-01	0.19080786E 00	-0.19023726E 00	-0.60657959E-01	0.20770994E 00	0.21449953E 00
909	0.85150853E-02	-0.51156832E-01	0.41244083E-01	0.96292155E-02	-0.50803427E-01	-0.54646243E-02

DETERMINISTIC ERRORS

	607	608	609	701	704	707
607	0.23112985E-01					
608	0.18153809E 00	0.10615442E-01				
609	-0.30369989E 00	0.17440807E 00	0.21562597E-01			
701	-0.54117403E-01	-0.46999499E 00	-0.12061781E 00	0.12397690E-01		
704	-0.13331529E 00	0.38231868E-01	-0.76817136E-01	-0.38375583E 00	0.40264042E-04	
707	0.30194765E 00	0.12788477E-01	0.14126943E 00	-0.63521548E 00	0.56645507E 00	0.24600063E-01
708	-0.38112070E-01	0.72537810E 00	0.17261595E 00	-0.83660942E 00	0.13968219E 00	0.22802103E 00
709	0.26698819E 00	0.10199019E 00	0.28573175E 00	0.24118859E 00	-0.74281954E 00	-0.49171221E 00
801	0.24074252E-01	0.29851523E 00	0.75984033E-01	-0.25559948E 00	0.11432222E-01	0.31047866E-01
804	0.10090136E 00	-0.16802906E-02	0.79540808E-01	-0.11244256E-01	-0.33024402E-01	0.67526412E-01
807	0.20530541E 00	0.10649900E 00	0.55444396E-01	-0.14066613E 00	-0.45769566E-01	0.16205020E 00
808	0.37281887E 00	-0.25829114E 00	0.98456517E-02	0.13359673E 00	-0.12015251E 00	0.26774060E 00
809	-0.49017978E-01	0.16136801E-01	0.36361946E-01	0.33444910E-01	0.61124074E-02	-0.43089582E-01
901	0.10689915E-01	0.13044783E 00	0.36372642E-01	-0.11834774E 00	0.48813185E-02	0.12795163E-01
904	0.72864835E-01	-0.20434783E-01	0.53221151E-01	0.17523296E-01	-0.26563320E-01	0.47543427E-01
907	0.17697239E 00	-0.62038746E-01	-0.28601954E-01	-0.11204912E-01	-0.43802951E-01	0.13878929E 00
908	0.18120362E 00	-0.30509626E 00	-0.74661815E-01	0.22849822E 00	-0.65786406E-01	0.12914287E 00
909	-0.26351413E-01	0.28878554E-01	0.56791823E-01	-0.38965002E-02	0.19834056E-02	-0.27302597E-01

DETERMINISTIC ERRORS

	708	709	801	804	807	808
708	0.10592908E-01					
709	0.46483937E-01	0.28213489E-01				
801	0.29691165E 00	0.47680041E-01	0.12042965E-01			
804	-0.55460755E-02	0.87205524E-01	-0.47314195E 00	0.39093596E-04		
807	0.10042004E 00	0.71151707E-01	0.86030883E 00	-0.60230610E 00	0.20495570E-01	
808	-0.26913501E 00	0.88709626E-01	0.12215208E 00	-0.38164100E 00	0.56970511E 00	0.96500909E-02
809	0.16859886E-01	0.25063304E-01	0.46815481E 00	-0.78015997E 00	0.64787725E 00	0.47190665E 00
901	0.12958419E 00	0.24105576E-01	0.15173276E 00	0.57438817E-02	0.78420653E-01	-0.94442385E-01
904	-0.23253629E-01	0.61077052E-01	-0.29589798E-01	0.18958811E-01	0.78905704E-02	0.77383096E-01
907	-0.66383328E-01	0.47181860E-02	0.17576322E-01	0.16572768E-01	0.15414604E 00	0.28305649E 00
908	-0.30907349E 00	-0.15345976E-01	-0.31802702E 00	0.45396405E-02	-0.13523384E-01	0.54707918E 00
909	0.28730079E-01	0.45886267E-01	0.99268950E-02	0.10477094E-01	-0.44494148E-01	-0.11561815E 00

DETERMINISTIC ERRORS

	809	901	904	907	908	909
809	0.25422265E-01					
901	-0.28831106E-01	0.34634672E-01				
904	0.10668612E-01	-0.27265326E 00	0.42525116E-04			
907	-0.66275773E-01	0.83161184E 00	-0.40380356E 00	0.38907436E-01		
908	0.13965372E-01	-0.61514533E 00	-0.87979196E-01	-0.10016623E 00	0.24979372E-01	
909	0.24315539E-01	0.11262220E 00	-0.66958137E 00	0.30486801E 00	0.26410571E 00	0.40554877E-01

REFERENCES

1. Neighbors, A. K., Cole, J.W., and Daniel, F., "Error Analysis of Saturn Guidance Hardware as Applied to a Lunar Mission, MTP-ASTR-A-63-4, March 1963, Marshall Space Flight Center, Huntsville, Alabama.

2. "Users Manual for Powered Flight Optimization and Error Analysis Programs", Philco WDL-TR2759, Palo Alto, California, 15 February 1966.

3. Schmidt, S. F., "The Application of State Space Methods to Navigation Problems", Philco WDL-TR4, Guidance and Control System Engineering Department, July 1964.

4. Tyler, J. S., Jr., "Improved Techniques for Statistical Error Analysis and Parametric Studies of Space Systems", Philco WDL-TR2892, 1 May 1966, Palo Alto, California.

5. AF ETR Instrumentation Handbook, ETR-TR-65-9, Pan American World Airways, Inc., Guided Missiles Range Division Development Planning, August 1965.

6. Junkin, Bobby G., "A Tracking System Error Model Regression Analysis for Systematic Error Evaluation of Apollo - Saturn Radar Flight Test Data", NASA TMX-53487, July 5, Marshall Space Flight Center, Huntsville, Alabama.

TASK 3
EFFECT OF BIAS ERRORS ON INTERPLANETARY NAVIGATION AND GUIDANCE SYSTEM PERFORMANCE

(SUMMARY)

Contract No. NAS8-20358

20 October 1967

Prepared by
Paul J. Rohde
PHILCO-FORD CORPORATION
Space and Re-entry Systems Division
Palo Alto, California

for
National Aeronautics and Space Administration
Marshall Space Flight Center
Huntsville, Alabama

SECTION 1
INTRODUCTION

1.1 GENERAL OBJECTIVES AND SCOPE

The primary objective of the Navigation and Guidance research task of Contract NAS8-20358 is to critically assess the influence of the constraints imposed on the study performed under Contract NAS8-11198 on the results obtained[(1)]*. Research under Contract NAS8-11198 established the basic requirements for an Advanced Spaceborne Detection, Tracking and Navigation System capable of performing future interplanetary missions. The constraints on the original study that are analyzed in this research report are the following:

(1) The assumption that the only significant error sources are random in nature.

(2) The original choice of 1975 round-trip Mars trajectory.

In order to analyze the influence of these constraints on the previous results, several tasks had to be completed:

(1) Research and analysis of the literature available on the techniques used to estimate the various physical constants that are required to specify an interplanetary trajectory. The uncertainty associated with each of these estimates constitutes a bias error in the equations of motion of a spacecraft.

(2) Determine the types of measurement bias errors to be considered.

(3) Derive suitable mathematical models to analyze the influence of the equation of motion and measurement bias errors on the trajectory estimation process.

(4) Develop methods for data presentation which indicate the importance of the bias error sources.

(5) Determine the areas which require future research.

---

* Superscripts refer to references.

The scope of the study includes an evaluation of the onboard navigation system performance under the influence of the following bias errors.

(1) Equation of Motion Errors

a. Uncertainty in the Astronomical Unit conversion
b. Uncertainty in the Earth's mass
c. Uncertainty in Mars' mass
d. Uncertainty in the solar radiation pressure

(2) Measurement Biases

a. Sextant bias in onboard measurement
b. Time bias in onboard clock

1.2 STUDY FORMAT

The effect of bias errors on the navigation system performance may vary considerably depending on the mission itself. This study is designed to identify the error sources and show their effect on the system performance for a variety of trajectories.

The study was performed in four basic steps. The results of each step are presented in the order that they were performed.

(1) Analysis of applicable filter theory
(2) Analysis of bias error sources
(3) Computer simulation
(4) Generation of results.

SECTION 2

THEORETICAL ANALYSIS OF OPTIMAL ESTIMATION PROCESS

The function of the navigation system, as defined in this report, is to obtain an estimate of vehicle state based on either direct observations of the vehicle (Earth-based tracking) or observations of celestial bodies whose positions are known (on-board tracking). The purpose of this section is to summarize the error analysis techniques that have been used to study the effects of measurement and equation of motion parameter uncertainties on the vehicle state estimation process.

The analysis of the orbit estimation process is based on the filtering theory of Kalman[2] and the orbit determination application by Schmidt[3,4,5]. The theory for including measurement and equation of motion bias type errors into the optimal orbit estimation process is presented in References 1 and 6. These references show three different techniques by which the bias errors in the estimation process can be handled. Each technique produces an optimal estimate but under a different assumption concerning the modeling of the dynamic and/or measurement bias error sources. The techniques are as follows:

(1) Neglect - In this case, the state being estimated is simply the three components of vehicle position and velocity. The dynamic and measurement models are assumed to be known perfectly and there are no bias errors in the physical process being analyzed. The effect of uncertainties in system parameters are neglected.

(2) Include - This technique allows for an expansion of the state vector to include specified dynamic and measurement parameters that produce bias error sources. The optimal estimation process fits the measurement data to the model to obtain a best estimate of the vehicle state and the system parameters simultaneously.

(3) Consider - With this type of analysis, the measurement and dynamic parameters are not included in the state vector being estimated but the effects of the uncertainties in these parameters are considered in the estimation process. An optimal estimate of the state is obtained under the constraint that specified unsolved-for system parameters have constant uncertainties (standard deviations) associated with their fixed estimates.

Each of these techniques has both favorable and unfavorable aspects. If the bias errors are neglected, the state vector is reduced in dimension and correspondingly the number of computations required in the estimation process is reduced. Alternately, the removal of bias errors from a problem in which they can significantly influence the results being obtained causes the state estimates that are obtained to have optimistic uncertainties attached to them. The implication here is that an analysis must be made to establish the relative importance of measurement and dynamic bias error sources to a particular orbit estimation process. On the basis of this analysis, the method for treating each of the error sources can be established. The allowable total size of the state vector would be limited by the computer capability either ground or onboard in terms of its size and speed. Within these limitations, the filtering techniques used for the various bias errors sources in the order of decreasing importance would be to include, consider, and neglect them.

Section 2 of the final report presents a detailed mathematical description of the derivation of the optimal filter for each of the three processing techniques described above. Due to the length of the derivations, they are omitted from this summary document. Section 2 also contains a description of some recent developments on techniques for efficient parametric analysis of navigation system performance. The mathematical theory is based primarily on the fine work of Gunckel[7]. The analysis techniques apply to two areas: (1) the effect of bias errors that are not included in the optimal filter and (2) the effect of varying the initial state variable (bias errors) uncertainty covariance matrix. The important feature of these techniques is that they are applied to the data obtained at the conclusion of a single computer run of an orbit determination simulation. The parametric analysis is accomplished by means of matrix manipulations of the end point data and thereby eliminates the need for making a large number of computer analysis runs when scanning a range of parametric values of the initial error variances.

SECTION 3
ANALYSIS OF BIAS ERROR SOURCES

This section presents a description of the bias error sources that are considered in this study. There are two basic types of bias error sources of interest: (1) equation of motion parameters and (2) measurement parameters. These parameters enter the estimation process because even though an estimate is available for each parameter there is some degree of uncertainty associated with it. The use of the term bias error to describe these errors arises from the fact that although the expected difference between the parameter estimate and its true value is zero, the uncertainty (standard deviation) in the estimate allows for a constant error to exist. The actual difference between the estimate and the true value enters the estimation process as a constant.

The equation of motion error sources that are included in the analysis are: (1) astronomical unit conversion, (2) mass of the Earth, (3) mass of Mars, and (4) solar radiation pressure. The measurement error sources evaluated are a bias in the on-board sextant measurement and a bias in the onboard clock.

The information presented in this section is a summary of the final report and the midterm progress report, entitled, "Influence of Uncertainties In the Astronomical Unit Conversion and Mars Planetary Mass on Earth-Mars Trajectories."[8]

3.1 EQUATION OF MOTION BIASES

The various methods used in estimating the heliocentric and planetary constants are described in References 9 through 14. They present the results of several determinations of the ratio of the astronomical unit to laboratory units and the planetary masses of Earth and Mars.

3.1.1 Astronomical Unit Conversion

The analysis of the astronomical unit (A.U.) presented here and the results in Section 5 are an extension and generalization of the work reported in Reference 5 by S. Henrick, et al.

The ratio of the A.U. to the equatorial radius is the "solar parallax" expressed in radians (Figure 1). Then the desired ratio of the kilometer

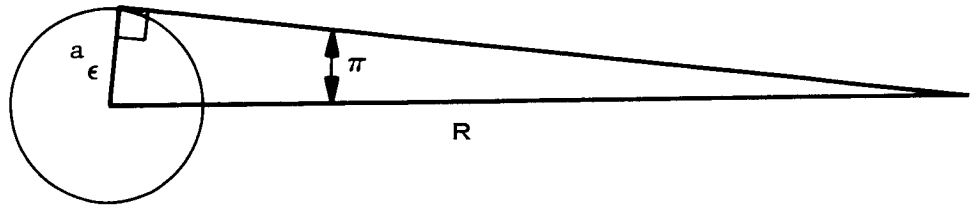

WHERE a_ϵ = EARTH EQUATORIAL RADIUS (KM)
R = EARTH SUN MEAN DISTANCE (KM)
π = SOLAR PARALLAX

Figure 1 Solar Parallax

to the A.U. embodied in the mean Earth distance, R, is related to the solar parallax as follows:

$$R \doteq \frac{a_\epsilon}{\pi} \qquad (3\text{-}1)$$

where

a_ϵ = Earth equatorial radius

π = Solar parallax

R = Earth-Sun mean distance

The relative uncertainty in the ratio is

$$\frac{\Delta R}{R} = - \frac{\Delta \pi}{\pi} - \frac{\Delta a_e}{a_e} \qquad (3\text{-}2)$$

or neglecting the smaller uncertainty in a_e

$$\frac{\Delta R}{R} = - \frac{\Delta \pi}{\pi} \equiv - \pi' \qquad (3\text{-}3)$$

The effect of the relative uncertainty, π', in the ratio will appear in the initial geocentric position and velocity of the vehicle if they are expressed in the astronomical unit. The result of this uncertainty on a Hohmann transfer to Mars is shown in Figure 2.

3.1.2 Planetary Mass

The target approach phase of an interplanetary trajectory is a target centered hyperbola. The characteristics of this trajectory are determined by the vehicle velocity state relative to the target at the time the "sphere of influence"[16] is reached and the planetary mass of the target body. The vehicle velocity state relative to the target at this time is determined by the particular heliocentric transfer trajectory that is used. The following is a summary of the effect of a planetary mass uncertainty on an approach trajectory.

The error in planetary mass is related to an error in the semi-major axis of the approach hyperbola through the vis-viva equation.

$$a = \frac{\mu}{v_\infty^2} \qquad (3\text{-}4)$$

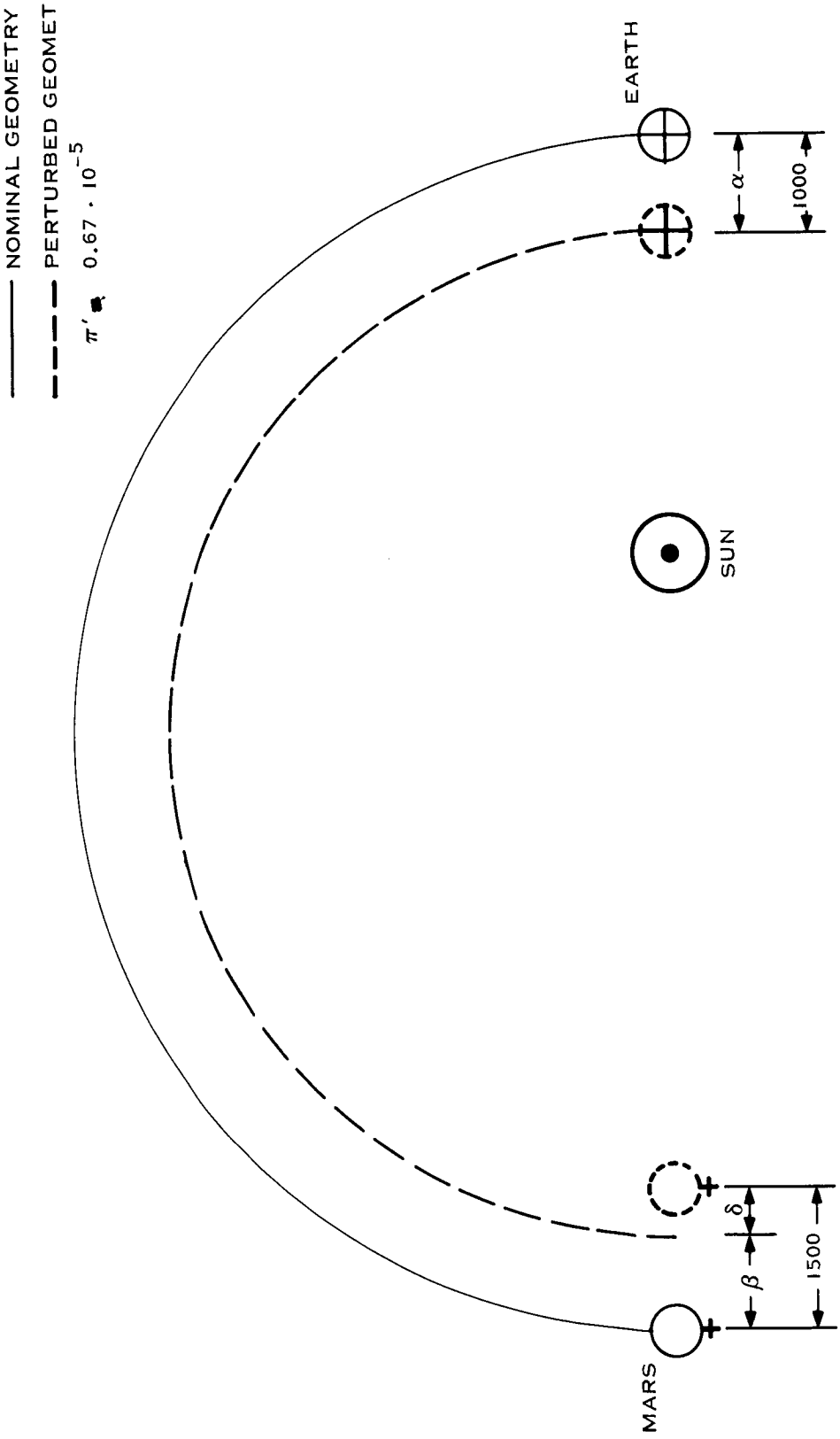

α = 1000 KM $\alpha + \beta$ = 1940 KM δ = 560 KM

Figure 2 Effect of Error in Solar Parallax

where

a = semi-major axis

μ = planetary mass

v_∞ = hyperbolic excess velocity

or

$$\frac{\Delta\mu}{\mu} = \frac{\Delta a}{a} \tag{3-5}$$

The uncertainty in the angle between the approach and regression asymptotes, $\Delta\delta$, can be expressed in terms of v_∞ and the semi-minor axis, b, as

$$\Delta\delta = -\frac{2b}{v_\infty^2}\left[\frac{\Delta\mu}{\mu^2/v_\infty^4 + b^2}\right] \tag{3-6}$$

Figure 3 presents the deviations in the scattering angle at Mars as a function of v_∞ and distance of closest approach. The planetary mass uncertainty,

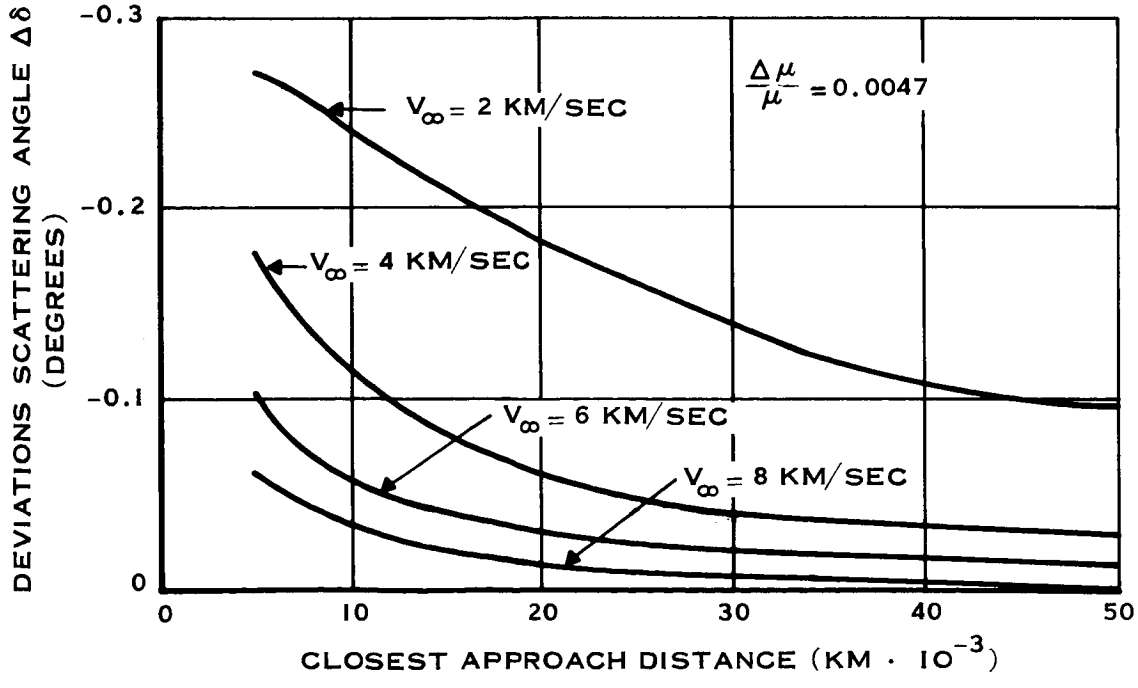

Figure 3 Mars' Scattering Angle Deviation

$\frac{\Delta\mu}{\mu}$, is 0.0047. These data were obtained by taking the difference between a nominal scattering angle and scattering angles obtained when using perturbed values of the planetary gravitational constant, μ, in a conic trajectory program. The difference results obtained in this manner for the stated planetary mass deviation agree quite well with the linear deviation expressed by equation (3-6).

The deviation in Mars close approach distance as a function of planetary mass and close approach distance (RCA) is shown in Figure 4. The data in Figure 4 indicate that an uncertainty in the planetary mass of the order of 150 km^3/sec^2 causes close approach deviations from ±2 km for a high energy trajectory to ±15 km for a very low energy trajectory. The deviations on the low energy trajectory increase to ±35 km for a close approach distance of 50,000 km. These data show that the planetary mass uncertainty is an important factor for missions requiring terminal accuracies on the order of 15 km and less.

The entry corridor at Mars with a 5 mb atmosphere is approximately 20 km[17] or ±10 km from a nominal trajectory. This indicates that for an atmospheric entry mission, a low energy approach trajectory could have significant deviations due to the uncertainty in the planetary mass.

The deviation in close approach distance at Earth is less than ±1 km for a planetary mass uncertainty of 15 km^3/sec^2. This indicates that for an entry mission at Earth the planetary mass uncertainty is not a very significant factor. The data shown in Reference 18 indicates that the entry corridor at Earth is 21 km for a vehicle with a L/D ratio of one and a speed of 18 km/sec.

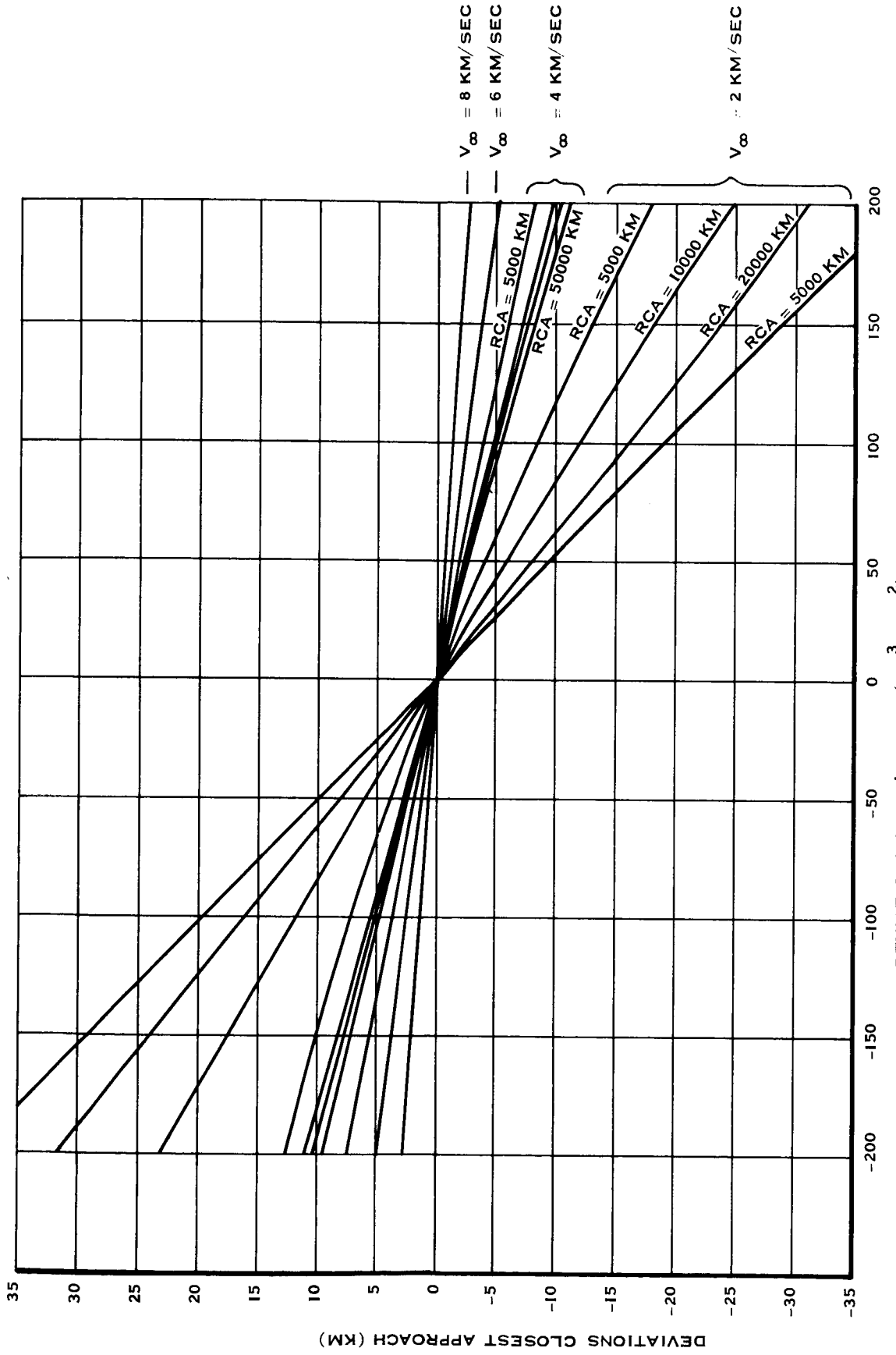

Figure 4 Deviations in Closest Approach Distance

3.1.3 Solar Radiation Pressure

In the trajectory analysis of a spacecraft, a knowledge of the environmental forces acting on the vehicle is required. An important component of the spacecraft environmental force is that due to radiation. While radiation is generally considered as a mode of energy transfer, it is well known that momentum is also transferred by radiation. The forces resulting from this momentum transfer can have an important influence on the trajectory of a spacecraft.

The primary interest in this study centers on the effects of uncertainties in the solar radiation force acting on the vehicle. The analysis presented in Section 5 treats the solar radiation force uncertainty as a bias error. The analysis examines the ensemble behavior of the vehicle state through the state convariance matrix. The solar pressure enters the equations of motion as follows.

The equation of motion of the spacecraft may be written as follows:

$$\dot{X} = F(X, U, t) \tag{3-7}$$

where

$$X = \begin{bmatrix} R \\ V \end{bmatrix}$$

Using the partitioned form of equation (3-7)

$$\ddot{R} = F'(R, V, U, t) \tag{3-8}$$

The function F' may be written as follows:

$$F' = -\mu_{CB} \frac{R}{r^3} - \sum_{i=1}^{N} \mu_i \left(\frac{\Delta_i}{\delta_i^3} + \frac{R_i}{r_i^3} \right) + \sum_{j=1}^{k} P_j \tag{3-9}$$

where

p_j are perturbation accelerations due to drag, oblateness, solar pressure, etc.

The form of the solar radiation pressure in the p_j term of (3-9) is assumed to be an inverse square repulsive acceleration relative to the sun.

$$p = k_{sp} \frac{R_s}{r_s^3} \qquad (3\text{-}10)$$

where

R_s is the radius vector from the sun to the vehicle

r_s is the magnitude of R_s

k_{sp} is a constant including the reflectance of the vehicle, the vehicle's mean sun-directed surface area and the vehicle's mass.

An uncertainty in the constant, k_{sp}, of (3-10) produces an uncertainty in the solar radiation pressure acceleration.

3.2 MEASUREMENT BIASES

The measurement biases considered in the analysis of Section 5 are: (1) onboard clock bias, and (2) an angle bias in the sextant measurements. The manner in which these bias errors enter the estimation process is through the gradient of the measurement with respect to the biases. The following is the measurement gradient for the sextant type planet-star observation that is used in the analysis. The measurement sensitivity to the following quantities is shown.

R Position state-radius vector from the central body to the vehicle

V Velocity state-inertial velocity relative to the central body

τ Time bias-error in onboard clock

δ Angle bias-error in sextant instrument

The sextant star-planet angle measurement is made in the plane defined by the vector from the vehicle to the star and the vector from the vehicle to the body being observed.

The total measurement gradient that is desired is the following:

$$H_z = \left(\frac{\partial \alpha}{\partial R} ; \frac{\partial \alpha}{\partial V} ; \frac{\partial \alpha}{\partial \delta} ; \frac{\partial \alpha}{\partial \tau} \right) \qquad (3\text{-}11)$$

The total measurement gradient with respect to the state and the two biases is shown below.

$$H_z = \left(- \frac{1}{|P|} \left[\frac{\hat{P} x \hat{S}}{|\hat{P} x \hat{S}|} x \hat{P} \right] ; 0; 1 ; - \frac{1}{|P|} \left[\frac{\hat{P} x \hat{S}}{|\hat{P} x \hat{S}|} x \hat{P} \right] [\dot{P}_p - V] \right) \qquad (3\text{-}12)$$

where

$\hat{P}$ = Vehicle-planet vector

$\hat{S}$ = Unit vector vehicle-star

$\dot{P}_p$ = Planet velocity

V = Vechicle velocity

SECTION 4
DIGITAL COMPUTER PROGRAMS

The analysis of the bias errors described in Section 3 has been performed using three digital computer program simulations. They are: (1) Patched Conic A.U. Program, (2) Planetary Mass Program, and (3) Mark II Error Propagation Program.

4.1 PATCHED CONIC A.U. PROGRAM

The Patched Conic A.U. Program simulates the effect of a change in the A.U. Conversion to a laboratory unit on the planetary ephemeris and shows the resulting effect on an interplanetary trajectory. In the ephemeris model used, a change in the A.U. is accompanied by changes in the radial distances of the planets and the mass of the Sun. These changes maintain the angular frequencies of the planets constant.

The program obtains an Earth-Mars (Mars-Earth) heliocentric conic trajectory with a specified flight time and transfer angle. The heliocentric conic is then patched to a Mars (Earth) centered conic trajectory at the sphere of influence. The A.U. conversion factor is then perturbed causing changes in the positions and velocities of Earth and Mars. The gravitational constant is also changed. The result of these changes is that the initial vehicle state relative to the Sun deviates from the nominal conditions. The vehicle position is changed with the change in the Earth's positon. The vehicle velocity relative to the Sun is changed through the change in the Earth's velocity. The perturbed heliocentric trajectory is patched to Mars and the approach trajectory differences from the nominal computed.

4.2 PLANETARY MASS PROGRAM

The Planetary Mass Program is designed to analyze the effect of uncertainties in planetary mass on interplanetary approach trajectories. The characteristics of a planetary approach trajectory are determine by vehicle velocity state relative to the planet at the "sphere of influence" and the

planetary mass. The program uses a conic trajectory. The magnitude of the vehicle velocity state at the sphere of influence, V_∞, is a program input used to simulate approach trajectories of different energies. The flight path angle of the approach velocity vector is used as a control by the program to obtain a trajectory with a specified distance of closest approach. After the generation of the desired nominal approach trajectory, the program perturbs the planetary mass and computes the differences between the perturbed approach trajectory and the nominal.

4.3 MARK II ERROR PROPAGATION PROGRAM

The Mark II Error Propagation Program is used in the statistical analyses of the effects of the bias errors on the navigation system performance. The Mark II program, with modifications incorporated during the study, is capable of statistically analyzing the effects of the bias errors for each of the three techniques described in Section 2: (1) Neglecting, (2) Including, and (3) Considering. The parametric analysis techniques described in Section 2 have also been added to the program capability.

The program is capable of analyzing the effects of the following bias errors.

a. Sextant Bias (Modification added during study)
b. Onboard Clock Bias
c. Earth Planetary Mass Uncertainty
d. Mars Planetary Mass Uncertainty
e. Solar Radiation Pressure Uncertainty

A basic assumption used in the program is that linearity is satisfied in the neighborhood of a nominal trajectory. The state covariance matrix is propagated along the nominal trajectory with the transition matrix. At each measurement time the covariance matrix is updated through the use of a Kalman optimal filter.

SECTION 5
MIDCOURSE NAVIGATION STUDY

The results presented in this section show the effects of bias errors on the performance of an onboard navigation system. These results are an evaluation of the navigation system requirements generated in the original study[1] with the constraint that only random errors were considered in the analysis. The analysis is performed for the midcourse phases of both the outbound Earth to Mars trajectories and the return Mars to Earth trajectories.

The navigation analysis is limited to the use of an onboard sextant measuring device with a random error of 10 arc seconds. The initial study showed that an instrument of approximately this accuracy was capable of performing the Earth-Mars round trip navigation such that ± 3.5 km entry corridors were achieved at both Mars and Earth. The onboard measurement schedules used for the outbound and return trajectories were selected in the original study. The analysis of the schedule selection is in Reference 1.

There are several trajectories utilized in the following summary analyses. The statistical analyses with the Mark II program use the same round trip nominal trajectory used in the original study. This nominal trajectory has a 235 day outbound and 296 day return with a 40 day stay at Mars. The Patched Conic A.U. Program and Planetary Mars program are used to analyze equation of motion error effects on a large number of trajectories. The trajectories analyzed include transfer and approach trajectories of practical interest.

5.1 EARTH-MARS TRANSFER

The results of two forms of analysis are presented below for the outbound trajectories. The first type of analysis evaluates the trajectory deviations or differences from a nominal trajectory that are introduced by

deviations in the equation of motion parameters. These analyses are performed with the Patched Conic A.U. Program and the Planetary Mass Program. The second type of analysis is a statistical evaluation of the effect of bias errors on the navigation system performance. These results are obtained with the Mark II Error Propagation Program.

5.1.1 Equation of Motion Errors

The equation of motion bias errors analyzed are uncertainties in the following: (1) A.U. conversion, (2) Earth and Mars planetary masses, and (3) solar radiation pressure.

5.1.1.1 A.U. Conversion. The sample data and results presented in this section were generated using an uncertainty in the conversion of the A.U. to kilometers of $\pm$1000 km. This is slightly larger than the uncertainty for the 1963 adopted value.

The approach phase of a number of Earth-Mars trajectories is analyzed to determine the navigation and guidance requirements due to the uncertainty in the A.U. conversion. Five heliocentric transfer angles are used with flight times for each from 100 to 500 days. Three trajectories of interest are included in the analysis. They are: (1) Hohmann transfer 180 degrees, 260 days, (2) Mariner IV trajectory 160 degrees, 228 days, and (3) High energy outbound leg of round-trip trajectory 270 degrees, 235 days. The results presented here are restricted to the 160 degree transfer trajectories with various flight times.

The trajectory data and corresponding target approach deviations are shown in Figures 5A and 5B. Part A of the figure shows the flight time, launch velocity, and target approach velocity as a function of the direction of the hyperbolic approach asymptote, $\hat{s}$. Part B shows the deviation in close approach distance for a 1000 km change in the A.U. conversion to kilometers. The 160 degree transfers show two deviation minimums. These data show the possibility of selecting trajectories that minimize the

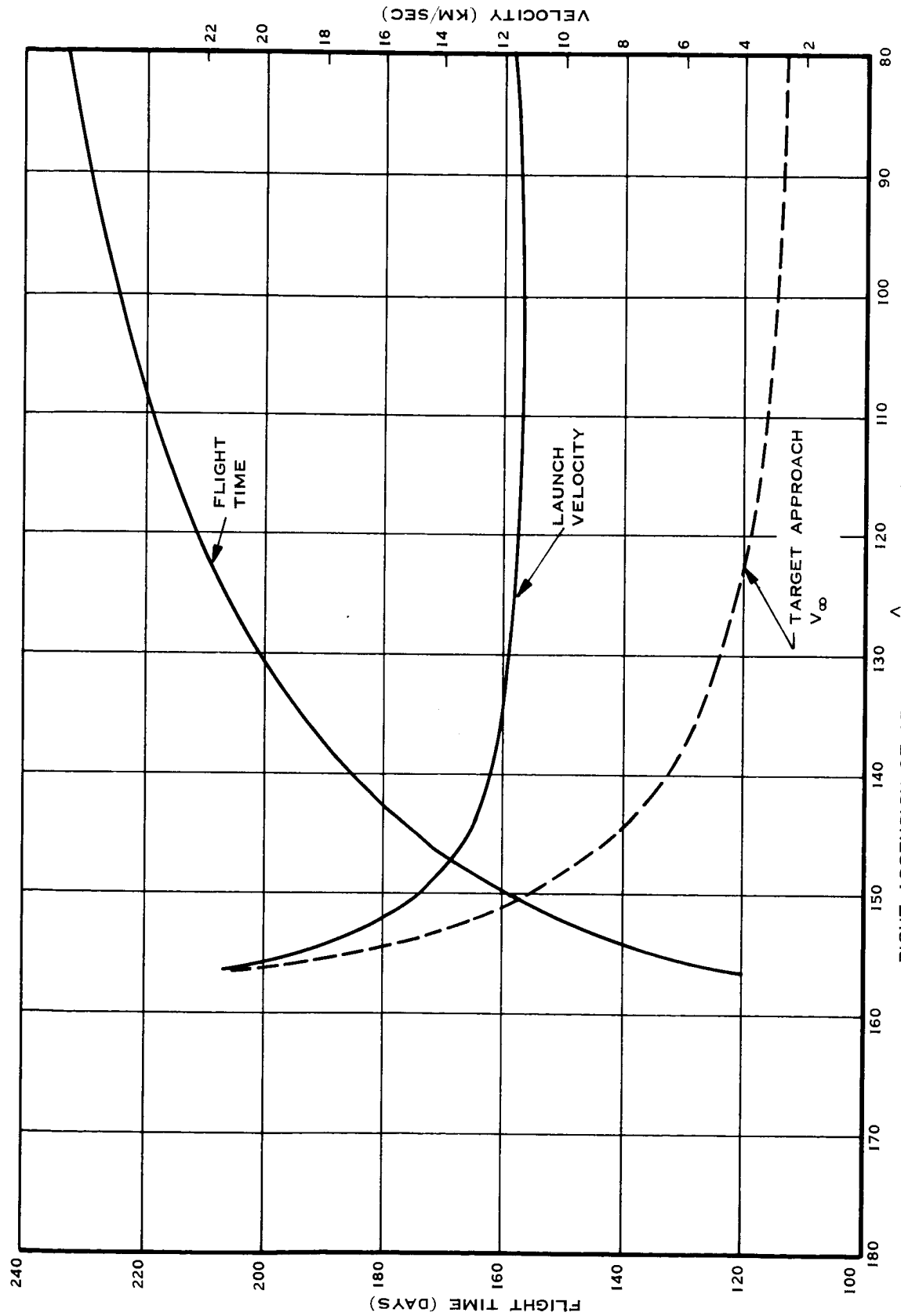

Figure 5A Trajectory Characteristics - 160° Transfer, Earth-Mars

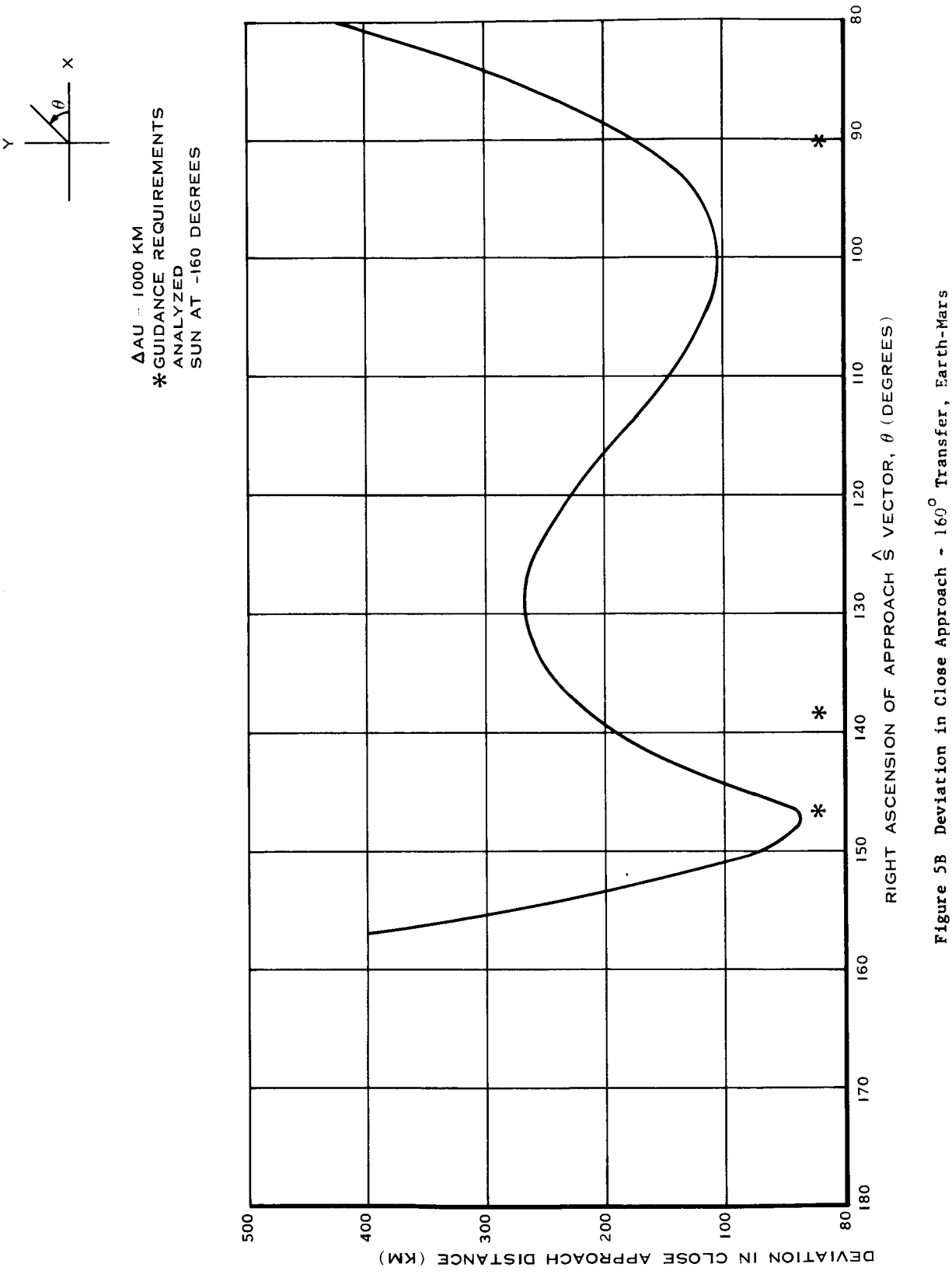

Figure 5B Deviation in Close Approach - 160° Transfer, Earth-Mars

effect of the uncertainty in the A.U. conversion on the close approach distance. The Mariner IV trajectory is one that is near a minimum. The 228 day 160 degree transfer has a deviation of 175 km for a 1000 km uncertainty in the conversion.

The trajectories marked with an asterisk on Figure 5B are analyzed to determine the approach guidance velocity required to correct the deviations. The results of this analysis are shown in Figure 6. The solid lines indicate the ΔV required for a fixed time of arrival (FTA) and the dotted lines the requirements for a variable time of arrival (VTA). The curves show that the requirements for FTA are nearly the same for all the trajectories shown. A correction at the sphere of influence requires about 10 meters/second and grows to approximately 200 meters/second as periaries is approached. The ΔV requirements for the VTA guidance law show a wide variation depending on the specific trajectory selected.

The trajectory that has a small close approach deviation, curve 1 in Figure 6, has a velocity requirement that ranges from less than 1 meter/second at the sphere of influence to 8 meters/second at periaries. The remaining VTA curves in Figure 6 show larger ΔV requirements that range from 2 meters/second to 40 meters/second for the trajectories with larger deviations. These requirements are considerably smaller than those required with a FTA guidance law.

The time at which a reasonable guidance correction can be made is determined by the navigation system. The error in estimate of the end constraints must be below a predetermined level before the guidance maneuver can be executed. The selection of an entry mission at Mars with a $\pm$10 km entry corridor defines tolerable limits on the end constraint deviations.

Figure 7 shows the error in estimate of the end constraints for three approach trajectories of different energies. The navigation measurements are made with a 10 arc second sextant. Measurements are taken every 15 minutes. The initial error in estimate of state is assumed to be 1000 km

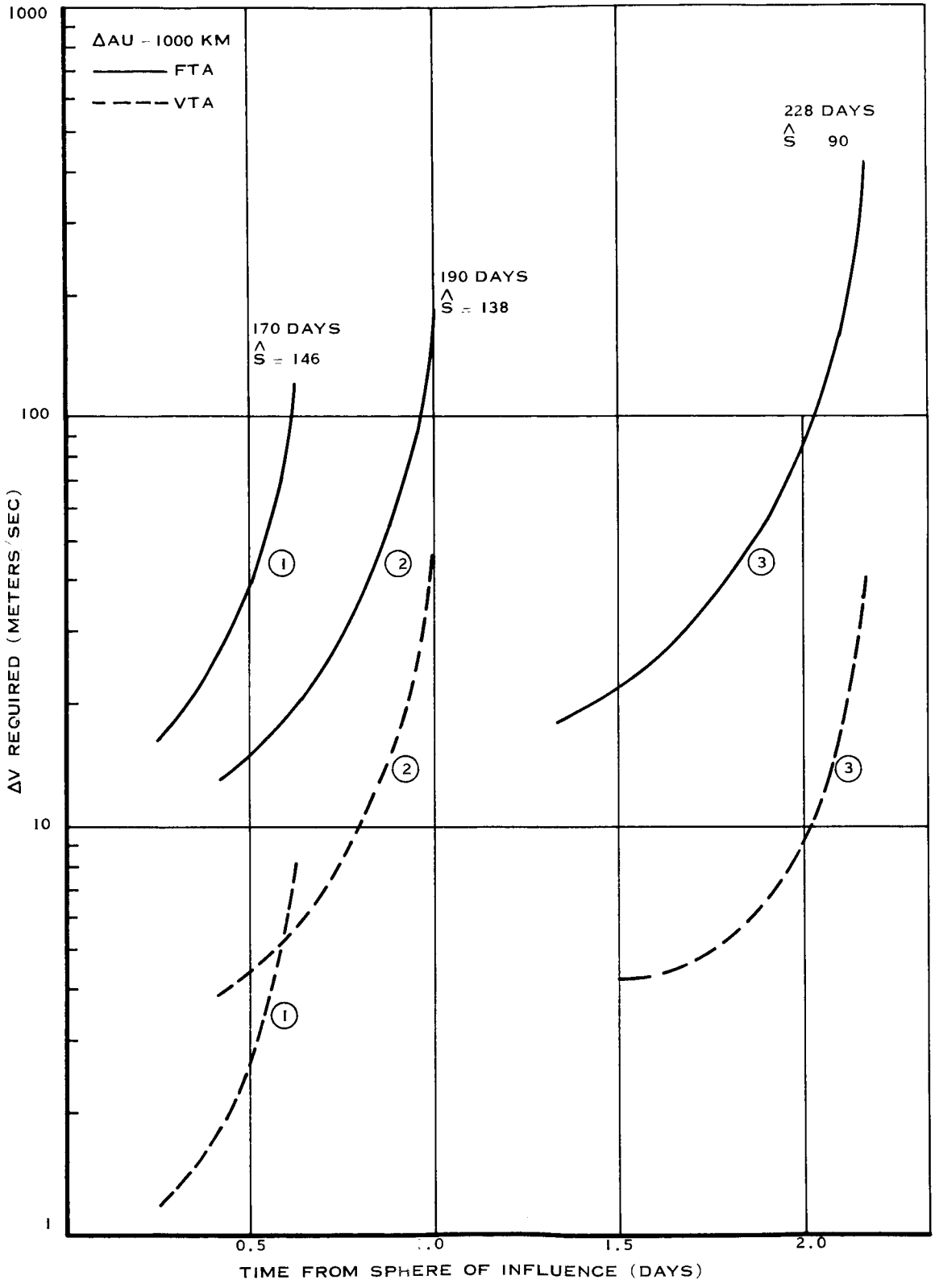

Figure 6 Approach ΔV Required for 160° Transfer

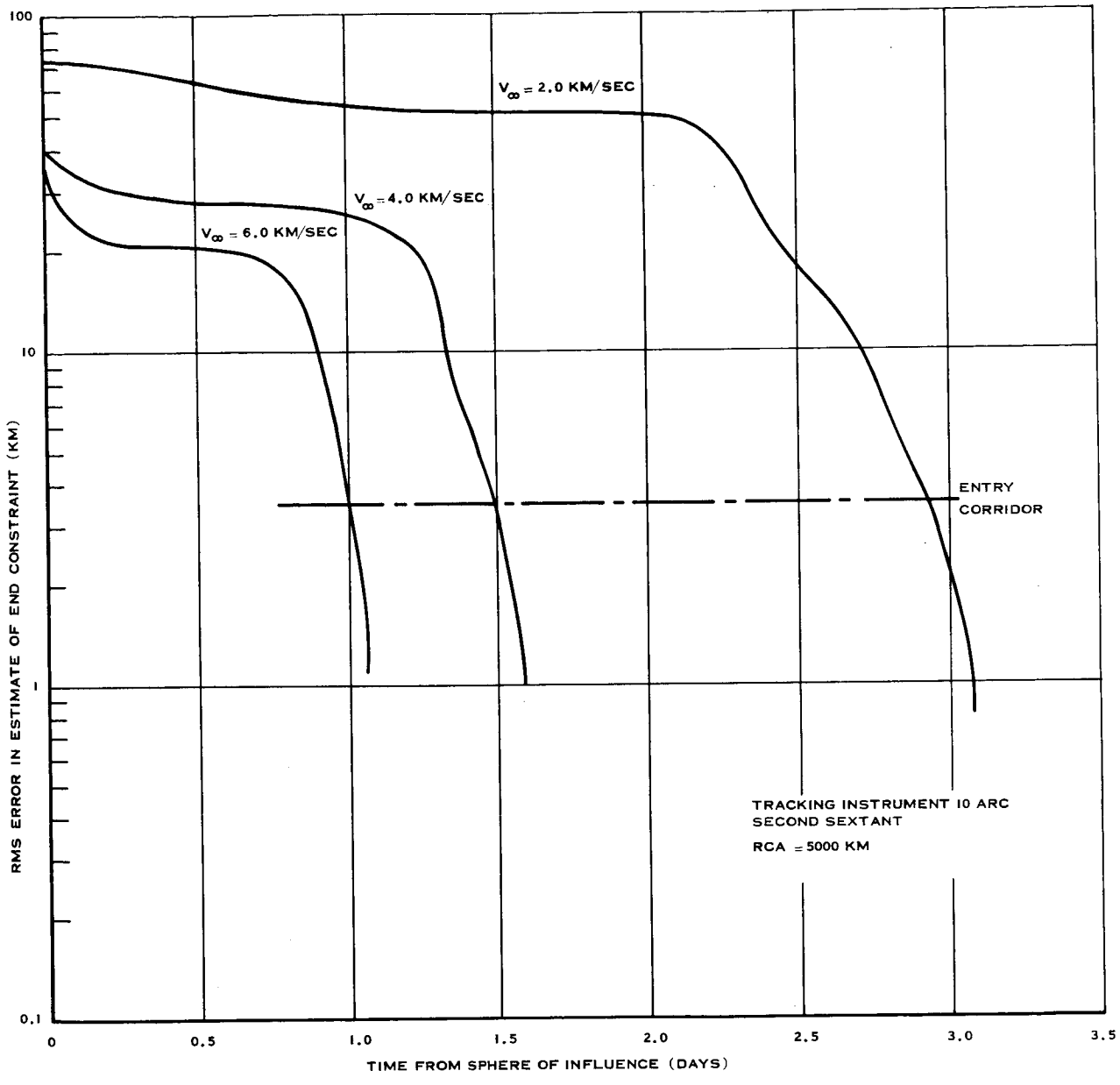

Figure 7 Error in Estimate of $\vec{B}$ Magnitude

in each of the inplane position coordinates and 0.2 meters/second in the velocity coordinates. These errors correspond to the actual deviations that occur at the time of patch to the target due to a 1000 km uncertainty in the A.U. conversion. Due to the onboard observations, the error in estimate of the constraints is quickly reduced to less than 100 km. It then remains relatively constant until the last few hours of the approach. The error in estimate is sufficiently small for an entry mission approximately 3 or 4 hours prior to periaries on each trajectory.

Figure 6 indicates that this time corresponds to corrections of 50 to 70 meters/second for a FTA guidance law. The VTA guidance requirements at this time are less than 10 meters/second. A FTA guidance policy allowing for two approach corrections could reduce the total ΔV required considerably from the 50-70 meters/second required for a single correction.

5.1.1.2 Mars' Planetary Mass. The results presented in this section show the navigation and guidance requirements for controlling the approach trajectory under the influence of an uncertainty in the planetary mass. The results assume that the midcourse guidance system has controlled the vehicle to the sphere of influence perfectly. The only equation of motion uncertainty considered is the planetary mass.

The time history of the growth in the predicted deviations in close approach distance and $\vec{B}$ magnitude based on the state deviation is shown in Figure 8. These data were obtained using a planetary mass uncertainty of 130 km^3/sec^2 and a close approach distance of 5000 km. The curves all display the characteristic of having very small deviations until 4 to 8 hours before periaries. The deviations then grow rapidly to values from 2 to 15 kilometers. The approach guidance ΔV required to correct these deviations is shown in Figure 9 as a function of time along the trajectory. The requirements are shown for both FTA and VTA guidance laws. The ΔV required on these trajectories for each guidance law is between 1 and 10 meters/second during the last few hours. The VTA velocity requirements are smaller in all cases.

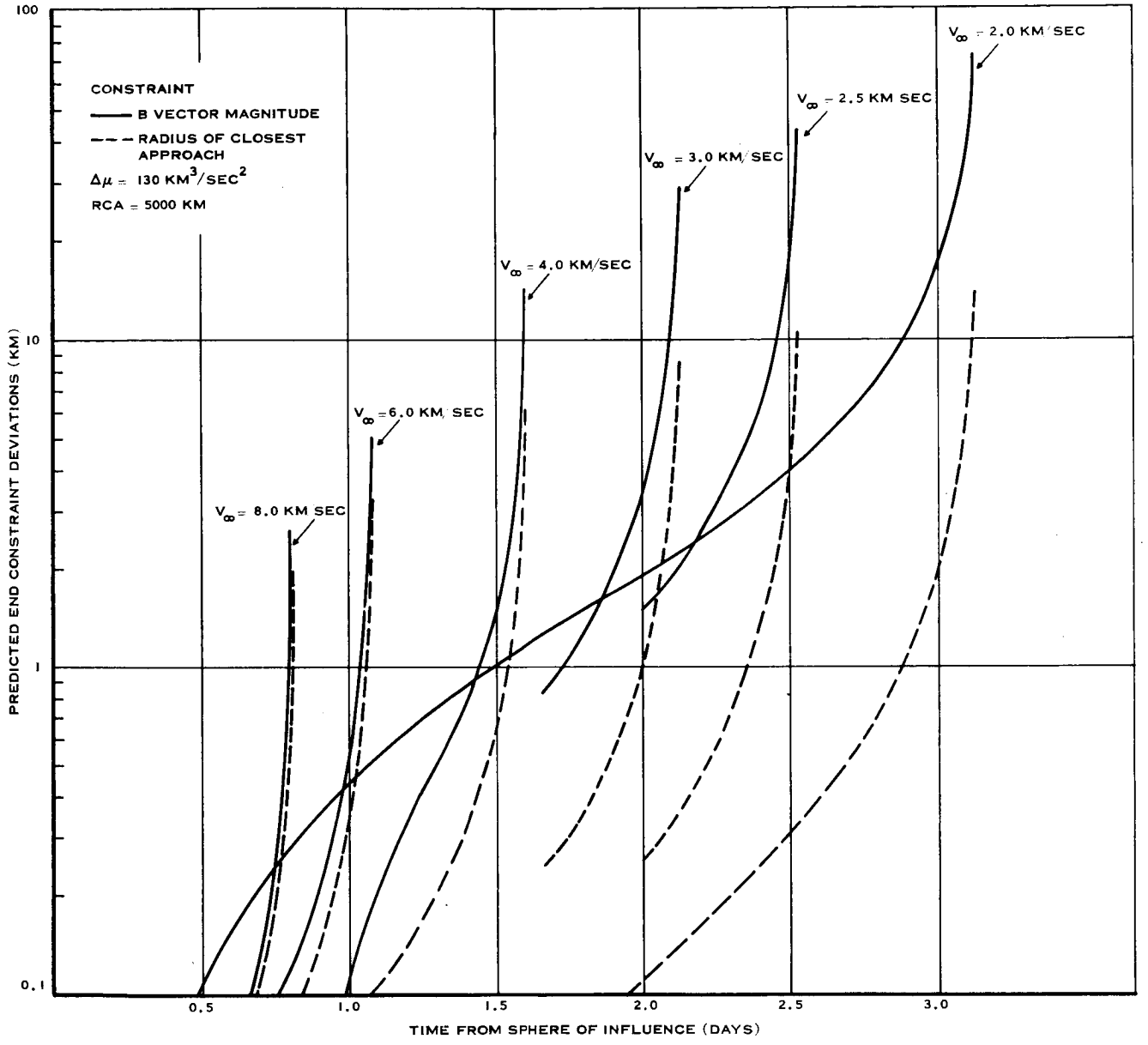

Figure 8 Time History of Predicted End Constraint Deviations

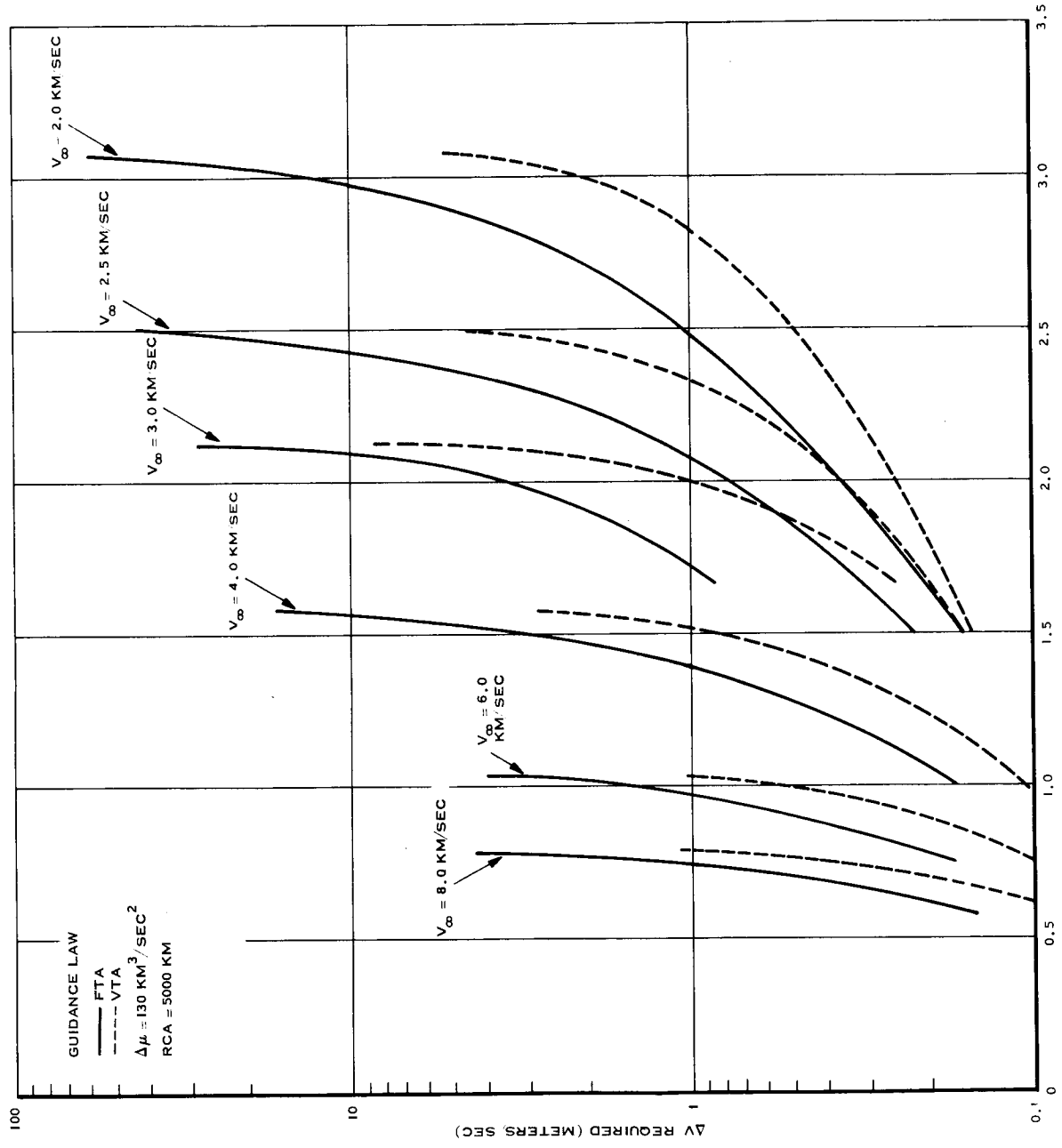

Figure 9 ΔV Required for Approach Guidance

The time at which a guidance correction can be made is determined by the capability of the navigation system to estimate the end point deviations to a satisfactory accuracy. The capability of an onboard navigation system using a 10 arc second sextant to estimate the end constraints is shown in Figure 10. The results are shown for three nominal trajectories with different energies. The parameters being estimated include the vehicle state and the planetary mass. The initial vehicle state uncertainty is assumed to be zero and the uncertainty in the planetary mass is 130 km^3/sec^2. The tolerable error in estimate for an entry mission is shown on Figure 10 as $\pm$3.3 km. The times on these trajectories that this level is reached are 2 days 19 hours for the trajectory with V_∞ = 2.0 km/sec and 1 day 12 hours for the V_∞ = 4.0 km/sec trajectory. Using these correction times in Figure 10 shows the guidance velocity requirements are approximately 1 meter/sec for a VTA guidance law and 3 meters/sec for FTA guidance law. The significance of these approach corrections in terms of the total mission is discussed in Section 6.

5.1.1.3 Statistical Analysis. The statistical analysis of the navigation system is performed with the Mark II Error Propagation Program. The measurement instrument is a 10 arc second accuracy sextant.

The results presented in Figure 11 show the effect of neglecting the equation of motion bias errors on the error in estimate of the end point constraint, $\vec{B}\cdot\hat{T}$. The $\hat{T}$ vector is in the trajectory plane. The number 4 curve in each figure shows the expected error in estimate of the end constraint under the assumption of a perfect physical model. These uncertainties are due to injection errors and random errors in the measurements. These results correspond to those obtained in the original study.(1) The three remaining curves in each figure show the additional error in estimate due to the neglected uncertainties in the planetary masses of Earth and Mars and the solar radiation pressure. The planetary mass uncertainties used are 15 km^3/sec^2 for the Earth and 150 km^3/sec^2 for Mars. These are approximately the uncertainties for the 1961 adopted values. The assumed form of the solar radiation pressure acceleration is

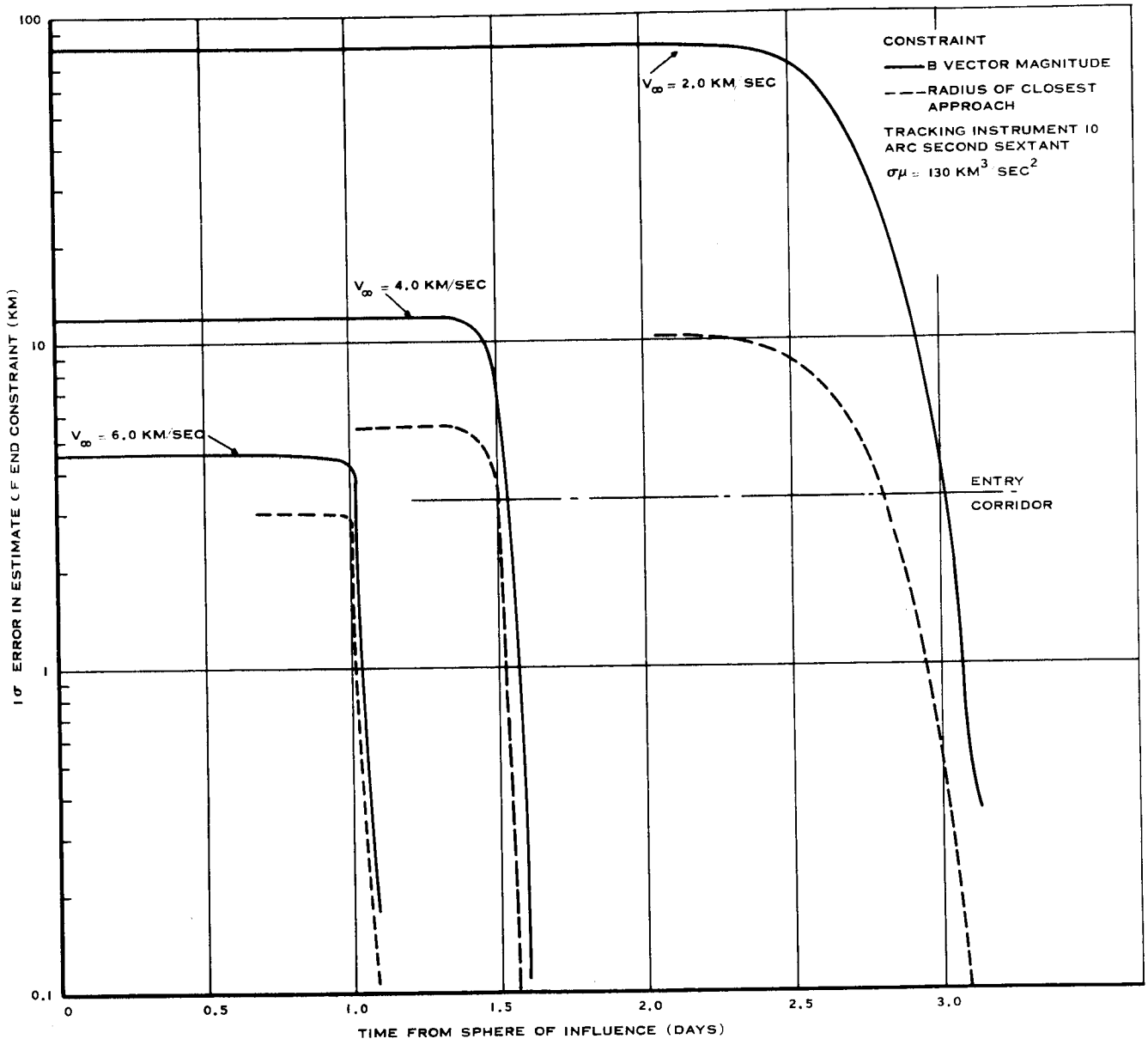

Figure 10 Error in Estimate of End Constraints

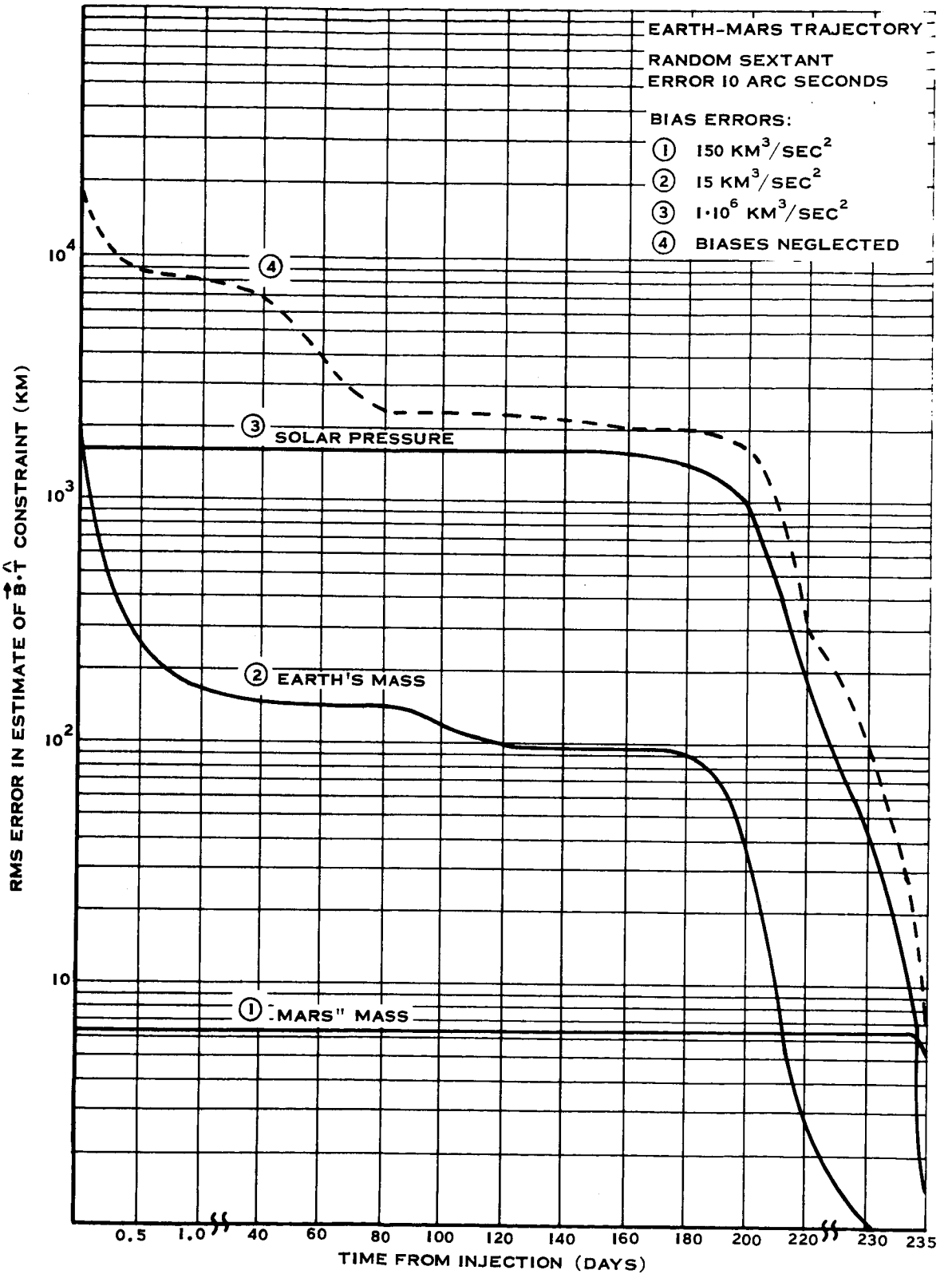

Figure 11 Error in Estimate of B·T Due to Neglecting Bias Errors

$$p = k_{sp} \frac{R_s}{r_s^3}$$

The solar radiation constant, k_{sp}, is a function of the vehicle mass, vehicle area projected normal to the vehicle-sun line, and the surface reflectance. For a hypothetical vehicle with a reflectance of one, a constant normal area of 100 square feet, and a weight of 200 pounds, the constant, k_{sp}, is approximately 10^7 km^3/sec^2. The results shown in Figure 11 are for an uncertainty in the solar radiation pressure constant of 10^6 km/sec^2 or 10%.

The characteristics of the three curves in Figure 11 showing the error due to neglecting the uncertainties in the planetary masses and solar radiation pressure are the result of the following effects. The initial uncertainties show the error each would introduce if no navigation measurements were taken. At different points in time, each of the errors begins decreasing due to the measurements that are being taken. The decrease in error begins to occur at a time when the equation of motion error source has had some influence on the trajectory and the navigation system is estimating the perturbed trajectory. For example, the planetary mass of Earth has an immediate strong effect on the trajectory. A large portion of the effect of this error is quickly removed by the navigation system. In contrast, the mass of Mars has essentially no effect on the trajectory until the sphere of influence is reached (234 days). Therefore, the error in the constraint estimate due to neglecting this bias error remains constant (number 2 curve) until the last day. At this time the mass of Mars does influence the trajectory and the effects of its uncertainties can be removed.

The total error in estimate of the end constraint due to neglecting the three equation of motion parameters is shown in Figure 12 by the number 1 curve. This curve is obtained by taking the root sum square of the errors due to the individual error sources. Curve number 2 in Figure 12 is the error in estimate when the bias errors are neglected. Curve 3 in this figure is the

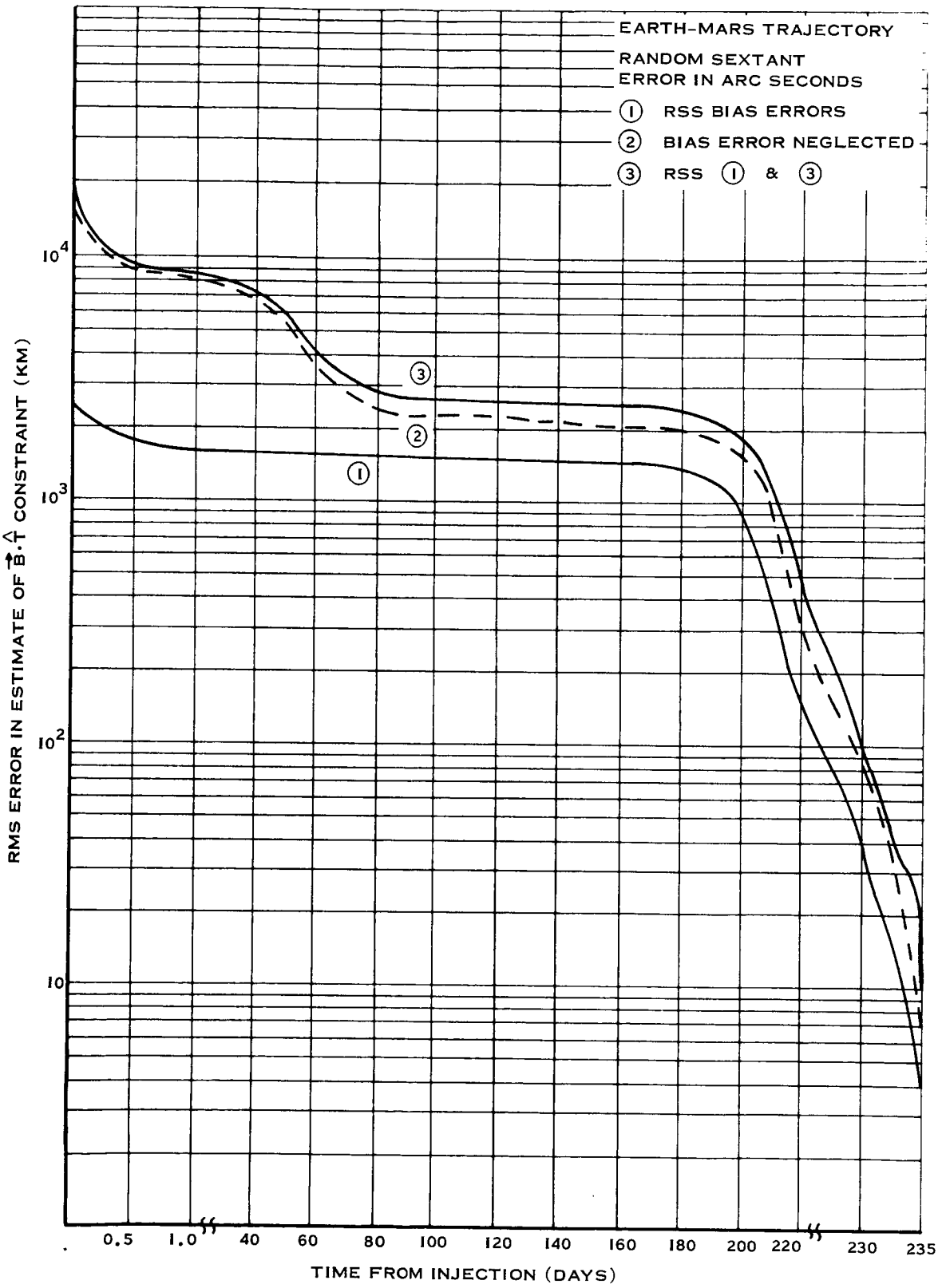

Figure 12 Composite Effect of Bias Error on $\vec{B}\cdot\hat{T}$ Estimate

total error in estimate of the constraint. This curve is the root sum square of curves 1 and 2. The difference between curves 2 and 3 shows the degree to which the results of the original study concerning the navigation system performance were optimistic due to neglecting the bias errors.

The $\vec{B}\cdot\hat{T}$ constraint estimate is critical because it indicates the accuracy to which the entry altitude is known. As indicated earlier, for an entry mission at Mars the altitude corridor is ± 3.5 km. Figures 11 and 12 show that the error in $\vec{B}\cdot\hat{T}$ due to neglecting the uncertainty in Mars planetary mass is 4 to 5 km. The effect of an error of this magnitude must be evaluated in terms of mission requirements. While this error makes an entry mission at Mars marginal, it would have only a minor effect on a flyby or orbiter mission.

5.1.2 Measurement Bias Errors

The analysis of the effects of the measurement biases is performed with the Mark II Error Propagation Program. The bias errors are analyzed by two techniques. One technique is that of including them as part of the state and estimating them. The second technique used is that of considering the effect of a bias error. The Mark II program is not capable of analyzing the error due to completely neglecting measurement biases as was done for the equation of motion errors.

The results shown in Figure 13 are for the two methods of treating the bias error in the sextant measurement. Curve 1 shows the error in estimate of the end constraint for an instrument with a 10 arc second random error and no bias error. Curve 2 shows the error in estimate for the addition of a 10 arc second bias that is included in the state and estimate. The third curve is for the case in which the 10 arc second bias is considered in the estimation process but is not estimated (variance is held constant) as part of the state. Curves 1 and 2 in Figure 13 show that the increase in the error due to an instrument bias error that is solved for is negligibly small (less than 1 km at the end time).

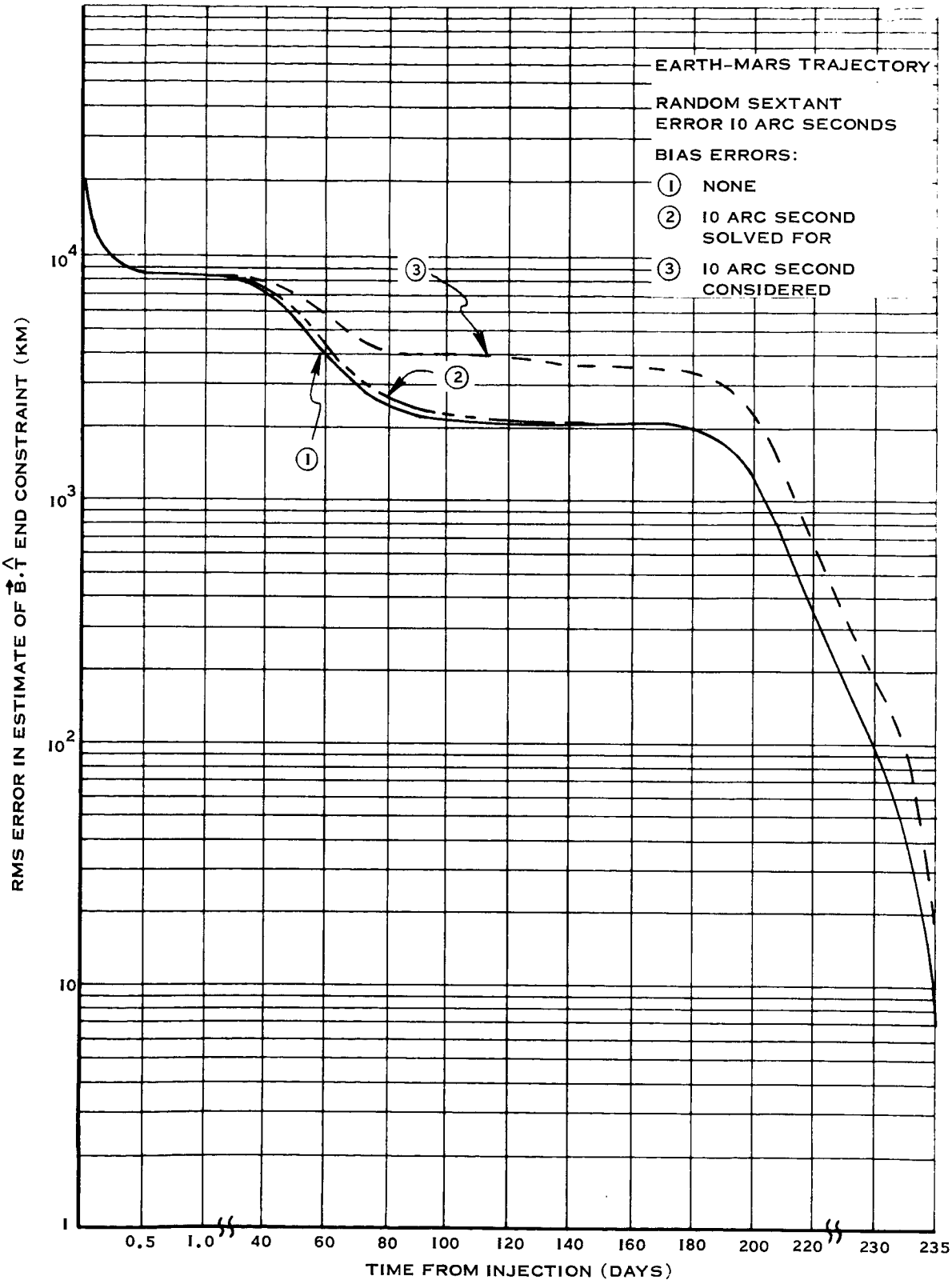

Figure 13 Effect of Sextant Angle Bias on $\vec{B}\cdot\hat{T}$

Curve 3 shows that there is a considerable increase in the error in estimate when the bias error is considered but not estimated. The end point estimate error in $\vec{B}\cdot\hat{T}$ is increased from 7 to 14 km. This result indicates that if the error source were neglected completely, the error due to neglecting it would be larger than the 7 km difference shown above.

The clock bias was analyzed by including it in the state and estimating it. The results indicate that the clock bias can be estimated rapidly and its effect removed from the estimation process. The effect of completely neglecting this error source is not presented. The high correlation between the clock bias and the estimate, as shown by the ability to solve for the bias, indicates it would be a significant error if present and neglected.

5.2 MARS-EARTH TRANSFER

The result obtained on the effects of bias errors on the Mars-Earth trajectories are presented in this section. The data presentation is restricted because the results and conclusions that can be reached are in general the same as obtained for the outbound portion of the mission.

The analysis of the measurement bias errors is omitted. The analysis in Section 5.1.2 indicates that these are error sources that cannot be neglected without introducing significant errors. This conclusion applies to the return trajectories equally well.

The results presented in Figure 14 show the effect of neglecting the equation of motion bias errors on the estimate of the end constraint $\vec{B}\cdot\hat{T}$. The number 4 curve in each figure shows the expected error in estimate of the constraint under the assumption of a perfect physical model. These uncertainties are due to the injection errors and random errors in the measurements. These results correspond to those obtained in the original study.[1] The three remaining curves in each figure show the additional error in estimate due to the neglected uncertainties in planetary masses of

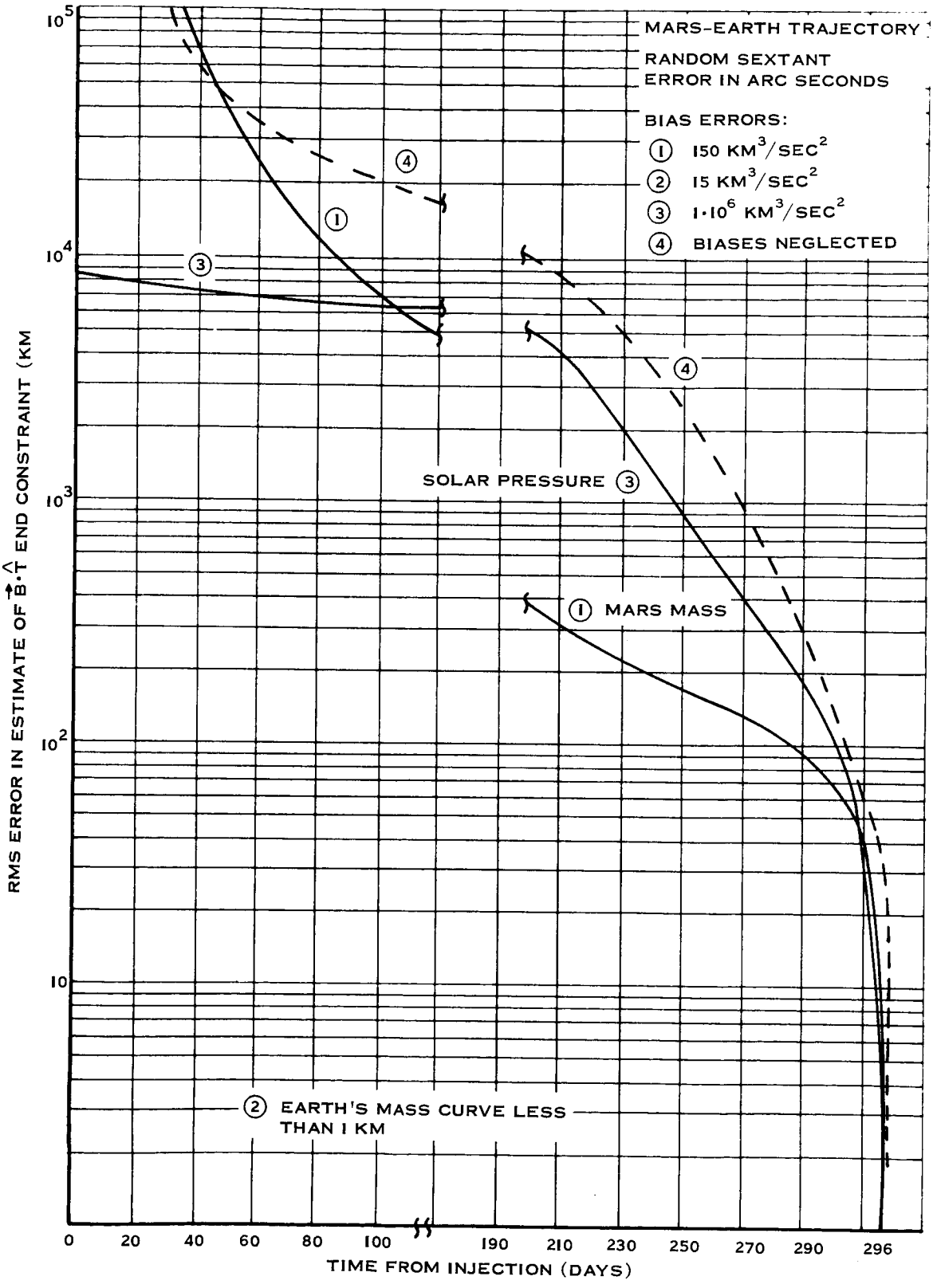

Figure 14 Error in Estimate of $\vec{B}\cdot\hat{T}$ Due to Neglecting Bias Errors

Earth and Mars and the solar radiation pressure. The planetary mass uncertainties used are 15 km^3/sec^2 for the Earth and 150 km^3/sec^2 for Mars. These are approximately the uncertainties for the 1963 adopted values. The uncertainty in the solar radiation constant, k_{sp}, is taken as 10^6 km^3/sec^2.

The curves in Figure 14 have the same character as those shown in Figure 11 for the outbound trajectory with the roles of Earth and Mars planetary masses interchanged. In the return case, the uncertainty in the mass of Earth is so small that it has negligible effect on the terminal accuracy. The mass of Mars and the solar radiation pressure exhibit an effect until late in the flight. During the final day, their effects become quite small.

SECTION 6

SUMMARY AND CONCLUSIONS

The theoretical analysis in Section 2 presents some new developments in the analysis of the effects of bias errors on an orbit estimation process. These developments concern three areas of interest. They are the following: (1) the effect of neglecting bias errors in the modeling of the physical process, (2) the separable properties of the effects due to random errors and those due to bias errors, and (3) techniques for efficient parametric analysis by means of matrix manipulations.

The data results obtained on the effects of equation of motion bias error sources on the navigation system performance indicated the following. The uncertainty in Mars planetary mass produces deviations in close approach of 10 to 20 km for practical Mars approach trajectories. The error in the state estimate due to neglecting this uncertainty is on the order of 4 to 5 km at the end point. This is a significant error when considering an entry mission with a 3.5 km corridor requirement. The effect of Mars mass uncertainty on the return trajectory is negligible following the navigation measurements that are used.

The uncertainty in the planetary mass of Earth causes approach deviations of less than 1 km on the practical approach trajectories. On the Earth-Mars outbound trajectory, the effect of this mass uncertainty is removed by the navigation measurements.

The effects of a solar radiation pressure uncertainty of 10 percent can be removed on both the outbound and return trajectories by means of the navigation measurements.

The effect of an uncertainty in the A.U. conversion to laboratory units is

a strong function of the particular heliocentric trajectory being used. The analysis of 5 heliocentric transfer angles for various flight times for both the outbound and return trajectories shows one or two minimums in the close approach deviations for each transfer angle. The deviation minimums vary from near zero to 550 km for a 1000 km uncertainty in the A.U. The minimum deviations are near zero for a 180 degree transfer and increase for larger and smaller transfer angles. The deviations can be estimated by the navigation system to a satisfactory accuracy for an entry mission.

The guidance analysis is restricted to the determinations of the velocity required to correct the deviations caused by the Mars planetary mass uncertainty and the A.U. conversion uncertainty. The ΔV required is a function of the time at which the correction is applied. The ΔV required to control the deviations due to Mars mass uncertainty for a FTA guidance law vary from 5 to 10 meters/second and from 1 to 5 meters/second with a VTA guidance law. The velocity requirements for an uncertainty in the A.U. are quite trajectory dependent. The guidance velocity corrections for a FTA guidance law are from 50 to 70 meters/second when using only one correction. The corrections for a VTA law vary considerably. The trajectories with small deviations (less than 100 km) require corrections from 1 to 10 meters/second. The trajectories with the larger deviations require corrections of 10 to 30 meters/second.

The guidance requirements for an Earth-Mars mission obtained in the original study while neglecting the two uncertainties that have been described above are shown in Table 1. The results in Table 1 for a VTA guidance law include the effects of errors in an onboard navigation system and guidance system execution errors. The approach trajectory deviations due to a planetary mass uncertainty cannot be estimated until the last few hours of the approach trajectory. It would therefore be necessary to control these deviations with the final correction. The 1 meter/second final correction shown in Table 1 would increase to a

TABLE 1

GUIDANCE PERFORMANCE VTA GUIDANCE LAW

Correction	End Constraint Deviations (KM)		Δv Req'd M/Sec	Time
	$\vec{B}\cdot\hat{T}$	$\vec{B}\cdot\hat{R}$		
1	10300	2390	10.56	1^D
2	269	153	8.18	220^D
3	12.8	8.6	3.53	234^D
4	6.54	2.01	.92	$234^D 20^h$

TABLE 2

VELOCITY REQUIREMENTS WITH EQUATION OF MOTION UNCERTAINTIES

Correction	Δv Req'd M/Sec
1	10.56
2	8.18
3	3.53 10.00 (AU)
4	0.92 5.00 (u) 3.00 (AU)
TOTAL	41.19

maximum of approximately 5 meters/second with a mass uncertainty of 150 km^3/sec^2. The trajectory deviations due to the uncertainty in the A.U. conversion can be estimated with an error of 30 to 40 km one day prior to periaries with a 10 arc second instrument. This allows the possibility of making a correction at this time that will correct the deviations to an accuracy consistent with the estimate. The deviations remaining after the correction could then be removed with the final maneuver. On the trajectories with large deviations due to the A.U. conversion, this would increase the third correction of Table 1 by approximately 10 meters/second. The final correction would be increased by 2 to 3 meters/second.

The discussion of guidance ΔV requirements above is summarized in Table 2. These results were obtained by algebraically adding the velocity requirements caused by the two uncertainties in the equation of motion to those due to injection errors, navigation errors, and guidance system execution errors. This very pessimistic analysis of adding these independent effects algebraically increases the total velocity requirements from 23 meters/second to 41 meters/second.

The sextant angle measurement bias and onboard clock bias both have a significant influence on the navigation system accuracy. If these errors are neglected, the results imply a degradation in the end point estimate accuracy of greater than 7 km. This is not satisfactory for an entry mission. If the bias error sources are included as part of the state being estimated their effect can be eliminated by the "calibration" of the sextant instrument and clock.

SECTION 7

REFERENCES

1. Interplanetary Navigation and Guidance Study, 3 Volumes, WDL-TR2629, Philco-Ford, Palo Alto, California, 30 October 1965.

2. Kalman, R. E., "A New Approach to Linear Filtering and Prediction Theory," ASME, Journal of Basic Eng., March 1960, pp. 35-45.

3. Schmidt, S. F., "State Space Techniques Applied to the Design of a Space Navigation System," JACC Conference paper, 1962.

4. Smith, G. L., Schmidt, S. F., and McGee, J. A., Application of Statistical Filter-Theory to the Optimal Estimation of Position and Velocity Onboard a Circumlunar Vehicle, NASA Technical Report R-135, Ames Research Center, 1962.

5. McLean, J. D., Schmidt, S. F., and McGee, J. A., Optimal Filtering and Linear Predictions Applied to a Midcourse Navigation System for the Circumlunar Mission, Technical Report D-1208, NASA Ames Research Center, March 1962.

6. Schmidt, S. F., The Application of State Space Methods to Navigation Problems, WDL-TR4, Philco-Ford WDL Guidance and Control Systems Engineering Department, Palo Alto, California, July 1964.

7. Gunckel, T. L., "Parametric Analyses of Optimal Estimation," Unnumbered Memo, Autonetics Division of North American Aviation, Inc., December 1965.

8. Rohde, P. J., "Influence of Uncertainties in the Astronomical Unit Conversion and Mars Planetary Mass on Earth-Mars Trajectories, " WDL-TR 3040, Philco-Ford, Palo Alto, California, September 1966.

9. Makemson, M. W., Baker, R. M. L., Jr., Westrom, G. B. "Analysis and Standardization of Astrodynamic Constants," The Journal of Astronautical Sciences, Volume VIII, Number 1, Spring 1961

10. Brouwer, D., "System of Constants," Progress in Astronautics and Aeronautics, Volume 14, Academic Press, New York, 1964.

11. Muhleman, D. O., "Relationship Between the System of Astronomical Constants and the Radar Determinations of the Astronomical Unit," TR-32-477, California Institute of Technology, Jet Propulsion Laboratory, January 15, 1964.

12. Marsden, B. G., "An Attempt to Reconcile the Dynamical and Radar Determinations of the Astronomical Unit" Symposium #21, I.A.U., on Fundamental Constants of Astronomy, Paris, June 1963.

13. Anderson, J. D., Null, G. W., Thorton, C. T., "The Evaluation of Certain Astronomical Constants from the Radio Tracking of Mariner II," Academic Press, New York, 1964.

14. "Astrodynamic Constants Analysis," LR 17571 Lockheed California Company, Burbank, California, June 1963.

15. Herrick, S., Westrom, G. B., Makemson, M. W., "The Astronomical Unit and the Solar Parallax," U.C.L.A. Astrodynamical Report No. 5, 1959.

16. Battin,R. H., Astronautical Guidance, McGraw-Hill Book Company, 1964, pp. 12-14.

17. Swenson, B. L., Carlson, R. W., Tindle, E. L., "Some Requirements on Lifting Vehicles for Manned Mars Operation," AIAA/AAS Stepping Stones to Mars Meeting, Baltimore, Maryland, March 28-30, 1966.

18. Manned Mars Mission Study, Report for NASA Ames, Contract No. NAS 2-1409 by TRW, STL Redondo Beach, California, 28 March 1964.